THE NOVEL PHARMACOLOGICAL ACTIONS OF ISONIAZID: A PROPOSAL FOR ITS MODE OF ACTION

By
Md. Saifur Rahman Khan

A thesis submitted in partial fulfillment of the requirements for the degree of

DOCTOR OF PHILOSOPHY

IN

PHARMACY AND PHARMACEUTICAL SCIENCES

Department of Pharmacy and Pharmaceutical Sciences
University of Alberta

Abstract

Isoniazid (INH) is one of the first-line anti-tuberculosis (TB) drugs against both active and latent TB, which is caused mainly by *Mycobacterium tuberculosis* (*Mtb*). The inhibition of bacterial cell wall synthesis has been previously proposed as the mode of action of INH. However, it cannot explain a number of queries such as: (a) how does INH kill waxy granuloma-residing *Mtb* (since INH cannot penetrate into granuloma due to very low lipophilicity); (b) how does INH kill latent TB bacteria which do not a possess typical cell wall, and (c) why being an antibiotic, INH treatment time is remarkably long (6 to 9 months). These limitations suggest INH may have another mode of action(s) which can be deciphered by comprehending the role of INH on the host immune system. To do so, a number of *in vitro* studies were conducted here. In the first study, human neutrophil myeloperoxidase was found capable of forming the INH-NAD^+ adduct, which inhibits cell wall synthesis (as does bacterial KatG). This suggests neutrophils could play a very important role against active TB during INH treatment. In the second study, INH showed a significant cytoprotective effect against oxidative stress-induced phagocytic cell necrosis which is the decisive cause of the granuloma degradation followed by active TB infection. This study suggests that INH ensures latency by defending necrotic degradation. In the third study, INH showed significant capacity to stimulate monocytic differentiation. Since monocyte-derived macrophages are considered as the major immune defense within granuloma due to their nitric oxide, INH-induced monocytic differentiation most likely has a contribution to both latent and active TB eradication. These three novel pharmacological actions of INH together have been presented in order to propose other modes of action of INH, which explain the previously mentioned limitations.

Preface

This thesis is an original work by Md. Saifur Rahman Khan (myself) supervised by Dr. Arno G. Siraki at Pharmacy and Pharmaceutical Sciences, University of Alberta. In certain experiment where human neutrophils were isolated from healthy donors, appropriate ethics approval was obtained from the University of Alberta Human Research Ethics Office (Protocol name: Neutrophil Isolation, Protocol No.: **Pro00008304).** The quantitative global proteomics (SILAC) studies design, mass spectroscopy and data acquisition followed by data normalization of both chapter 3 and 4 were conducted in the collaboration with Alberta Proteomics and Mass Spectrometry Facility (formerly known as IBD) and Professor Dr. Richard Fahlman at the University of Alberta. The mass analysis of INH-NAD^+ was carried out by Dr. Randy M. Whittal at Mass Spectroscopy Facility of the chemistry department, University of Alberta. The most of the experiments were carried out by me under direct supervision of Dr. Arno G. Siraki. However, some were conducted and/or assisted by other lab members (Dr. Michael Karim – post doctoral fellow, Naif Aljuhani – PhD candidate, Argishti Baghdasarian – Masters' student, Andrew G.M. Morgan – Masters' student, and Nutan Srivastava – Lab technician). The Chapter 2 of this thesis has been published as S.R. Khan *et. al.*, "Metabolism of isoniazid by neutrophil myeloperoxidase leads to isoniazid-NAD+ adduct formation: A comparison of the reactivity of isoniazid with its known human metabolites," Biochemical Pharmacology, vol. 106, 46 – 55, 2016. The Chapter 3 of this thesis has been published as S.R. Khan *et. al.*, "Cytoprotective effect of isoniazid against H2O2 derived injury in HL-60 cells," Chemico-Biological Interactions, vol. 244, 37 – 48, 2016. I was responsible for the data collection and analysis as well as the manuscript composition under supervision of Dr. Arno G. Siraki.

Dedication of the thesis

This thesis is dedicated to my parents, my beloved wife and my sweet daughter "Ashalina Khan Arisha"

Acknowledgments

First of all, I want to acknowledge the Almighty Allah for his willingness and blessings that I could accomplish this work.

This was an incredible experience that started with the conversation with Dr. Arno Siraki after my first supervisor Dr. Mavanur Suresh left the department within few months of my admission due to serious illness and ended up with this thesis. I am very thankful to my both supervisor Dr. Mavanur Suresh and Dr. Arno Siraki for providing me the opportunity of joining their labs at the University of Alberta. I express my deep esteemed gratitude to my present supervisor Dr. Arno Siraki for his constant support and encouragement throughout the course of this study. Working in the ingenious atmosphere of his lab has been a rare and gratifying experience. I must thank him for giving me freedom to choose my projects and sharing his vast experience on research day-to-day basis. I sincerely appreciate his inspiring lessons on writing quality scientific manuscripts. I am grateful for his priceless advice, enthusiasm, confidence in my work and freedom to realize my scientific pursuit. This piece of work would have been a distant dream for me without my present supervisor.

I am thankful to Dr. Richard Fahlman and Dr. Paige Lacy, my committee members for their interest in my work. The enthusiastic participation of all my committee members in the discussions relating to the study has made it possible to complete this project on time. The lab environment plays an immense role in the productivity of any student. I would like to thank all my lab mates for being cooperative, helpful, and providing congenial atmosphere. No words suffice to thank my incredible lab members Dr. Karim Michael, Naif Aljuhani, Argishti Baghdasarian, Andrew G.M. Morgan, and Nutan Srivastava for their affection, care, and support.

My heartfelt thanks to my supportive and caring community friends and numerous well-wishers, whose help and good wishes contributed, in one or another way, to the completion of this work.
The contribution of my beloved wife Aysha Akter in this entire phase of work and life is immense and beyond any description. Her supportive, encouraging and motivating attitude keep my spirits high and inspiring me to aim higher. I bow in ovation to my wife and daughter "Ashalina Khan Arisha" for their love and support. The two noble ones stood by me all through with patience and tolerance.

I would also like to acknowledge Alberta Innovate Technology Futures and the University of Alberta for their support. Last but not the least, I express my gratitude to my parents and younger brother for their never-ending prayers for me.

Md. Saifur Rahman Khan

Table of Contents

List of figures in introduction

CHAPTER 2: METABOLISM OF ISONIAZID BY NEUTROPHIL MYELOPEROXIDASE CAN PRODUCE INH-NAD$^+$ ADDUCT

CHAPTER 3: ISONIAZID INCREASES OXIDATIVE STRESS TOLERANCE OF IMMUNE CELLS

CHAPTER 5: DISCUSSION

List of the figures in discussion

ABBREVIATIONS

ABAH	4-Aminobenzoic acid hydrazide
ANOVA	Analysis of variance
ATP	Adenosine triphosphate
BSA	Bovine serum albumin
CCCP	Carbonyl cyanide 3-chlorophenylhydrazone
C VPS	Macrophage class C vacuolar protein sorting complex
DAPI	4', 6-Diamidino-2-phenylindole
$\Delta\psi_m$	Mitochondrial membrane potential
DMPO	5,5-Dimethyl-1-pyrroline-N-oxide
DPI	Diphenyleneiodonium
DTPA	Diethylenetriaminepentaacetic dianhydride
EPR	Electron paramagnetic resonance
FBS	Fetal bovine serum
FITC	Fluorescein isothiocyanate
GM	Granulocyte-macrophage
GOx	Glucose oxidase
GST	Glutathione-S-transferase
HL-60 cells	Human promyelocytic leukemia cell
H_2O_2	Hydrogen peroxide
HOCl	Hypochlorous acid
HRP	Horseradish peroxidase
HZ or Hz	Hydrazine
IgG	Immunoglobulin gamma
$INH^{\bullet}$	Isonicotinoyl radical
$INH\text{-}NAD^{+}$	Isonicotinoyl-nicotinamide adenine dinucleotide
InhA	Enoyl acyl-carrier-protein reductase
iNOS	Inducible nitric oxide synthase
MPO	Myeloperoxidase
NAcINH	N-acetylisoniazid
NAcHZ	N-acetylhydrazine
NAD^{+}	Oxidized form of nicotinamide adenine dinucleotide
NADPH	Nicotinamide adenine dinucleotide phosphate
NaF	Sodium Fluoride
NAT2	N-acetyl transferase 2
NBT	Nitrotetrazolium blue chloride
NO	Nitric oxide
NSE	Non-specific esterase
PtpA	Protein tyrosine phosphatase
PBS	Phosphate buffered saline
PBST	Phosphate buffer saline Tween-20
PBMC	Peripheral blood mononuclear cells
PI	Propidium iodide
PMA	Phorbol 12-myristate 13-acetate
RA	Retinoic acid

RNS	Reactive nitrogen species
ROS	Reactive oxygen species
RS	Reactive species
SD	Standard deviation
SOD	Superoxide dismutase
TB	Tuberculosis
V-ATPase	Vacuolar H^+-ATPase
VitD3	1α, 25-Dihydroxyvitamin D_3

CHAPTER 1:

INTRODUCTION

1.1 ISONIAZID (INH)

1.1.1 Brief history

Isoniazid (INH) is one of the first-line drugs for both active and latent tuberculosis (TB) which is caused by *Mycobacterium tuberculosis* (*Mtb*) and *Mycobacterium tuberculosis* complex (MTBC) (which includes *M. bovis, M. africanum, M. pinnipedii, M. microti, M. caprae* and *M. canettii*) (http://www.cdc.gov/tb/). Isoniazid was first synthesized by two Ph.D. candidates, Hans Meyer and Josef Mally of German Charles University in Prague, as a part of their doctoral requirements in 1912; however, its enormous potential against TB was unknown at the time. In 1951, researchers at Hoffmann-La Roche and E.R. Squibb & Sons in the U.S. and at Bayer in West Germany concurrently demonstrated the high degree of INH efficacy against TB (https://pubs.acs.org/cen/coverstory/83/8325/8325isoniazid.html). INH was later approved as an anti-tuberculosis drug against both active and latent TB by FDA in 1952 and 1967, respectively (www.fda.gov/).

1.1.2 Physicochemical properties of INH

INH, chemically referred to as isonicotinoyl hydrazine or isonicotinic acid hydrazide ($C_6H_7N_3O$, mol. Wt. 137.14), belongs to the class of organic compounds known as pyridine carboxylic acids and derivatives. It is a freely water-soluble compound (14 g/100 mL of water at 25ºC). Its solubility decreases with decreasing polarity of solvent. Its melting point is 171.4°C, lipophilicity is very low (logP = -0.70), and it is slightly basic (pKa = 1.82, at 20°C) [DrugBank: Isoniazid (DB00951)]. The high water solubility of INH ensures its rapid absorption and systemic distribution which describe why it is the ideal form of the drug to exert its systemic pharmacological action. At the same time, it also explains where its limitation such as

penetration into waxy regions of the body (e.g., granulomas in TB infection; which has been described in later) due to very poor lipophilicity.

1.1.3 Pharmacokinetics of INH

Due to its high water solubility, INH absorbs rapidly from the gastrointestinal tract after oral administration and undergoes the first-pass metabolism. It is also distributed rapidly throughout the body (volume of distribution: 0.57 to 0.76 L/kg) and excreted approximately 95% through urine within 24 hours. Its protein binding capacity is very low: only 0 to 10%. Food, especially fatty food, significantly reduces its absorption and distribution [DrugBank: Isoniazid (DB00951)]. The pharmacological concentration of INH (C_{max}) is 20 µM to 60 µM (5.53 ± 2.92 µg/ml) [1]. The liver is the main site for INH metabolism. The metabolism steps of INH are: **(1) *acetylation:*** INH is acetylated by N-acetyl transferase-2 (NAT2) to N-acetyl-INH; **(2) *hydrolysis:*** one step hydrolysis of N-acetyl-INH forms both isonicotinic acid (water soluble and excreted trough urine) and acetylhydrazine; (3) ***further acetylation:*** acetylhydrazine undergoes further acetylation by NAT2 to form water soluble diacetylhydrazine which can be excreted through urine [DrugBank: Isoniazid (DB00951)].

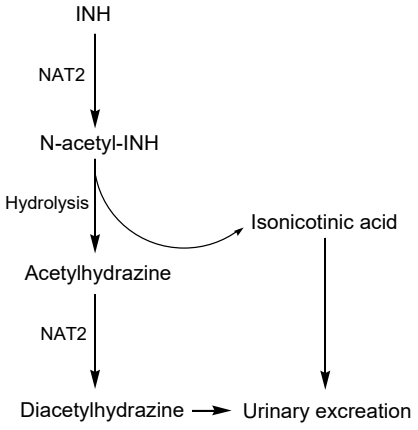

Figure - 1: The metabolism of INH in liver.

1.1.4 Pharmacodynamics/Mode of action of INH

The extensive research on the mode of action of INH was started at the very beginning of INH approval by the FDA, and took approximately half-a-century to institute a general consensus. Among these studies, some highlighting studies have been mentioned below:

In 1952: It was found that INH decreased the synthesis of fatty acids with chain lengths longer than 16 carbons. It was first proposed that the mechanism of INH was as an inhibitor of the mycolic acid biosynthesis [2]. However, it was unknown how INH could inhibit mycolic acid biosynthesis.

In 1954: The same group published another study on INH resistance. It showed that the INH-resistant *Mtb* expressed no or little mycobacterial catalase-peroxidase (KatG). It concluded that INH mode of action relies on KatG functions [3].

In 1995**:** The composition of the mycobacterial envelope was first identified, and also proposed that *Mtb* utilizes enoyl acyl-carrier-protein reductase (InhA) to synthesize mycolic acids [4].

1n 1998: It was found that the activated form of INH formed a covalent bond with nicotinamide adenine dinucleotide (NAD), which blocked the active site of InhA [5].

In 1998-2006: The mode of anti-bacterial action of INH was proposed and is generally agreed upon as shown in Figure 1 (below) [6, 7].

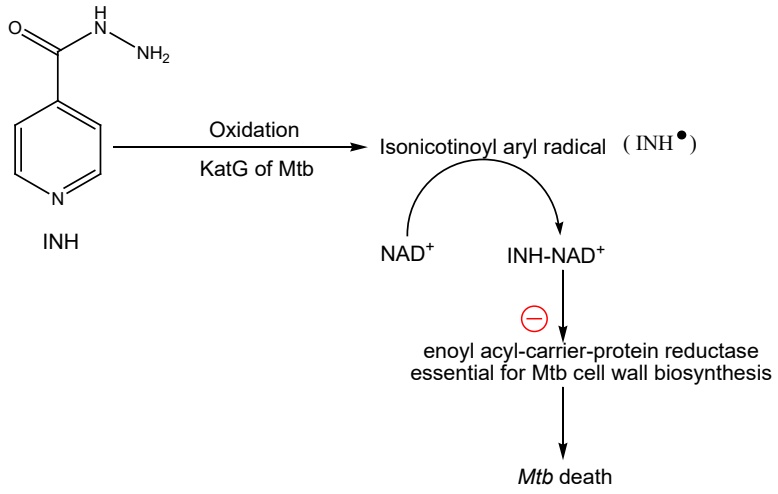

Figure - 2: The mode of action of INH.

Being a prodrug, INH can be oxidized to the isonicotinoyl radical ($INH^{\bullet}$) through the peroxidation cycle of the bacterial catalase-peroxidase, KatG. Thereafter, $INH^{\bullet}$ reacts with the oxidized form of nicotinamide adenine dinucleotide (NAD^{+}) and produces the INH-NAD^{+} adduct, a potent inhibitor of enoyl acyl-carrier-protein reductase (InhA) which is an essential enzyme of mycolic acid biosynthesis of the *Mtb* cell wall [6, 7]. In drug-resistant TB, mutations on KatG were confirmed with lower INH-NAD^{+} adduct formation as well as lower antibacterial activity [8]; in this instance, INH therapy is not effective.

1.1.5 Limitations of the proposed mode of action

A number of limitations have already been identified against the consensus on the mode of action of INH, which was based on all *in vitro* studies. Although these *in vitro* studies were useful, some recent knowledge of the pathophysiology of TB along with some long-standing clinical queries has questioned the mechanism of action. As such, a recent study showed that INH penetration into the granuloma (where *Mtb* resides in TB) was very low in a rabbit model of TB infection [9]; this is possibly due to both its low lipophilicity (log*P* = - 0.70) and very low

protein binding (0 – 10%) [DrugBank: Isoniazid (DB00951)]. If INH cannot penetrate into the site of infection, its anti-bacterial activity would not kill bacteria. Again, several *in vitro* studies showed that INH demonstrated rapid killing of *Mtb*; however it takes 6 to 9 months for clinical efficacy [10], which still remains puzzling. In addition, a latent stage of *Mtb* has been described as non-replicating but energy-generating within granulomas [11]. A recent study on the populations of latent *Mtb* was conducted for their cell wall evaluation, and found that all populations of latent *Mtb* remain in cell-wall free stage [12]. However, INH functions through inhibiting cell wall biosynthesis. If latent *Mtb* does not possess a cell wall, how could INH demonstrate effectiveness against latent TB? All these limitations or questions regarding the mode of action of INH lead one to surmise that INH may have more than one mechanism(s) of action which have yet to be identified.

1.1.6 Alternative modes of actions of INH

As a part of alternative modes of action search, two studies can be mentioned here. Both showed that suprapharmacological concentration (35 mM) of INH can produce nitric oxide (NO) through the peroxidation cycle of KatG [13, 14]. To produce NO from INH, the oxidation site of the hydrazide nitrogen atom was proposed as the carbonyl of INH, which is decomposed to NO and INH$^{\bullet}$.

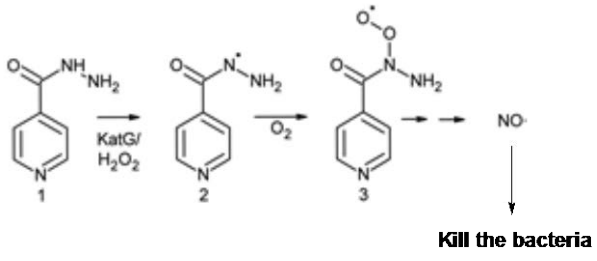

Figure – 3: The alternative mode of action of INH [13, 14].

Recently a study on the temperature-dependent rate constants for the hydroxyl radical oxidation and solvated electron reduction of INH concealed such possibility. It found the distal nitrogen of hydrazyl moiety as the initial oxidation site, and revealed the decomposition products as diazene (HN=NH) and INH$^{\bullet}$ [15]. Moreover, this alternative mode of action does not address any earlier limitations described.

1.1.7 INH metabolism and toxicity

Chronic use of INH is well-known for drug-induced idiosyncratic toxicity, presented as hepatotoxicity, systemic lupus erythematosus, and rarely agranulocytosis. Although the mechanisms of these idiosyncratic drug reactions are yet to be elucidated, it is suspected that INH reactive metabolites induced immune responses. Several studies showed that INH-induced toxicity mainly depends on following factors: (1) *N*-acetyltransferase 2 (NAT2) polymorphisms [slow and rapid acetylator phenotypes]; (2) increased CYP2E1 activity; (3) co-administration of rifampicin, and (4) absence (null) of Glutathione-S-transferase (GST) M1 [16].

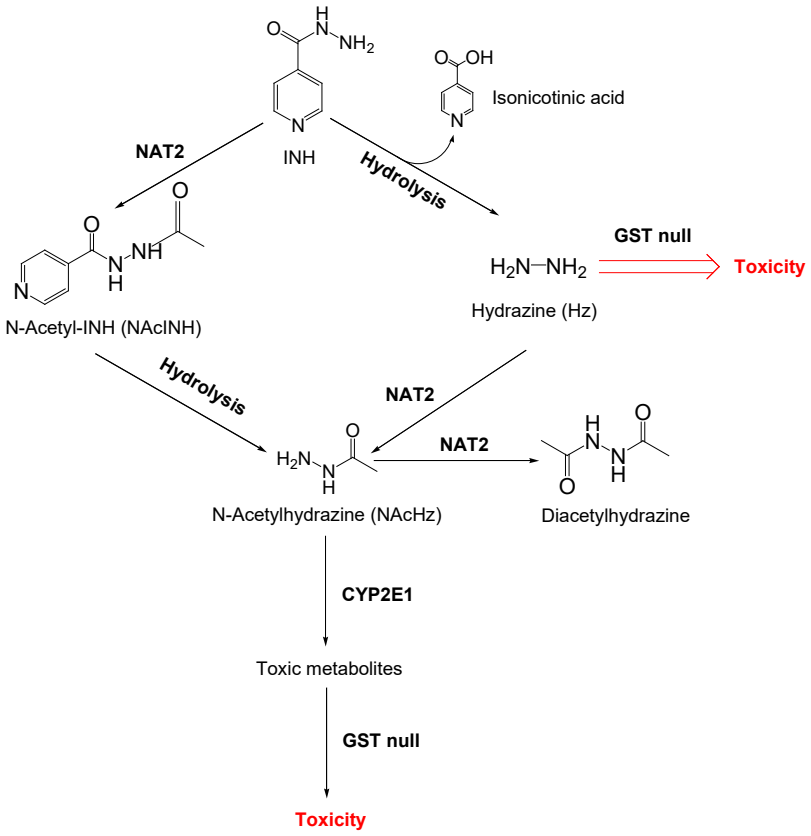

Figure - 4: A scheme of the possible reactive metabolites involved in INH-induced (hepatotoxicity) toxicity.

During INH metabolism, INH is first converted into N-acetyl-INH by NAT2, followed by hydrolysis and another step of either acetylation by NAT2 or oxidation by CYP2E1. The acetylation forms a non-toxic compound, diacetylhydrazine, whereas the oxidation forms toxic metabolites. Interestingly, the slow acetylator phenotype of NAT2 has been found as more toxic metabolite producer [17-19]. A possible cause might be that slow acetylation of acetylhydrazine would allow CYP2E1 relatively more time to oxidize it. In addition, INH can produce hydrazine (Hz) through hydrolysis. These all together can contribute to toxicity directly and/or by producing protein-adduct-antigen (haptens) to induce adaptive immune responses, if there is a

lack of Glutathione-S-transferase (GST) M1 expression which can effectively neutralize these reactive toxic metabolites from the body [16, 18]. Additionally, rifampicin is also found as a contributor for more toxic metabolite production due to its capacity to increase CYP2E1 expression [17].

1.2 TUBERCULOSIS (TB)

1.2.1 Preamble

TB is thought as a prehistoric scourge for human beings based on archeological studies [20]. A recent comparative genomic analysis of bacterial DNA from 1000 years old mummies disagreed with this archeological finding and revealed that TB originated from Africa less than 6000 years ago [21]. Although TB is an ancient disease and nowadays scientific endeavors are at the zenith being well-equipped with a number of first-line and second line drugs for different regiments of anti-TB therapies, TB is still one of the major causes of death in developing countries. 9 million new TB cases have been reported worldwide in 2013 as per the WHO report of March 2015. Among them, 1.14 million died due to TB alone and another 0.36 million died due to both TB and HIV coinfection. As per the Canada communicable disease report 2015, 1640 new active and re-treatment TB cases were also reported in 2013 (http://phac-aspc.gc.ca/publicat/ccdr-rmtc/15vol41/dr-rm41s-2/assets/pdf/15vol41-S2-eng.pdf). It has spurred WHO to launch an "End TB strategy" in 2015 where novel research initiatives have also got priority with other prevention strategies to achieve "zero TB death" goals by 2035 (http://www.who.int/tb/post2015_strategy/en/).

1.2.2 Mycobacterium tuberculosis (Mtb)

Mtb is a fairly large non-motile rod-shaped bacterium (2 – 4 µm in length and 0.2 – 0.5 µm in width), first discovered by Robert Koch as a causative agent of TB in 1882. It is an obligate aerobe pathogenic bacterial species (capable of growing and reproducing inside the well-aerated cells of a host). As such, *Mtb* can be always found in the well-aerated upper lobes of the infected lungs. However, inside the macrophage where *in situ* conditions are not favorable for aeration,

Mtb slows down its generation time (15 – 20 h). In this condition, *Mtb* is defined as a facultative intracellular parasite (http://textbookofbacteriology.net/tuberculosis.html).

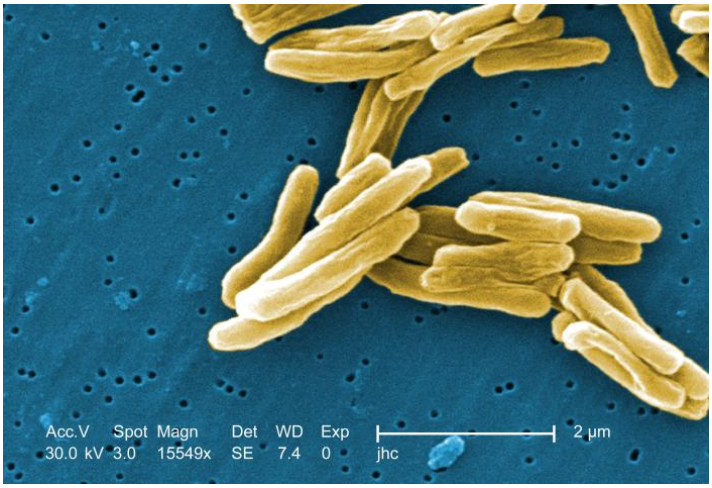

Figure - 5: The electron micrograph (Magnification 15549X) of *Mtb*. (www.cdc.gov).

Due to the highly waxy nature of the *Mtb* cell wall (described later), the general Gram-staining procedure does not apply here. Hence, *Mtb* is not classified based on Gram-staining (neither Gram-positive nor Gram-negative). Rather the acid-fast staining method is applied on *Mtb*. The Ziehl-Neelsen-carbolfuchsin-stain is used to stain the fixed *Mtb*, particularly its cell-wall component - mycolic acid, followed by decolorization with an acid-alcohol solution. The *Mtb* cells are then checked against contrasting background of methylene-blue. It appears as pink cells; it means that *Mtb* is an acid-fast bacterium (http://textbookofbacteriology.net/tuberculosis.html).

1.2.3 The cell-wall structure of Mtb

The cell-wall of *Mtb* is a thick waxy construction which prevents it from dehydration and provides adequate protection against both acidity and free radicals that are deployed by host immune systems to kill the bacilli. This characteristic cell wall also protects *Mtb* from various

antibiotics [22]. In general, the cell-wall of *Mtb* is a distinct layer on the phospholipid bilayer of the cytoplasmic membrane. The cell wall has three distinct sublayers of mycolic acid, arabinogalactan, and peptidoglycan (outer to inner side); all of which are covalently attached to each other. The outer sublayer (mycolic acid sublayer), in addition, is also covalently attached to free lipids, lipoglycans, and phosphotidyl inositols which make the outer capsule [23]. In latency, *Mtb* changes their shape from rod to round, and loses the typical cell wall outside of cytoplasmic membrane [24].

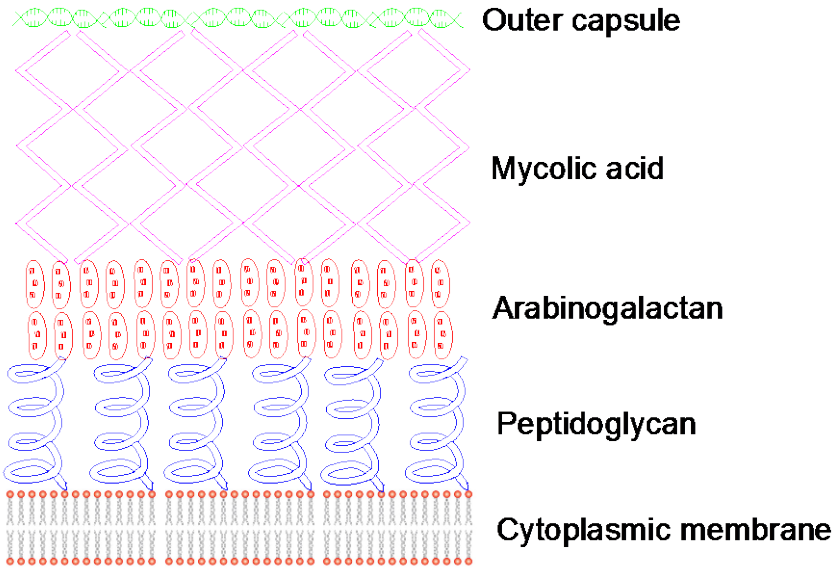

Figure - 6: The structure of *Mtb* cell wall. It consists of three distinct layers: peptidoglycan, arabinogalactan and mycolic acid. The mycolic acid is covered by an outer capsule.

1.3 PATHOPHYSIOLOGY OF TB AND HOST DEFENSE

1.3.1 Pathophysiology of TB and Granuloma formation

It is certain that human immune system plays the most important role to defend the progression of TB. The infectious dose for a person is reported to be between 1 and 200 bacilli. The invasion of *Mtb* is primarily defended by the alveolar macrophages which eventually form granulomas in the lungs. The cellular composition of TB granuloma has been well characterized. The main cellular components are infected macrophages, uninfected macrophages, and different modified forms of macrophages such as foamy macrophages, epithelioid cells, and multinucleated giant cells (Langerhans cells). The granuloma also consists of B lymphocytes, T lymphocytes, and fibroblasts [25].

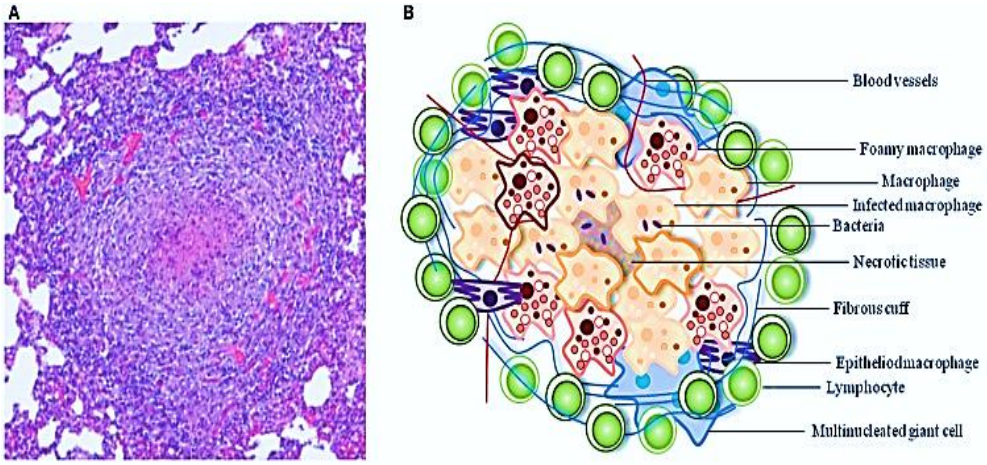

Figure - 7: The typical TB granuloma and its composition, taken from elsewhere [25]. (A) A representative pig lung TB granuloma with central necrosis. (B) A schematic presentation of the cellular constituents of a TB granuloma.

The pathological condition of TB is described as two states: (A) Latent TB where *Mtb* remains inside the granuloma; and (B) Active TB where *Mtb* comes out from granuloma through necrosis.

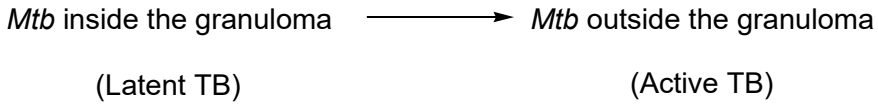

Figure – 8: Types of TB.

1.3.2 Host immune defense

The granuloma formation stops the spreading of *Mtb* throughout the body. However, the success of eradication of *Mtb* by macrophages in granulomas depends on the number of functional macrophages and bacilli's capacity to modulate the macrophagic signals for being activated as fully functional (e.g., the fusion of lysosome and phagosome). Healthy people usually have sufficient immunity to either eradicate or halt the progression of *Mtb* infection which results in either complete remedy or latent TB respectively. Only five percent of infected individuals, who have weak immunity due to malnutrition or diseases like HIV would succumb to active TB [26-28]. Therefore, it is clear how important the host immune system is to defend against TB.

1.3.3 Immune escaping strategies of Mtb

Mtb which is phagocytized by macrophages interferes with the phagosome maturation signals and destroys the digestive capacity of macrophages. Afterward, *Mtb* acts as a parasite and uses the infected macrophage for their nutrition and propagation. In general, the intracellular phagocytic killing of micro-organisms by macrophage/monocyte involves (A) surface binding, (B) uptake and vacuole/phagosome formation, and (C) maturation by fusion with lysosome to

trigger digestion, and (D) initiation of apoptosis. Macrophage has different types of cell surface receptors. These are (I) complement receptors, (II) mannose receptors, (III) pulmonary surfactant proteins, and (IV) others including CD14, scavenger receptors, and Fcy receptors [29]. These receptor expressions may vary depending on the state of differentiation and the state of activation of macrophages. However, there is no information about the certain type of surface receptor binding and *Mtb* survival inside macrophages [29]. *Mtb* possesses a number of ligands on its surface which make it easy to bind with macrophage surface. After surface binding, *Mtb* enters into the macrophage by forming a fused cell membrane containing vacuole which is known as phagosome. Usually, phagosomes are fused with lysosome to acquire antimicrobial activity and digest the micro-organisms. However, *Mtb* stops this fusion by adapting and modulating several molecular signals in active TB.

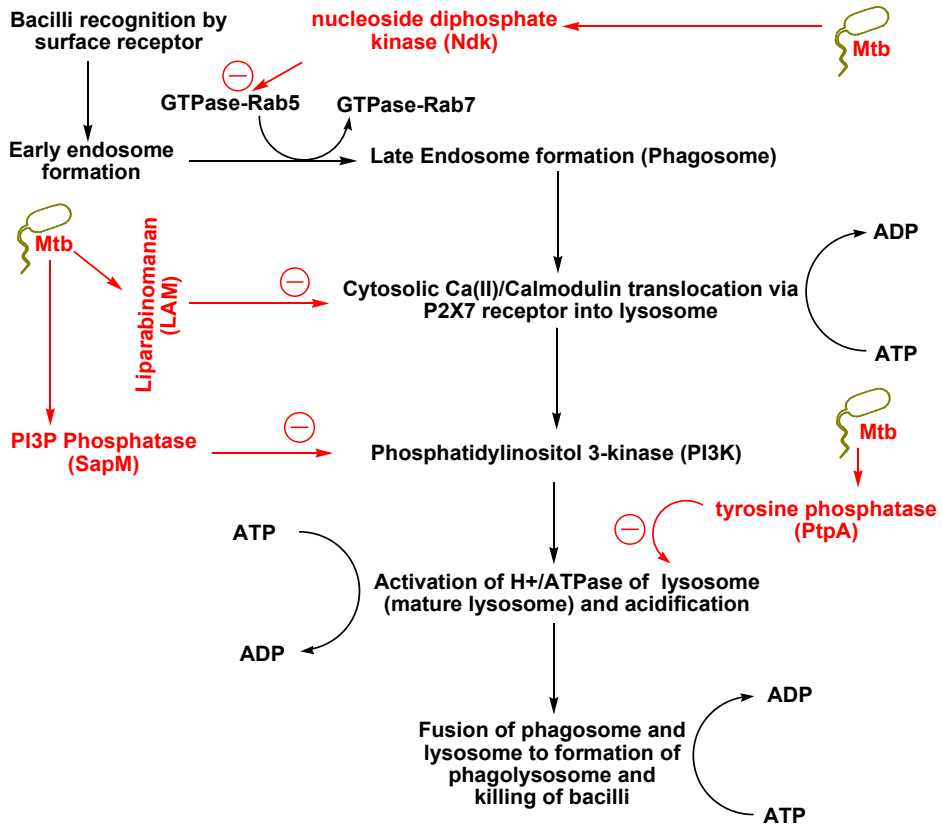

Figure - 9: The schematic diagram of phagocytosis process and the modulation of phagocytosis by *Mtb*. *Mtb* produce a number of signaling modulators such as nucleoside diphosphate kinase (Ndk), lipoarabinomanan (LAM), PI3P phosphatase (SapM), and tyrosine phosphate (PtpA) which modulate the phagocytosis process and help to survive inside the phagocytic cells.

In general, *Mtb*-induced modulation of macrophage signals are as follow: (1) inhibition of lysosome formation by the production of eukaryotic-like signaling molecules such as kinases or phosphatases to interfere with host signals trafficking, (2) inhibition of sphingosine kinase to block Ca(II)/calmodulin translocation into lysosome, (3) inhibition of lysosome maturation and acidification, and (4) *Mtb* propagation inside macrophages and release through necrosis which leads to active TB [30-32].

1.3.4 Role of ATP in host defense against TB

Macrophages, after engulfing pathogens, acidify the phagosomal lumen by recruiting vacuolar H^+-ATPase (V-ATPase), a multi-subunit protein-pump complex that actively transports protons across membranes using energy from ATP hydrolysis and is structurally similar to ATP synthase. This acidification not only inhibits the bacterial growth but also regulates the lysosomal fusion through macrophage class C vacuolar protein sorting (C VPS) complex, a key regulator of endosomal membrane fusion. However, *Mtb* inhibits phagosome acidification and maturation by secreting protein tyrosine phosphatase (PtpA) which binds to subunit H of V-ATPase; and subsequently stops lysosome fusion by inhibiting C VPS complex through dephosphorylation of VPS33B, a member of the class C VPS complex and a cognate substrate of PtpA [33]. A study showed that addition 3 mM ATP can induce rapid autophagy (30 minutes of post-treatment) of *Mtb*-infected macrophages, which was accompanied by rapid phagolysosomal

fusion and loss of mycobacterial viability within infected cells [34, 35]. Therefore, it can be surmised that inhibition of V-ATPase is the rate-limiting step of the *Mtb*-induced phagocytic modulation. However, it is not yet known if INH has any role in V-ATPase activity or in ATP biogenesis.

1.4 ENZYMES RELATED TO INH METABOLISM

1.4.1 Preamble

As INH is a pro-drug; the activation of INH (formation of isonicotinyl free radical, $INH^{\bullet}$) requires a one electron enzymatic oxidation step. In the mode of action section, it has already been mentioned that bacterial catalase-peroxidase enzyme, KatG, possesses such capacity. However, there are a number of functionally similar enzymes in the host system. Myeloperoxidase (MPO) is one of them. These two enzymes are described here in detail due to their importance in this study.

1.4.2 KatG

KatG, a multifunctional heme-protein, belongs to a catalase-peroxidase group of enzymes. It is the major bacterial machinery which detoxifies antibacterial reactive oxygen species (e.g., $O_2^{-\bullet}$) and acidic compounds (e.g., HOCl) generated by host phagocytic cells and ensures the survival of *Mtb* [36]. KatG is also well-known for its critical role in INH metabolism, activation, and antibacterial INH-NAD^+ adduct formation. Beside its catalase-peroxidase activity, KatG also shows Mn(II)-dependent peroxidase activity, peroxynitrite activity (decomposition of ONOOH moiety), and participates in bacterial DNA repair [37].

Figure - 10: The crystal structure of KatG (taken from PDB 3VLM).

As per recent developments on the KatG-structure, it is a homodimer (consists of identical two subunits, 82-kDa each) with one haem per subunit. The N-terminal domain of each subunit possesses both the catalase and peroxidase activities and the C-terminal domain is necessary for the overall functional capability of KatG [37]. The activated KatG forms compound-I (an unstable but catalytically competent oxyferryl iron-protoporphyrin IX:π-cation radical intermediate) which can metabolize INH into $INH^{\bullet}$ [38]. The most common INH-resistant *Mtb* phenotype has been identified as a Ser-315 mutation in KatG. A study showed that this mutation did not reduce the enzymatic activity; however, it interfered with the INH binding site which causes less INH activation and INH-resistance [39].

1.4.3 Myeloperoxidase (MPO)

Myeloperoxidase (MPO), a member of the haem peroxidase-cyclooxygenase superfamily, is the major component of the azurophilic granules of neutrophils; it is also found to a lesser extent in the lysosome of monocytes and certain types of macrophages [40]. The 150-kDa MPO is a cationic homodimer bound to a prosthetic heme group. Each dimer consists of a heavy chain and a light chain. The light chains are glycosylated and possess the active site, modified iron protoporphyrin IX ring. The dimers are connected to each other through a cysteine bridge at

Cys153. It also contains a calcium-binding site [41, 42]. In the comparison between MPO and KatG for peroxidase activity, MPO possesses approximately 10^4 times stronger peroxidase activity than KatG [43]. However, it is unknown if MPO has any role in INH-NAD^+ adduct formation, which formed the basis for one of the chapters of this thesis.

1.5 FREE RADICAL DETECTION METHODS

1.5.1 Electron Paramagnetic Resonance (EPR)

The involvement of a free radical (an atom, molecule or compound containing an unpaired electron) in biochemical reactions is a well-known phenomenon. To detect free radicals, the electron paramagnetic resonance (EPR) technology was developed. The principle of EPR relies on the fact that in the presence of the (external) magnetic field, an (unpaired) electron acts as a tiny bar magnet which can spin around its axis. This is known as the paramagnetic behavior of an electron and is named as a paramagnet. It will align itself with the direction of the applied external field in one of two orientations: align with external magnetic field, known as parallel orientation (Ms = - ½); or oppositely align, known as anti-parallel orientation (Ms = ½). The anti-parallel spin orientation possesses higher energy state whereas parallel state possesses lower energy level (http://www.chemistry.jhu.edu/NMR/WhatsEPR.pdf). A molecule with one unpaired electron in an external magnetic field, the energy states of the electron can be defined as~

$$E = g\mu_B B_0 M_s$$

$$E = \pm 1/2 g\mu_B B_0$$

Where E is the energy state, g is the proportionality factor, μ_B is the Bohr magneton, B_0 is the static magnetic field, M_s is the spin orientation (± ½). Here g is not a constant; it varies with the nature of the microenvironment of the electron. Usually for an organic paramagnetic compound, g is 2.0023 whereas g for a metallic paramagnetic compound is 1.4.

The unpaired paramagnetic electron initially remains at the lower energy level (parallel orientation). It can jump from lower energy level to another energy level while another weaker alternative magnetic field is applied to it from its right angles, and only if the microwave frequency is equal to the precession frequency of the external magnetic field. This transition of a unpaired paramagnetic electron from lower energy state to higher energy state is known as "resonance" which is recorded in EPR spectrometer as signals (http://www.uottawa.ca/publications/interscientia/inter.2/spin.html).

1.5.2 Hyperfine splitting

In typical chemical bonds, electrons remain in a pair. Hence, these bonds containing compounds are not paramagnetic compounds as well as not giving EPR signals. An only unpaired electron can act as paramagnetic. Hence, an unpaired electron-containing compound is a paramagnetic compound which can be analyzed through EPR. An EPR signal sometimes contains several lines. These are hyperfine splitting or coupling structure arising from the electrons interacting with nucleus spins. The hyperfine interactions give following information: (1) the number and identity of atoms in a molecule or compound, and (2) distance from the unpaired electron. The number of peaks in an EPR spectrum resulting from hyperfine splitting of radicals can be predicted from the following equation:

$$\text{Number of peaks in the EPR spectrum} = 2NI + 1$$

Where I is the spin number, and N is the number of equivalent nuclei. There is a number of rules to determine I (http://chemwiki.ucdavis.edu/). These are:

(A) If both the atomic number and the mass number of nuclei are even, the spin number will be zero (I = 0).

(B) If the atomic number of nuclei is odd but the mass number is even; the spin number will be 1 (I = 1).

(C) If both the atomic number and the mass number of nuclei are odd, the spin number will be ½ (I = ½).

For an example, the EPR spectrum of •CH-CH_2 will be 6 in total in 3:3 pattern. The calculation has been shown below:

CH = 2.NI + 1 = (2 x 1 x 1/2) + 1 = 2

CH_2 = 2NI + 1 = (2 x 2 x 1/2) + 1 = 3

So, •CH-CH_2 = 2 x 3 = 6; and they will show up as 3: 3 pattern (http://chemwiki.ucdavis.edu/).

1.5.3 Spin trapping

For direct EPR, the prerequisites are: (1) radical must be stable or, at least, metastable; and (2) radical cannot be diatomic. The direct detection of the free radicals in such system is a challenge due to its very low concentration, instability, and high reactivity. To overcome these problems and acquire the suitable platform for EPR, spin-trapping was introduced. The spin traps which are diamagnetic molecules can react with unstable free radicals to form relatively stable free radicals. They are not only used in EPR technique to identify free radicals but also can be

deployed in immune blot which is known as immuno-spin trapping [44]. There are two major classes of spin traps: (A) nitrones, and (B) nitroso compounds [45].

The nitrones are N-oxides of an imine. Since the simplest form of the nitrone is very unstable and forms polymers, the structural modification was required to overcome these problems. Nowadays, a number of stable nitrones are commercially available. They are free from all above mentioned problems. Among them, DMPO (5,5-dimethyl-1-pyrroline N-oxide) and PBN (phenyl-N-butyl nitrone) are the most popular. They are quite stable and are not particularly toxic. Hence, it can be used in a biological system without exerting any toxic effect. However, DMPO adducts are convertible from superoxide radical trapped adduct (DMPO/•OOH) to hydroxyl radical trapped adduct (DMPO/•OH). They are also subjected to rare nucleophilic addition across their double bonds. In addition, there is a chance of hydroxylamine silent EPR signal due to oxidation. On the other hands, nitroso compounds can trap free radical to its nitrogen atom of a C-nitroso compound. MNP (2-methyl-2-nitrosopropane) is the most popular nitroso spin trap. Due to acutely toxic nature, it cannot be used *in vivo*, and is problematic in cells. In addition, high reactivity nature makes it so prone to give false nitroxide signals [45].

1.6 HL-60 CELLS AND NEUTROPHILS

The human promyelocytic leukemia (HL-60) cell line which is a model cell for granulocyte-monocyte (GM) progeny stem cell is inducible for differentiation into various myeloid immune cells, e.g., granulocytes, monocytes [46-48]. Additionally, HL-60 cells have abundant amounts of the catalase-peroxidase enzyme, myeloperoxidase (MPO). In the presence of H_2O_2, MPO catalyzes the production of hypochlorous acid, a strong oxidant, through the chlorination cycle. It also can oxidize a number of endogenous substrates and several drugs to form various reactive

species through peroxidation cycle. In general, these species result in oxidative stress which can induce different types of cell death (apoptosis/necrosis) depending on their concentration and mechanism of cell damage [49-52]. The higher concentration of reactive species leading to oxidative stress is associated with necrotic cell death due to excessive mitochondrial damage, whereas moderate concentrations of reactive species can cause moderate mitochondrial damage and apoptotic cell death [52]. Although HL-60 cells can be differentiated into two major types of immune cells such as monocytes and neutrophils, neutrophil is considered as the prominent type. Neutrophils, which are the most abundant type of phagocyte in blood, constitute 50% to 60% of the total circulating white blood cells. This short-lived (approximately 5 days) immune cell has a multi-lobed nucleus and two types of granules based on the presence of MPO. The primary azophilic granule which consists of MPO, elastase, and defensins, is acidic in nature. The secondary granule does not have MPO. After engulfing pathogens, neutrophils form a phagosome where azophilic granules release their contents and participate in phagocytosis [53].

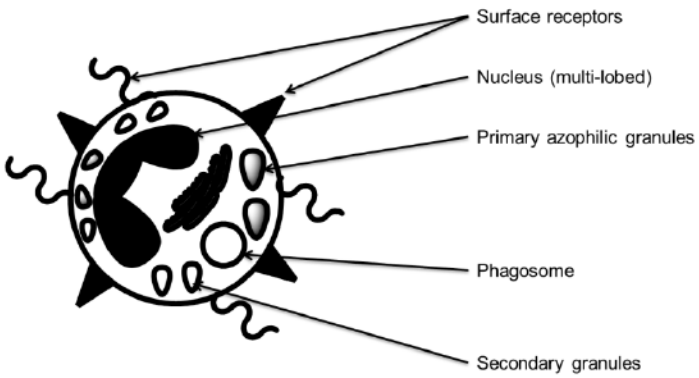

Figure 11: The morphology of a typical neutrophil.

1.7 RATIONALE AND HYPOTHESES

Isoniazid (INH) is still the mainstay treatment of both active and latent tuberculosis (TB) **[10, 54]**. In early 21st century, the molecular mechanism of INH antibacterial activity was proposed to involve enzymatic oxidation of INH by bacterial catalase-peroxidase KatG to form isonicotinoyl radical which in turn forms a key chemical adduct (INH-NAD^+ adduct) with nicotinamide adenine dinucleotide. This adduct is a potent inhibitor of enoyl acyl-carrier-protein reductase, an essential enzyme for mycolic acid biosynthesis of *Mtb* cell wall, which causes bacterial killing **[6]**. In drug-resistant TB, mutations in KatG were confirmed with lower INH-NAD^+ adduct formation as well as the lower antibacterial activity of INH **[8]**; this scenario is resulted in the removal of INH from clinical therapy. The host neutrophil possesses myeloperoxidase (MPO), a human catalase-peroxidase enzyme, which has higher peroxidase activity than KatG **[55].** It suggests that neutrophil may play a prominent role in the mode of action of INH. However, it is yet to be established that INH-NAD^+ adduct formation occurs in TB patients and healthy volunteers even after extensive EPR (electron paramagnetic resonance) studies and metabolomics studies **[56, 57]**. In this study, the role of neutrophil MPO as an alternative site for the formation of INH-NAD^+ adduct was aimed to be evaluated. Therefore**,** it has been hypothesized here that ***metabolism of INH by neutrophil MPO can produce INH-NAD^+ adducts (Hypothesis 1).***

From extensive studies on TB pathophysiology, it is known that virulent *Mtb* strains induce necrosis in infected phagocytic cells via mitochondrial inner membrane disruption [58]. Reactive species (RS) are one of the main causes of such mitochondrial damage [59]. In the case of *Mtb* infection, host phagocytic cells induce the formation of RS to kill bacteria; however *Mtb* has extraordinary strategies to defend itself against such killing, especially against reactive oxygen

species (ROS) [60]. Therefore, the induction of ROS by phagocytic cells cannot kill bacteria; however it causes their self-destruction through necrosis. To combat *Mtb*, phagocytic cells first have to survive against self-destruction through oxidative stress-induced necrosis (oxidative necrosis). The effect of INH against oxidative necrosis has never been investigated. However, the limitations of the proposed mode of action of INH (described in the section 1.1.5) suggest that INH may have other pharmacological action(s). If INH is cytoprotective against oxidative necrosis, this novel phenomenon can justify its effectiveness against TB by overcoming some limitations of its aforementioned proposed antibacterial mechanism. Therefore, ***we hypothesize that INH increases oxidative stress tolerance of immune cells (Hypothesis 2).***

For pathogen killing during phagocytosis, macrophages mainly rely on their reactive nitrogen species (RNS) production whereas neutrophils rely on their reactive oxygen species (ROS) production. Each type of phagocytic cell usually can produce nanomolar (nM) to micromolar (μM) amounts of their respective reactive species (RNS/ROS). However, *Mtb* possesses a very high tolerance for ROS (up to 50 mM H_2O_2 [61]) whereas tolerance against RNS is relatively lower (few nM to 5 mM of reactive nitrogen species is bacteriostatic; above 5 mM of that is bactericidal [61]). Additionally, few macrophages can merge together to form giant cells within the granuloma [62]. The formation of the giant cell ceases its microbial uptake function but strengthens its antigen presentation property (similar to dendritic cells). It is necessary to activate T-cells which can reactivate the inactivated macrophages within the granuloma [62]. All of above reasons indicate why the macrophage is the main host immune defense against TB. For more macrophages to combat *Mtb* successfully, more monocytes are required to be recruited from the circulation, which necessitates more monocytic differentiation from granulocyte-monocyte (GM) progeny stem cells. One study revealed that niacin

(structurally similar to INH) can induce granulocytic differentiation of HL-60 cells (human promyelocytic leukemia cell line which can be differentiated like GM progeny stem cells) [63]; and another study in HL-60 cells showed that isonicotinic acid (a metabolite of INH) can induce expression of CD38, a surface marker of resting monocytes [64]. However, there is no extensive study on INH-induced differentiation. Additionally, if INH induces monocytic differentiation, this novel phenomenon of INH can further justify its effectiveness in anti-TB therapy by overcoming some other limitations of proposed antibacterial mechanism of INH. **Therefore, *we hypothesize that INH induces monocytic differentiation of HL-60 cells (Hypothesis 3).***

1.8 HYPOTHESES AND OBJECTIVES

1.8.1 Hypothesis 1: Metabolism of INH neutrophil MPO can produce INH-NAD$^+$ adduct.

Specific objectives:

1) To evaluate the free radical generation in INH metabolism by both MPO and human neutrophils through EPR spectroscopy.
2) To identify the INH-NAD$^+$ adduct in INH metabolism by MPO through both UV-spectroscopy and LC-MS.
3) To identify the biochemical nature of INH that makes it different from other human metabolites.
4) To compare NAD$^+$ with its different components and reduced form (NADH) for INH-NAD$^+$ adduct formation.

1.8.2 Hypothesis 2: INH increases oxidative stress tolerance of immune cells.

Specific objectives:

1) To determine the effect of INH in human promyelocytic leukemia (HL-60) cell line challenged by oxidative stress.
2) To determine the morphological type of cell death/cytoprotection for objective 1.
3) To determine the effect of INH on oxidative stress-induced mitochondrial damage.
4) To determine the global proteomic changes for objective 1.
5) To determine the role of INH-protein adducts for objective 1.
6) To determine the role of MPO for objective 1.

1.8.3 Hypothesis 3: INH induces monocytic differentiation of HL-60 cells.

Specific objectives:

1) To determine the global proteomic changes in INH-treated HL-60 cells.
2) To identify the involved signaling pathways in objective 1.
3) To determine whether INH has the ability to induce differentiation.
4) To identify the type of differentiation.

REFERENCES

[1] Peloquin CA, Namdar R, Dodge AA, Nix DE. Pharmacokinetics of isoniazid under fasting conditions, with food, and with antacids. Int J Tuberc Lung D. 1999;3:703-10.

[2] Middlebrook G. Sterilization of Tubercle Bacilli by Isonicotinic Acid Hydrazide and the Incidence of Variants Resistant to the Drug Invitro. Am Rev Tuberc Pulm. 1952;65:765-7.

[3] Middlebrook G. Isoniazid-Resistance and Catalase Activity of Tubercle Bacilli - a Preliminary Report. Am Rev Tuberc Pulm. 1954;69:471-2.

[4] Brennan PJ, Nikaido H. The Envelope of Mycobacteria. Annual Review of Biochemistry. 1995;64:29-63.

[5] Rozwarski DA, Grant GA, Barton DHR, Jacobs WR, Sacchettini JC. Modification of the NADH of the Isoniazid Target (InhA) from Mycobacterium tuberculosis. Science. 1998;279:98-102.

[6] Timmins GS, Deretic V. Mechanisms of action of isoniazid. Molecular microbiology. 2006;62:1220-7.

[7] Miesel L, Rozwarski DA, Sacchettini JC, Jacobs WR, Jr. Mechanisms for isoniazid action and resistance. Novartis Foundation symposium. 1998;217:209-20; discussion 20-1.

[8] Ando H, Kondo Y, Suetake T, Toyota E, Kato S, Mori T, et al. Identification of katG Mutations Associated with High-Level Isoniazid Resistance in Mycobacterium tuberculosis. Antimicrobial agents and chemotherapy. 2010;54:1793-9.

[9] Kjellsson MC, Via LE, Goh A, Weiner D, Low KM, Kern S, et al. Pharmacokinetic Evaluation of the Penetration of Antituberculosis Agents in Rabbit Pulmonary Lesions. Antimicrobial agents and chemotherapy. 2012;56:446-57.

[10] Sia IG, Wieland ML. Current concepts in the management of tuberculosis. Mayo Clinic proceedings. 2011;86:348-61.

[11] Ehlers S, Schaible UE. The Granuloma in Tuberculosis: Dynamics of a Host–Pathogen Collusion. Frontiers in Immunology. 2012;3:411.

[12] Velayati AA, Abeel T, Shea T, Konstantinovich Zhavnerko G, Birren B, Cassell GH, et al. Populations of latent Mycobacterium tuberculosis lack a cell wall: Isolation, visualization, and whole-genome characterization. International Journal of Mycobacteriology.

[13] Timmins GS, Master S, Rusnak F, Deretic V. Nitric Oxide Generated from Isoniazid Activation by KatG: Source of Nitric Oxide and Activity against Mycobacterium tuberculosis. Antimicrobial agents and chemotherapy. 2004;48:3006-9.

[14] Timmins GS, Master S, Rusnak F, Deretic V. Requirements for Nitric Oxide Generation from Isoniazid Activation In Vitro and Inhibition of Mycobacterial Respiration In Vivo. Journal of Bacteriology. 2004;186:5427-31.

[15] Rickman KA, Swancutt KL, Mezyk SP, Kiddle JJ. Isoniazid: Radical-induced oxidation and reduction chemistry. Bioorganic & Medicinal Chemistry Letters. 2013;23:3096-100.

[16] Fukino K, Sasaki Y, Hirai S, Nakamura T, Hashimoto M, Yamagishi F, et al. Effects of N-acetyltransferase 2 (NAT2), CYP2E1 and Glutathione-S-transferase (GST) genotypes on the serum concentrations of isoniazid and metabolites in tuberculosis patients. The Journal of toxicological sciences. 2008;33:187-95.

[17] Yue J, Peng R. Does CYP2E1 play a major role in the aggravation of isoniazid toxicity by rifampicin in human hepatocytes? British journal of pharmacology. 2009;157:331-3.

[18] Raquel Lima de Figueiredo Teixeira, Márcia Quinhones Pires Lopes, Suffys PN, Santos AR. Tuberculosis Pharmacogenetics: State of The Art: InTech; 2013.

[19] Pirmohamed M. Pharmacogenetics: past, present and future. Drug Discovery Today. 2011;16:852-61.

[20] Gomez i Prat J, de Souza SM. Prehistoric tuberculosis in america: adding comments to a literature review. Memorias do Instituto Oswaldo Cruz. 2003;98 Suppl 1:151-9.

[21] Bos KI, Harkins KM, Herbig A, Coscolla M, Weber N, Comas I, et al. Pre-Columbian mycobacterial genomes reveal seals as a source of New World human tuberculosis. Nature. 2014;514:494-7.

[22] Wolfe LM, Mahaffey SB, Kruh NA, Dobos KM. Proteomic Definition of the Cell Wall of Mycobacterium tuberculosis. Journal of Proteome Research. 2010;9:5816-26.

[23] Brennan PJ. Structure, function, and biogenesis of the cell wall of Mycobacterium tuberculosis. Tuberculosis (Edinb). 2003;83:91-7.

[24] Velayati AA, Abeel T, Shea T, Konstantinovich Zhavnerko G, Birren B, Cassell GH, et al. Populations of latent Mycobacterium tuberculosis lack a cell wall: Isolation, visualization, and whole-genome characterization. International Journal of Mycobacteriology. 2016;5:66-73.

[25] Guirado E, Schlesinger LS. Modeling the Mycobacterium tuberculosis Granuloma - the Critical Battlefield in Host Immunity and Disease. Front Immunol. 2013;4:98.

[26] Sakamoto K. The Pathology of Mycobacterium tuberculosis Infection. Veterinary Pathology. 2012;49:423-39.

[27] Balasubramanian V, Wiegeshaus EH, Taylor BT, Smith DW. Pathogenesis of tuberculosis: pathway to apical localization. Tubercle and Lung Disease. 1994;75:168-78.

[28] Smith I. Mycobacterium tuberculosis Pathogenesis and Molecular Determinants of Virulence. Clin Microbiol Rev. 2003;16:463-96.

[29] Ernst JD. Macrophage receptors for Mycobacterium tuberculosis. Infect Immun. 1998;66:1277-81.

[30] Hestvik AL, Hmama Z, Av-Gay Y. Mycobacterial manipulation of the host cell. FEMS microbiology reviews. 2005;29:1041-50.

[31] Wong D, Bach H, Sun J, Hmama Z, Av-Gay Y. *Mycobacterium tuberculosis* protein tyrosine phosphatase (PtpA) excludes host vacuolar-H^+–ATPase to inhibit phagosome acidification. Proceedings of the National Academy of Sciences. 2011;108:19371-6.

[32] Sun J, Singh V, Lau A, Stokes RW, Obregon-Henao A, Orme IM, et al. *Mycobacterium tuberculosis* nucleoside diphosphate kinase inactivates small GTPases leading to evasion of innate immunity. PLoS Pathog. 2013;9:e1003499.

[33] Wong D, Bach H, Sun J, Hmama Z, Av-Gay Y. *Mycobacterium tuberculosis* protein tyrosine phosphatase (PtpA) excludes host vacuolar-H^+-ATPase to inhibit phagosome acidification. Proceedings of the National Academy of Sciences of the United States of America. 2011;108:19371-6.

[34] Lammas DA, Stober C, Harvey CJ, Kendrick N, Panchalingam S, Kumararatne DS. ATP-induced killing of mycobacteria by human macrophages is mediated by purinergic P2Z(P2X7) receptors. Immunity. 1997;7:433-44.

[35] Fairbairn IP, Stober CB, Kumararatne DS, Lammas DA. ATP-Mediated Killing of Intracellular Mycobacteria by Macrophages Is a P2X7-Dependent Process Inducing Bacterial Death by Phagosome-Lysosome Fusion. The Journal of Immunology. 2001;167:3300-7.

[36] Manca C, Paul S, Barry CE, 3rd, Freedman VH, Kaplan G. *Mycobacterium tuberculosis* catalase and peroxidase activities and resistance to oxidative killing in human monocytes in vitro. Infection and immunity. 1999;67:74-9.

[37] DeVito JA, Morris S. Exploring the Structure and Function of the Mycobacterial KatG Protein Using trans-Dominant Mutants. Antimicrobial agents and chemotherapy. 2003;47:188-95.

[38] Chouchane S, Lippai I, Magliozzo RS. Catalase-Peroxidase (*Mycobacterium tuberculosis* KatG) Catalysis and Isoniazid Activation†. Biochemistry. 2000;39:9975-83.

[39] Yu S, Girotto S, Lee C, Magliozzo RS. Reduced affinity for isoniazid in the S315T mutant of *Mycobacterium tuberculosis* KatG is a key factor in antibiotic resistance. Journal of Biological Chemistry. 2003;278:14769-75.

[40] Tavora FR, Ripple M, Li L, Burke AP. Monocytes and neutrophils expressing myeloperoxidase occur in fibrous caps and thrombi in unstable coronary plaques. BMC Cardiovascular Disorders. 2009;9:27.

[41] Mathy-Hartert M, Bourgeois E, Grülke S, Deby-Dupont G, Caudron I, Deby C, et al. Purification of myeloperoxidase from equine polymorphonuclear leucocytes. Canadian Journal of Veterinary Research. 1998;62:127-32.

[42] Davies MJ. Myeloperoxidase-derived oxidation: mechanisms of biological damage and its prevention. Journal of Clinical Biochemistry and Nutrition. 2011;48:8-19.

[43] Khan SR, Morgan AGM, Michail K, Srivastava N, Whital RM, Aljuhani N, et al. Metabolism of Isoniazid by Neutrophil Myeloperoxidase Leads to INH-NAD^+ Adduct Formation: A Comparison of the Reactivity of Isoniazid with its Known Human Metabolites. Biochemical Pharmacology. 2016; 106: 46-55.

[44] Ramirez DC, Mason RP. Immuno-spin trapping: detection of protein-centered radicals. Current protocols in toxicology / editorial board, Mahin D Maines. 2005;Chapter 17:Unit 17 7.

[45] Janzen EG, Stronks HJ, Dubose CM, Poyer JL, McCay PB. Chemistry and biology of spin-trapping radicals associated with halocarbon metabolism *in vitro* and *in vivo*. Environmental Health Perspectives. 1985;64:151-70.

[46] Martin SJ, Bradley JG, Cotter TG. HL-60 cells induced to differentiate towards neutrophils subsequently die via apoptosis. Clinical and Experimental Immunology. 1990;79:448-53.

[47] Li D, Wang Z, Chen H, Wang J, Zheng Q, Shang J, et al. Isoliquiritigenin induces monocytic differentiation of HL-60 cells. Free Radical Biology and Medicine. 2009;46:731-6.

[48] Rebel VI, Ossenkoppele GJ, van de Loosdrecht AA, Wijermans PW, Beelen RHJ, Langenhuijsen MMAC. Monocytic differentiation induction of HL-60 cells by MC 903, a novel vitamin D analogue. Leukemia Research.16:443-51.

[49] Jiang XH, Wong BC, Yuen ST, Jiang SH, Cho CH, Lai KC, et al. Arsenic trioxide induces apoptosis in human gastric cancer cells through up-regulation of p53 and activation of caspase-3. Int J Cancer. 2001;91.

[50] Deguchi J, Horiguchi K, Wong CP, Hosoya T, Iihoshi A, Kaneda T, et al. Sucutinirane-diterpene derivatives induce apoptosis via oxidative stress in HL-60 cells. Journal of Natural Medicines. 2014;68:723-9.

[51] Plantin-Carrenard E, Bernard M, Derappe C, Bringuier A, Vadrot N, Feldmann G, et al. Differential responses of proliferative and non-proliferative leukemia cells to oxidative stress. Free radical research. 2005;39:1-13.

[52] Dickancaite E, Cenas N, Kalvelyte A, Serapiniene N. Toxicity of daunorubicin and naphthoquinones to HL-60 cells: an involvement of oxidative stress. Biochemistry and molecular biology international. 1997;41:987-94.

[53] Cieutat A-M, Lobel P, August JT, Kjeldsen L, Sengeløv H, Borregaard N, et al. Azurophilic Granules of Human Neutrophilic Leukocytes Are Deficient in Lysosome-Associated Membrane Proteins but Retain the Mannose 6-Phosphate Recognition Marker. Blood. 1998;91:1044-58.

[54] Gafter AKaU. Tuberculosis prophylaxis for the chronically dialysed patient--yes or no? . Nephrology Dialysis Transplantation. 1999;14: 2857-9.

[55] Jakopitsch C, Wanasinghe A, Jantschko W, Furtmüller PG, Obinger C. Kinetics of Interconversion of Ferrous Enzymes, Compound II and Compound III, of Wild-type Synechocystis Catalase-peroxidase and Y249F: PROPOSAL FOR THE CATALATIC MECHANISM. Journal of Biological Chemistry. 2005;280:9037-42.

[56] Ranguelova K, Suarez J, Magliozzo RS, Mason RP. Spin trapping investigation of peroxide- and isoniazid-induced radicals in Mycobacterium tuberculosis catalase-peroxidase. Biochemistry. 2008;47:11377-85.

[57] Mahapatra S, Woolhiser LK, Lenaerts AJ, Johnson JL, Eisenach KD, Joloba ML, et al. A Novel Metabolite of Antituberculosis Therapy Demonstrates Host Activation of Isoniazid and Formation of the Isoniazid-NAD+ Adduct. Antimicrobial agents and chemotherapy. 2012;56:28-35.

[58] Chen M, Gan H, Remold HG. A Mechanism of Virulence: Virulent Mycobacterium tuberculosis Strain H37Rv, but Not Attenuated H37Ra, Causes Significant Mitochondrial Inner Membrane Disruption in Macrophages Leading to Necrosis. The Journal of Immunology. 2006;176:3707-16.

[59] Belhadj Slimen I, Najar T, Ghram A, Dabbebi H, Ben Mrad M, Abdrabbah M. Reactive oxygen species, heat stress and oxidative-induced mitochondrial damage. A review. International Journal of Hyperthermia. 2014;30:513-23.

[60] Ehrt S, Schnappinger D. Mycobacterial survival strategies in the phagosome: Defense against host stresses. Cellular microbiology. 2009;11:1170-8.

[61] Voskuil MI, Bartek I, Visconti K, Schoolnik GK. The response of Mycobacterium tuberculosis to reactive oxygen and nitrogen species. Frontiers in Microbiology. 2011;2.

[62] Lay G, Poquet Y, Salek-Peyron P, Puissegur MP, Botanch C, Bon H, et al. Langhans giant cells from M. tuberculosis-induced human granulomas cannot mediate mycobacterial uptake. The Journal of pathology. 2007;211:76-85.

[63] Iwata K, Ogata S, Okumura K, Taguchi H. Induction of differentiation in human promyelocytic leukemia HL-60 cell line by niacin-related compounds. Bioscience, biotechnology, and biochemistry. 2003;67:1132-5.

[64] Ida C, Ogata S, Okumura K, Taguchi H. Changes in the Gene Expression of C-myc and CD38 in HL-60 Cells during Differentiation Induced by Nicotinic Acid-Related Compounds. Bioscience, Biotechnology, and Biochemistry. 2008;72:868-71.

CHAPTER 2:

METABOLISM OF ISONIAZID BY NEUTROPHIL MYELOPEROXIDASE CAN PRODUCE AN INH-NAD$^+$ ADDUCT

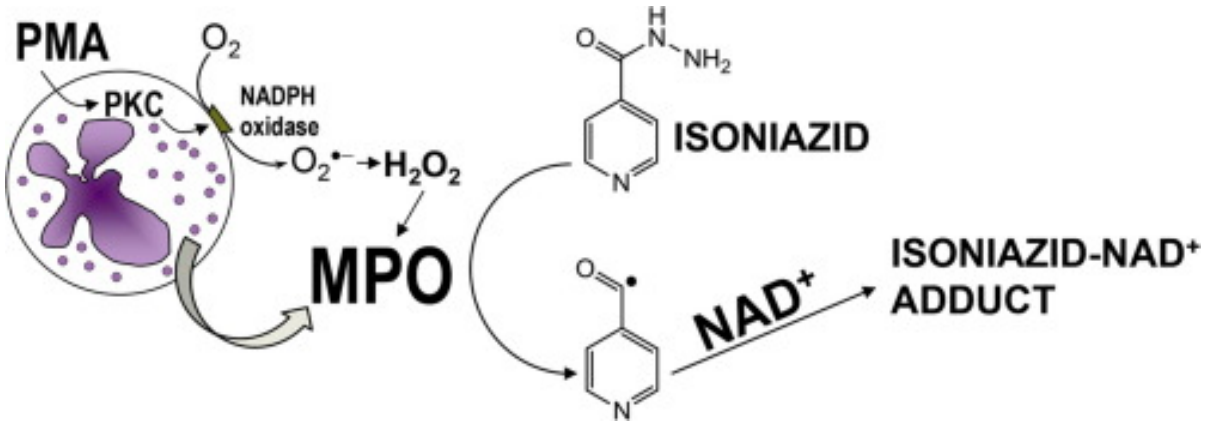

[This work has already been published as *Saifur R. Khan et.al., Metabolism of Isoniazid by Neutrophil Myeloperoxidase Leads to INH-NAD$^{\pm}$ Adduct Formation: A Comparison of the Reactivity of Isoniazid with its Known Human Metabolites*, Biochemical Pharmacology, http://dx.doi.org/10.1016/j.bcp.2016.02.003.]

2.1 ABSTRACT

The formation of isonicotinyl-nicotinamide adenine dinucleotide (INH-NAD^+) via the mycobacterial catalase-peroxidase enzyme, KatG, has been described as the major component of the mode of action of isoniazid (INH). However, there are numerous of human peroxidases that may catalyze this reaction. The role of neutrophil myeloperoxidase (MPO) in INH-NAD^+ adduct formation has never been explored; this is important, as neutrophils are recruited at the site of tuberculosis infection (granuloma) through infected macrophages' cell death signals. In our studies, we showed that neutrophil MPO is capable of INH metabolism using electron paramagnetic resonance (EPR) spin-trapping and UV-Vis spectroscopy. MPO or activated human neutrophils (by phorbol myristate acetate) catalyzed the oxidation of INH and formed several free radical intermediates; the inclusion of superoxide dismutase revealed a carbon-centered radical which is considered to be the reactive metabolite that binds with NAD^+. Other human metabolites, including N-acetyl-INH, N-acetylhydrazine, and hydrazine did not show the formation of carbon-centered radicals, and either produced no detectable free radicals, N-centered free radicals, or superoxide, respectively. A comparison of these free radical products indicated that only the carbon-centered radical from INH is reducing in nature, based on UV-Vis measurement of nitroblue tetrazolium reduction. Furthermore, only INH oxidation by MPO led to a new product (λ_{max} = 326 nm) in the presence of NAD^+. This adduct was confirmed to be isonicotinyl-NAD^+ using LC-MS analysis where the intact adduct was detected (m/z = 769). The findings of this study suggest that neutrophil MPO may also play a role in INH pharmacological activity.

Keywords: Isoniazid, myeloperoxidase, neutrophil, INH-NAD^+, free radicals

2.2 INTRODUCTION

Although isoniazid (INH) was introduced into tuberculosis (TB) therapy in 1952, its mode of action still remains elusive. It is generally accepted that INH is a prodrug and is oxidized to the isonicotinyl radical ($INH^{\bullet}$) through peroxidation by the bacterial catalase-peroxidase, KatG; $INH^{\bullet}$ then reacts with the oxidized form of nicotinamide adenine dinucleotide (NAD^{+}) producing the INH-NAD^{+} adduct. This adduct inhibits mycolic acid biosynthesis of *Mycobacterium tuberculosis* (*Mtb*) cell wall by blocking an essential enzyme named enoyl acyl-carrier-protein reductase [1, 2]. A number of limitations such as effectiveness of INH in latency (where *Mtb* does not possess typical cell wall), low penetration of INH into granuloma (where *Mtb* resides) and exceptionally long treatment duration as an antibiotic (as opposed to *in vitro* experiments) have been identified [3-5], which suggests that there are other additional mechanism(s) of action of INH.

Two studies reported that INH at suprapharmacological concentrations (35 mM) produces nitric oxide (NO) through the peroxidation cycle of KatG, which in turn is proposed to kill *Mtb* [6, 7]. The oxidation of the hydrazide nitrogen atom proximal to the carbonyl of INH was proposed as the primary site of oxidation in this study, which is decomposed to NO and $INH^{\bullet}$. Recently a study on the temperature-dependent rate constants for the hydroxyl radical oxidation and solvated electron reduction of INH revealed that the initial oxidation of INH by hydroxyl radical is the distal nitrogen of hydrazyl moiety. Therefore, the decomposition product is not expected to be NO, but rather would be diazene (HN=NH) and $INH^{\bullet}$ [8]. This study contradicted the report of NO generation, which has not been reported elsewhere. However, $INH^{\bullet}$ was produced in both cases of nitrogen atom oxidation either that is proximal or distal to the carbonyl of INH. In addition, the role of oxidation in the formation of $INH^{\bullet}$ has not been

challenged, where the oxidation can be enzymatic (in both *in vivo* and *in vitro*) or non-enzymatic auto-oxidation (*in vitro*). Auto-oxidation for $INH^{\bullet}$ formation requires a longer time period has been reported in several studies [9, 10].

There are several enzymes which usually catalyze xenobiotic oxidation, including the cytochrome P-450 enzymes, and peroxidase enzymes such as neutrophil myeloperoxidase (MPO). Recently, an INH-$NADP^+$ adduct (m/z 851.0) was identified in human liver microsomes through LC-MS experiments in an *in vitro* study that concluded cytochrome P450 was involved [9]. MPO has been shown to oxidize/metabolize INH [11-13], however, there has been no report of a subsequent interaction with NAD^+ or $NADP^+$. MPO is a peroxidase enzyme which is most abundantly expressed in neutrophils has some resemblance to bacterial KatG in terms of activity. However, a comparison between KatG and the plant peroxidase horseradish peroxidase (HRP) showed that KatG had very poor peroxidase activity (5.1± 0.5 units/mg) compared to HRP (6405 ± 170 units/mg) [14]. In another study, the capacity of tyrosine nitration from nitrite was compared between MPO and HRP and it was found that the peroxidation capacity of MPO was, at least, ten times more than that of HRP [15]. Therefore, MPO possesses approximately 10^4 times stronger peroxidase activity than KatG. Due to the high peroxidase activity of MPO, it is likely that MPO could rapidly oxidize INH to $INH^{\bullet}$, which has been previously been reported by others [11, 16]. However, the role of MPO or neutrophils in generating INH-NAD^+ adducts has not been explored.

Recently, a metabolomics study found the INH-nicotinamide adduct in urine from both TB patients and healthy mice treated with INH; it was argued that INH-nicotinamide could be a break-down product of the INH-NAD^+ adduct, which indirectly suggests the existence of an INH-NAD^+ adduct *in vivo* [17]. Furthermore, this study suggested that INH can be activated by a

host peroxidase, for example, lactoperoxidase. The cause of poor effectiveness of INH in the case of KatG mutants of TB (even though host peroxidases can activate INH) has been explained due to the distal proximity of host INH activation, which leads to other reaction pathways. It causes the degradation and modification of INH-NAD^+ adduct *in vivo* [17]. On the other hand, neutrophils which have a prominent role in the early stage of granuloma formation and further recruited at the site of TB infection (granuloma) through cell death signals of infected macrophages [18-21] are unknown whether they are able to form INH-NAD^+ adduct upon INH metabolism. In this study, we hypothesized that neutrophil MPO is another site of INH metabolism, and can metabolize INH into $INH^{\bullet}$ and lead to INH-NAD^+ adduct formation. To test this hypothesis, INH and its main human metabolites, including N-acetylisoniazid (NAcINH), N-acetylhydrazine (NAcHZ) and hydrazine (HZ, Figure 1) were investigated for reactive species generation through MPO oxidation using both isolated MPO and activated neutrophils.

2.3 MATERIALS & METHODS

2.3.1 Chemicals and Kits

NAcINH was purchased from Toronto Research Chemicals, Inc. (Toronto, ON). Nicotinamide adenine dinucleotide free acid form (NAD^+) was procured from Santa Cruz biotechnology, Inc. (Dallas, TX). Human purified neutrophil MPO (180-220 units per mg lyophilized protein) was purchased from Athens Research & Technology (Athens, GA). 5,5-Dimethyl-1-pyrroline-N-oxide (DMPO), manufactured by Dojindo Molecular Technologies, Inc. was purchased from Cedarlane Laboratories Ltd (Burlington, ON). Chelex®-100 was purchased from Bio-Rad Laboratories (Mississauga, ON). Superoxide dismutase (SOD), glucose oxidase (GOx), nicotinamide, nicotinamide adenine dinucleotide reduced form (NADH), nitrotetrazolium blue chloride (NBT), hydrogen peroxide (H_2O_2), INH, NAcHZ, HZ, 4-aminobenzoic acid hydrazide

(ABAH) and all other chemicals (unless otherwise noted) were purchased from Sigma-Aldrich Canada Co. (Oakville, ON).

2.3.2 Electron paramagnetic resonance (EPR) spin trapping and characterization

The free radical species were detected by spin trapping, where the free radical species covalently bind to the nitrone spin trap (DMPO) to produce a relatively stable paramagnetic adduct. Reactions were prepared by adding a final concentration of 2 mM of each chemical (INH, NAcINH, NAcHZ, HZ) and 100 mM DMPO in a 200 µL volume of Chelex®-100-treated 0.1 M sodium phosphate buffer (pH 7.4) containing 100 µM DTPA to a micro test tube containing either 0.1 µM MPO, or 6 x 10^4 or 5 x 10^5 neutrophils (freshly isolated from human blood – see below). To initiate the reactions, 100 µM of H_2O_2 was used in reactions with MPO, whereas a 15-minute incubation with 0.8 µM of phorbol 12-myristate 13-acetate (PMA) was used for neutrophil activation. SOD (2.5 µM) was used to rapidly dismutate superoxide radical. 2 mM of NAD^+ was used in reactions to study trapping of free radicals from INH (and its metabolites). To ensure the role of MPO in neutrophil-derived reactions, 100 µM ABAH was used to inhibit MPO. However, it was not carried out in the case of purified MPO enzymatic system as there was nothing but MPO. Reactions were briefly vortexed prior to transferring to a Suprasil quartz ESR flat cell (Bruker Canada, Milton, ON) for spectrum recording. EPR spectra were obtained with a Bruker Elexsys E-500 spectrometer (Billerica, MA) equipped with an ER 4122 SHQ cavity operating at 9.78 GHz and 100 kHz modulation field at room temperature with the following parameters: power = 20 mW, scan rate = 0.47 G/s, modulation amplitude = 0.4 G, and receiver gain = 6.32× 10^5. Spectra were recorded as a single scan.

2.3.3 Relative oxidation and reduction of INH and its metabolites

To identify the redox properties of INH and its metabolites, we used several approaches. The reductive capacity of the metabolite(s) of each compound (INH, NAcINH, NAcHZ, and HZ) was studied through NBT reduction, where 1 mM of each chemical was incubated with 200 μM of NBT, 50 nM of MPO, and 50 μM of H_2O_2. The absorption of the reduced NBT (formazan) was measured at 520 nm. The oxidative capacity of the compounds (INH and its metabolites) were measured through NADH oxidation where 1 mM of each chemical was incubated with 200 μM of NADH, 50 nM of MPO, and 50 μM of H_2O_2. The absorbance was measured at 339 nm and all data were acquired by using a SpectraMax M5 microplate reader with cuvette port (Molecular Devices, Sunnyvale, CA). In all experiments, 0.1 M sodium phosphate buffer (pH 7.4) containing 100 μM DTPA were used.

2.3.4 UV-Vis analysis for covalent adduct formation and other interactions

To identify the possible interactions between INH and endogenous molecules, 500 μM of four different nucleotides (thymine, guanine, cytosine, and adenine) nucleotide were exposed to 500 μM of INH, 1 μM of MPO, 10 milliunits (mU) glucose oxidase (GOx) and 5 mM glucose for 30 mins and the UV-spectrum was analyzed. In addition, 500 μM of each chemical (INH, NAcINH, NAcHZ, and HZ) was exposed to 500 μM of nicotinamide, adenine, or NAD^+. The reaction was initiated by the addition of 1 μM of MPO, 10 mU GOx, and 5 mM glucose and run for 30 minutes to 1 h using UV-Vis kinetic spectroscopy to compare the changes in the spectrum. The absorbance at specific adduct peaks was also monitored. In all experiments, 0.1 M sodium phosphate buffer (pH 7.4) containing 100 μM DTPA were used.

2.3.5 Neutrophil (PMN) isolation from human blood

Human neutrophils were collected from healthy donors by consent granted from the Human Ethics Research Office of the University of Alberta by a methodology described elsewhere [22]. In brief, 6 mL of whole blood was layered on top of 6 mL Histopaque™1119 in 15 mL polystyrene centrifuge tubes and spin for 20 min at 800 × g with the centrifuge brake set to off (i.e., zero deceleration). It produced four distinct layers of the blood. The third pink-reddish layer was collected into 15 ml polystyrene centrifuge tubes. Cells were washed twice with 1× PBS through centrifugation at 300 × g for 10 min. 100% Percoll™ solution was prepared by mixing 18 mL Percoll™ with 2 mL 10× PBS. From 100% Percoll™ solution, 5 mL of 85%, 80%, 75%, 70% and 65% Percoll™ gradients were prepared by using 1× PBS. 2 mL of the resuspended cells were layered onto the each Percoll™ gradients followed by spin tubes at 800 × g for 20 min with the centrifuge brake set to off. After centrifugation, the interphases were visibly distinguishable due to the highest cell density. By removing top layers, white interphase that contains neutrophils was collected into a clean 15 mL polystyrene centrifuge tube. The separated neutrophils were further washed by filling up the tube with 1x PBS followed by spin at 300 × g for 10 min. The supernatant was discarded and the cell sediment was re-suspended in 2 ml of PBS. Cells were plated at the required density in PBS.

2.3.6 INH-NAD$^+$ extraction and LC-MS analysis

For INH-NAD$^+$ adduct identification, 500 µM of INH was exposed to 500 µM of NAD$^+$, 1 µM MPO, 5 mM glucose and 10 mU GOx in 0.1 M sodium phosphate buffer (pH 7.4) containing 100 µM DTPA for 1 h while the INH-NAD$^+$ adduct formation was monitored at 326 nm in UV-Vis kinetic spectroscopy. After 1 h, the reaction content was passed through an Oasis® HLB 1 cc extraction cartridge followed by washing with deionized water. The final eluent was extracted

using methanol. LC-MS was performed on an Agilent 1200 UHPLC with an Agilent 6130 single quadrupole mass spectrometer equipped with an electrospray source. Samples were injected onto a 2.1 × 50mm Agilent Zorbax SB-C18 column with 1.8 μm silica particles and separated using a water /acetonitrile gradient with 0.1% formic acid added as a solvent modifier at a flow rate of 0.5 mL/min. After holding at 1% acetonitrile for 0.5 min the gradient is ramped linearly to 60% acetonitrile in 5 min. Column eluent is first monitored by an Agilent G4212B diode array detector, monitoring the UV signal at 326 nm followed by the mass spectrometer giving a small delay between the UV and MS signals of 0.02 min. The mass spectrometer is run in both positive and negative ion modes, switching modes continuously between scans. Exact mass LC-MS was performed on an Agilent 6220 time-of-flight mass spectrometer equipped with an ESI source to provide compound formulae in positive ion mode.

2.3.7 MPO activity of neutrophils

The MPO activity of neutrophils was measured indirectly. Firstly a MPO activity calibration curve was constructed for different concentration (1, 2, 5,7 and 10 nM) of commercially available human purified neutrophil MPO through guaiacol oxidation assay [23]. In brief, 10 mM of guaiacol was exposed to different concentration of MPO, and all reactions were triggered by 100 μM of H_2O_2. The UV absorbance of the initial rate of guaiacol oxidation was measured at 470 nm followed by the linear calibration curve (R^2 = 0.95) was constructed. Afterward, neutrophils (5 x 10^5 cells) were lysed by three cycles of freezing and thawing followed by centrifuging at 4000 g for 5 min. The neutrophil lysate was incubated with 0.8 μM of PMA for 15 minutes (as same as EPR studies) and the rate of guaiacol oxidation was measured to estimate the MPO activity of neutrophils.

2.3.8 Statistical analysis

All experiments were carried out, at least, three times ($n \geq 3$) using freshly prepared reagents to ensure reproducibility of data.

2.4. RESULTS

2.4.1 EPR studies for INH in MPO system and neutrophils

Studies were first carried out using commercially purchased MPO. The latter in the presence of INH showed a relatively weak but discernable DMPO/$^{\bullet}$OH spectrum using EPR (Fig. 2A). In the presence of H_2O_2, which activates MPO, the DMPO/$^{\bullet}$OH signals were found to be intensified along with a mixture of DMPO/$^{\bullet}$OOH and possibly carbon-centered free radicals (Fig. 2B). With the addition of SOD, DMPO/$^{\bullet}$OOH signals were eliminated and DMPO/$^{\bullet}$OH signals were further intensified (Fig. 2C). Moreover, carbon-centered radical signals appeared more clearly (Fig. 2C). By the addition of NAD^+, the EPR spectrum showed a significant decline of DMPO/$^{\bullet}$OH and carbon-centered radicals (DMPO/$^{\bullet}$C), and reappearance of DMPO/$^{\bullet}$OOH (Fig. 2D).

In the case of activated (PMA-treated) neutrophils, EPR spectra showed a similar composite spectrum as seen with commercial MPO (Fig. 3A). SOD was added to eliminate spectra arising from the trapping of superoxide ($O_2^{\bullet-}$) which is expected in activated neutrophils. The EPR spectrum of activated neutrophils incubated with SOD demonstrated no significant spin adduct (only a trace of DMPO/$^{\bullet}$OH signals were observed) (Fig 3B), indicating that the spectra were attributed to oxygen activation, which is well known and shown previously by others [24]. The EPR spectrum arising from the addition of metabolite/drug (NAcINH, NAcHZ, HZ, and INH) to PMA-activated neutrophils was not shown because the PMA-generated superoxide overwhelmed any metabolite/drug spectrum. Upon addition of SOD, EPR spectra resulting from

metabolite/drug was discernable (Fig. 3 C-F). In the case of INH (Fig. 3 F), two signals remained: DMPO/$^{\bullet}$OH and DMPO/$^{\bullet}$C; these were similar to what was observed using MPO with SOD (Fig. 2C), albeit less intense (likely due to MPO concentration described later in Section 3.6). When NAD^+ was added to the reaction (Fig. 3G), the DMPO/$^{\bullet}$OH and DMPO/$^{\bullet}$C radicals both were attenuated. In the case of MPO inhibited neutrophils (using ABAH, Fig. 3H), the signals of both DMPO/$^{\bullet}$OH and DMPO/$^{\bullet}$C were attenuated.

To better illustrate these effects, were used a greater density of neutrophils (5 x 10^5, which was equivalent to, which were shown in Fig 3I – K. This resulted in more intense spectra, with the same species being detected as Fig 3F-H. From these observations, it appears that isolated MPO produces the same free radical products as activated neutrophils in the presence of SOD; also, activated neutrophils demonstrate INH metabolism.

As the MPO content and activity depended on neutrophil density, we determined peroxidase activity using guaiacol to compare the activity of isolated MPO (100 nM) with neutrophils. We determined that the MPO activity of neutrophils (6 x 10^4 cells) was equivalent to 3.23 nM of purified human MPO.

2.4.2 EPR studies for the metabolites of INH in MPO and neutrophils

In the MPO system, NAcINH did not show any EPR signals in any of its reactions (Fig. 2E-H). However, NAcHZ (Fig. 2I-L) and HZ (Fig. 2M-P) showed detectable EPR spectra. NAcHZ showed an N-centered free radical (DMPO/$^{\bullet}$N) when incubated with MPO + H_2O_2 and was simulated (see Fig. 2J and Simulated K). The addition of SOD (Fig. 2K) or NAD+ (Fig. 2L) did not affect the spectrum. With HZ, we found DMPO/$^{\bullet}$OH signals which were enhanced by the addition of H_2O_2 (Fig. 2M, N). The addition of SOD caused a marked attenuation of DMPO/$^{\bullet}$OH

(Fig. 2O), suggesting that the DMPO/$^{\bullet}$OH signals were generated from $O_2^{\bullet-}$. Hence, DMPO/$^{\bullet}$OOH signals did not appear in any of HZ reactions. In NAcHz and HZ reactions, we did not find EPR-based evidence of interactions between NAD^+ and any free radicals generated with these compounds (Fig. 2L, P).

Using activated neutrophils with SOD, we observed DMPO/$^{\bullet}$N associated with NAcHZ (Fig. 3D) and DMPO/$^{\bullet}$OH associated with HZ (Fig. 3E). The spectrum of NAcHZ was similar to the spectrum using MPO both in characteristics and intensity; the spectrum derived from HZ in activated neutrophils, however, was significantly less intense compared to MPO although a weak DMPO/$^{\bullet}$OH was observed. Lastly, NAcINH (Fig. 3C) did not show any EPR spectra as was found with MPO.

2.4.3 Chemical nature of INH and its metabolites

In the NBT reduction assay, we compared the MPO metabolites of INH with its human metabolites; only INH showed the capacity to reduce NBT to form formazan which was measured at 520 nm in UV-Vis spectroscopy (Fig. 4). A previous study showed that only INH has the capacity to reduce NBT in comparison other hydrazine drugs (hydralazine and iproniazid) [11]. Therefore, an INH product(s) of MPO is/are reducing agent(s) which can donate electrons to NBT to form NBT-formazan. On the other hand, all other metabolites of INH, when oxidized by MPO, did not react with NBT. The absence of an MPO substrate ("no drug" in Fig. 4) also did not cause NBT reduction. Therefore, biochemically these radical metabolites were significantly different from the parent compound's initial free radical metabolite(s).

2.4.4 UV-Vis and LC/MS studies of INH-NAD^+ adduct formation

We carried out a series of UV-Vis studies where either INH or its metabolites (NAcINH, NAcHZ, and HZ) were incubated with NAD^+/MPO/H_2O_2. After 30 minutes of each reaction, we compared the spectrum with the initial time-point spectrum to determine if new products were found. No compound, except for INH, showed a change in its spectrum (Fig 5). Based on these findings, we investigated the UV-Vis absorbance kinetics at 326 nm (Fig. 5A inset). These findings demonstrated that only INH oxidation by MPO led to a new product in the presence of NAD^+. There was no change in the spectrum when NAD^+ was omitted from the reaction containing INH, MPO, and H_2O_2 (data not shown).

We further performed another series of UV-Vis studies where either NAD^+, the components of NAD^+ (nicotinamide and adenine) or NADH were added with INH and MPO/H_2O_2 (Fig. 6). After 30 minutes of each reaction, we compared the spectrum with the initial time-point spectrum to observe any changes. No new products were detected with any of the potential reactants used; only NAD^+ led to a new product as described above (Fig. 5A).

In another set of UV-Vis studies, four different nucleotides (guanine, cytosine, adenine and thymine) were added individually with INH in MPO/H_2O_2 system to investigate the interactions. As INH is electron rich (due to the hydrazide moiety) it behaved like a reducing agent; as such, it is possible to interact with electron acceptors, for example, NAD^+. However, our studies revealed that INH did not interact with any of four nucleotides (data not shown). It suggests that the reaction between INH and NAD^+ is rather unique.

2.4.5 Identification of INH-NAD$^+$ adduct in LC-MS

LC-MS was carried out after a reaction containing 500 μM INH, 500 μM NAD$^+$, 1 μM MPO, 5 mM glucose, and 10 mU GOx for 1 h in 0.1M phosphate buffer pH 7.4 containing 100 μM DTPA (sample preparation was described Materials & Methods). The LC chromatogram revealed three main peaks (λ = 326 nm) with retention times at 0.42, 3.70, and 5.77 min. (Fig. 7A). ESI-MS shows the INH-NADH adduct in both positive and negative ion modes at an RT of 0.44min. An extracted ion chromatogram of the positive mode ESI shows that the m/z 769 peak corresponding to INH-NAD$^+$ is observed only at 0.44 min (Figure 7B). Interestingly, in positive mode both the INH-NAD$^+$ and INH-NADH forms are observed at m/z 769 and m/z 771, respectively (Fig 7C). In negative mode, the INH-NADH form is observed (Fig. 7D). Reduction of NAD$^+$ to NADH can occur during the ESI process as NAD$^+$ has a more positive reduction potential (-0.18 V) than the iron metal (-0.41 V) in the ESI spray tip [25]; therefore, it is not surprising that both NAD$^+$ and NADH forms are observed, despite having added only NAD$^+$ to the reaction mixture. Fragmentation of INH-NAD$^+$ also occurs and results in the formation of fragment peaks at m/z 228, m/z 542 and m/z 664. The proposed structures of the fragments are shown in Fig. 7E and the proposed formulae were confirmed by high-resolution ESI LC-MS in a separate experiment (data not shown).

2.5 DISCUSSION

These studies demonstrated that there are fundamental differences in the behavior of INH compared to its major human metabolites (NAcINH, NAcHZ, and HZ). In addition, MPO is significant in the metabolism of INH and its human metabolites. By using EPR spectroscopy, a DMPO/$^{\bullet}$C (a carbon center radical) signal was identified in both MPO and isolated human

neutrophils. It is assumed that this DMPO/$^{\bullet}$C signal was generated due to INH$^{\bullet}$ formation from INH via the peroxidation cycle of MPO; the DMPO/$^{\bullet}$C signal was also identified for KatG INH$^{\bullet}$ generation [26, 27]. In addition, this study identified INH-NAD^{+} adduct formation catalyzed by MPO by the addition of NAD^{+} in reactions that generated INH$^{\bullet}$. The INH$^{\bullet}$ metabolite was a reducing radical, whereas other oxidized radical products of INH metabolites were not reductants; this characteristic is likely what leads INH$^{\bullet}$ to interact with NAD^{+}. The INH-NAD^{+} adduct has been postulated as a major anti-TB component of INH [1, 2]. The INH-NAD^{+} adduct was confirmed by using LC-MS in INH/MPO/H_2O_2. As the INH-NAD^{+} adduct was found in the MPO biochemical system and MPO is a key neutrophil enzyme, it is expected to be formed in activated neutrophils. Furthermore, our studies confirmed that the unique chemical properties of NAD^{+} are necessary for the interaction of the INH$^{\bullet}$ since the individual components of NAD^{+} (nicotinamide and adenine) did not interact with INH$^{\bullet}$ metabolite. To our knowledge, this is the first study to show that neutrophil MPO can form the INH-NAD^{+} adduct.

In EPR studies, the reaction between INH and MPO resulted in DMPO/$^{\bullet}$OH signals. A previous study had shown that INH in 0.1 M phosphate buffer (pH $\geq$ 7) produced apparent hydroxyl radicals in the presence of a potent metal chelator, phytic acid, with or without catalase; however, in acidic pH ($\leq$ 6) this apparent hydroxyl radical was non-detectable [28]. It suggested that the comparatively basic pH of 0.1 M phosphate buffer may facilitate the formation of hydroxyl radical from INH through slow auto-oxidation [24]. This may also be influenced by the reduction potential of the compounds as higher the reduction potential compounds may undergo a higher rate of autooxidation. From redox potential studies, it is known that INH has the highest redox potential (-1.5 V) [29], then HZ (-0.201 V) [30]. NAcHZ has very low redox potential (-

0.077 V) [30] which makes it not likely for auto-oxidation; and NAcINH is relatively inert regarding redox potential since its acetylation blocked its H^+ transfer capacity.

In the presence of H_2O_2, compound-I of MPO was formed and oxidized INH. EPR signals demonstrated at least three radical species (DMPO/$^{\bullet}$OH, DMPO/$^{\bullet}$OOH, and DMPO/$^{\bullet}$C) were formed. Goodwin *et al.* were the first to show similar findings in their studies for this reaction. However, the result of SOD addition was somewhat different in terms of DMPO/$^{\bullet}$OH signal intensity [11]. In our studies, we found that DMPO/$^{\bullet}$OH signals were intensified and DMPO/$^{\bullet}$OOH signals were eliminated by the addition of SOD. However, Goodwin *et al.* showed both signals were decreased [11]. Both experiments suggested that $O_2^{\bullet-}$ was the source for DMPO/$^{\bullet}$OOH signals. However, the contradiction between DMPO/$^{\bullet}$OH signals may vary due to the variation of pH variation of the buffer systems (discussed above). We speculate that at physiological pH, INH$^{\bullet}$ may reduce H_2O_2 to hydroxyl radical as the INH-induced DMPO/$^{\bullet}$OH spectrum was insensitive (and enhanced) by SOD, though further evidence is needed. Again, as HZ has very low redox potential in comparison to that of INH, its reduction capacity of H_2O_2 may be very weak. Therefore, SOD attenuated DMPO/$^{\bullet}$OH, arising from $O_2^{\bullet-}$, from HZ reactions.

In our studies, we introduced NAD^+ which has not been explored yet in MPO-mediated INH metabolism. The addition of NAD^+ into INH/SOD/MPO/H_2O_2 system caused a slight decrease of the entire spectrum of INH (DMPO/$^{\bullet}$C and DMPO/$^{\bullet}$OH) along with the reappearance of DMPO/$^{\bullet}$OOH. This suggested that carbon-centered radical of INH (INH$^{\bullet}$) reacted with NAD^+ to form INH-NAD^+ adduct which was confirmed in UV-Vis absorbance at 326 nm followed by identified in LC-MS. However, it is unknown how the formation of INH-NAD^+ adduct caused the significant decrease of DMPO/$^{\bullet}$OH signal and reappearance of DMPO/$^{\bullet}$OOH signal in EPR

spectrum. The reappearance of DMPO/$^{\bullet}$OOH signal suggests that INH-NAD^+ adducts may have an inhibitory effect on SOD activity, but this needs further investigation. In the case of other reactions (NAcINH, NAcHZ, and HZ), no spectral changes were observed after adding NAD^+. This again highlights the specific reaction between INH radical metabolites and NAD^+.

Similar to isolated MPO, EPR studies in activated human neutrophils were carried out. Firstly, SOD was needed in order to visualize the INH or INH metabolite associated free radicals due to oxygen activation by the respiratory burst. Activated PMNs showed a characteristic EPR spectrum, which is composed of a mixture of DMPO/$^{\bullet}$OOH and DMPO/$^{\bullet}$OH as reported previously [31]; the addition of SOD essentially abrogated the oxygen-derived free radical spectra. In the presence of INH, SOD resulted in a residual DMPO/$^{\bullet}$OH spectrum and a weak DMPO/$^{\bullet}$C. The addition of NAD^+ in the reaction caused even further attenuation. These observations were consistent with spectra from reactions using isolated MPO, except that the intensity was significantly less when using neutrophils. A higher neutrophil density increased the signals, and the MPO inhibitor, ABAH, attenuated the spectrum. Therefore, it is apparent that neutrophil MPO played a major role in INH oxidation and free radical generation. In addition, it was shown for the first time that neutrophils can produce carbon-centered radical, which we proposed to be derived from INH$^{\bullet}$. The metabolites of INH appeared to behave quite similar as they did when using MPO as the catalyst such that NAcINH did not produce detectable free radical products, NAcHZ formed nitrogen-centered radicals, and HZ formed superoxide. A summary of these findings regarding INH oxidation via neutrophil MPO is presented in Figure 8.

Studies evaluating the reducing or oxidizing effects of the free radical metabolites of INH and its human metabolites demonstrated that MPO metabolism of INH only led to a free radical metabolite which is reducing and can reduce NBT. This type of assay has been used in other

studies that used KatG [32, 33], or even when assaying superoxide radical [34, 35]. As per its redox potential, INH is a very strong reducing agent whereas HZ and NAcHZ are very weak [30, 36]. Therefore, we speculated that the intermediate species of INH during MPO metabolism may have higher reduction potential than the intermediates of other compounds tested. This is the likely explanation of why the INH intermediate radical solely reacted with NAD^+ (oxidized form), and others did not show any interaction. As NADH is the reduced form of NAD^+, it was not favorable to interact with $INH^{\bullet}$ which was also reducing in nature. These findings were characterized by LC-MS analyzes. Interestingly, a recent study in TB patients and healthy mice identified a similar species in urine [17].

In comparison with other immune cells, neutrophils are less studied with respect to TB infection. Although the role of neutrophils in host defense against TB is contradictory, the early recruitment of neutrophils at the site of *Mtb* infection is well documented [37]. After recruitment, they recognize *Mtb* directly or via opsonization and internalize them followed by deploying various killing mechanisms such as reactive oxygen species generation, NETs formation, and release of other antimicrobial peptides [37]. The successful killing causes the apoptosis of neutrophils which can recruit non-inflammatory macrophages and lead to disease recovery [38-40]. Many studies showed that neutrophil-derived killing, however, is not effective against *Mtb* [37], and causes the necrosis of neutrophils which recruits more neutrophils and inflammatory macrophages to the site of infection [40]; this causes more damage rather than recovery [37, 40, 41]. Our studies have shown that MPO can produce the postulated anti-bacterial component of INH, INH-NAD^+ adduct upon INH treatment, and suggests an alternative pathway to kill *Mtb*. Future studies should be directed at exploring the relationship between the immune cell-induced production of INH-NAD^+ in order to provide a beneficial TB outcome.

2.6 ACKNOWLEDGEMENTS

Saifur R. Khan (supervised by Arno G. Siraki) was supported by an Alberta Innovates Graduate Scholarship of Alberta Innovates Technology Futures (AITF). Mr. N. Aljuhani (also supervised by Arno G. Siraki) was supported by Taibah University through Saudi Arabian Cultural Bureau in Canada. This work was supported by the Canadian Institutes of Health Research (202034) and the Natural Sciences and Engineering Research Council (#RGPIN-2014-04878).

2.7 REFERENCES

[1] Timmins GS, Deretic V. Mechanisms of action of isoniazid. Mol. Microbiol. 62 (2006) 1220-27.

[2] Miesel L, Rozwarski DA, Sacchettini JC, Jacobs WR, Jr. Mechanisms for isoniazid action and resistance in Genetics and Tuberculosis: Novartis Found. Symp. 217 (1998) 209-20.

[3] Zumla A, Atun R, Maeurer M, Mwaba P, Ma Z, O'Grady J, et al. Viewpoint: Scientific dogmas, paradoxes and mysteries of latent Mycobacterium tuberculosis infection. Trop. Med. Int. Health 16 (2011) 79-83.

[4] Kjellsson MC, Via LE, Goh A, Weiner D, Low KM, Kern S, et al. Pharmacokinetic evaluation of the penetration of antituberculosis agents in rabbit pulmonary lesions. Antimicrob. Agents Chemother. 56 (2012) 446-57.

[5] de Steenwinkel JE, de Knegt GJ, ten Kate MT, van Belkum A, Verbrugh HA, Kremer K, et al. Time-kill kinetics of anti-tuberculosis drugs, and emergence of resistance, in relation to metabolic activity of Mycobacterium tuberculosis. J. Antimicrob. Chemother. 65 (2010) 2582-9.

[6] Timmins GS, Master S, Rusnak F, Deretic V. Nitric Oxide Generated from Isoniazid Activation by KatG: Source of Nitric Oxide and Activity against *Mycobacterium tuberculosis*. Antimicrob. Agents Chemother. 48 (2004) 3006-9.

[7] Timmins GS, Master S, Rusnak F, Deretic V. Requirements for nitric oxide generation from isoniazid activation *in vitro* and inhibition of mycobacterial respiration i*n vivo*. J. Bacteriol. 186 (2004) 5427-31.

[8] Rickman KA, Swancutt KL, Mezyk SP, Kiddle JJ. Isoniazid: radical-induced oxidation and reduction chemistry. Bioorg. Med. Chem. Lett. 23 (2013) 3096-100.

[9] Meng X, Maggs JL, Usui T, Whitaker P, French NS, Naisbitt DJ, et al. Auto-oxidation of isoniazid leads to isonicotinic-lysine adducts on human serum albumin. Chem. Res. Toxicol. 28 (2015) 51-58.

[10] Winder FG, Denneny JM. Metal-catalysed auto-oxidation of isoniazid. Biochem. J. 73 (1959) 500-7.

[11] Goodwin DC, Aust SD, Grover TA. Free Radicals Produced during the Oxidation of Hydrazines by Hypochlorous Acid. Chem. Res. Toxicol. 9 (1996) 1333-9.

[12] Forbes LV, Furtmüller PG, Khalilova I, Turner R, Obinger C, Kettle AJ. Isoniazid as a substrate and inhibitor of myeloperoxidase: Identification of amine adducts and the influence of superoxide dismutase on their formation. Biochem. Pharmacol. 84(2012) 949-60.

[13] Hofstra AH, Li-Muller SM, Uetrecht JP. Metabolism of isoniazid by activated leukocytes. Possible role in drug-induced lupus. Drug Metab. Dispos. 20 (1992) 205-10.

[14] Hillar A, Loewen PC. Comparison of isoniazid oxidation catalyzed by bacterial catalase-peroxidases and horseradish peroxidase. Arch. Biochem. Biophys. 323 (1995) 438-46.

[15] Sampson JB, Ye Y, Rosen H, Beckman JS. Myeloperoxidase and Horseradish Peroxidase Catalyze Tyrosine Nitration in Proteins from Nitrite and Hydrogen Peroxide. Arch. Biochem. Biophys. 356 (1998) 207-13.

[16] van der Walt BJ, van Zyl JM, Kriegler A. Aromatic hydroxylation during the myeloperoxidase-oxidase oxidation of hydrazines. Biochem. Pharmacol. 47 (1994) 1039-46.

[17] Mahapatra S, Woolhiser LK, Lenaerts AJ, Johnson JL, Eisenach KD, Joloba ML, et al. A Novel Metabolite of Antituberculosis Therapy Demonstrates Host Activation of Isoniazid and Formation of the Isoniazid-NAD+ Adduct. Antimicrob. Agents Chemother. 56 (2012) 28-35.

[18] Yang CT, Cambier CJ, Davis JM, Hall CJ, Crosier PS, Ramakrishnan L. Neutrophils exert protection in the early tuberculous granuloma by oxidative killing of mycobacteria phagocytosed from infected macrophages. Cell Host Microbe. 12 (2012) 301-12.

[19] Silva Miranda M, Breiman A, Allain S, Deknuydt F, Altare F. The Tuberculous Granuloma: An Unsuccessful Host Defence Mechanism Providing a Safety Shelter for the Bacteria? Clin. Dev. Immunol. 2012 (2012) 1-14.

[20] Eruslanov EB, Lyadova IV, Kondratieva TK, Majorov KB, Scheglov IV, Orlova MO, et al. Neutrophil Responses to Mycobacterium tuberculosis Infection in Genetically Susceptible and Resistant Mice. Infect Immun. 73 (2005) 1744-53.

[21] Seiler P, Aichele P, Bandermann S, Hauser AE, Lu B, Gerard NP, et al. Early granuloma formation after aerosol Mycobacterium tuberculosis infection is regulated by neutrophils via CXCR3-signaling chemokines. Eur J Immunol. 33 (2003) 2676-86.

[22] Oh H, Siano B, Diamond S. Neutrophil Isolation Protocol. J. Vis. Exp. 17 (2008) 745.

[23] Britigan BE, Rosen GM, Thompson BY, Chai Y, Cohen MS. Stimulated human neutrophils limit iron-catalyzed hydroxyl radical formation as detected by spin-trapping techniques. J. Biol. Chem. 261 (1986) 17026-32.

[24] Kebarle P, Verkerk UH. Electrospray: From ions in solution to ions in the gas phase, what we know now. Mass Spectrom. Rev. 28 (2009) 898-917.

[25] Johnsson K, Schultz PG. Mechanistic Studies of the Oxidation of Isoniazid by the Catalase Peroxidase from Mycobacterium tuberculosis. J. Am. Chem. Soc. 116 (1994) 7425-6.

[26] Magliozzo RS, Marcinkeviciene JA. Evidence for Isoniazid Oxidation by Oxyferrous Mycobacterial Catalase−Peroxidase. J. Am. Chem. Soc. 118 (1996) 11303-4.

[27] Van Zyl JM, Van Der Walt BJ. Apparent hydroxyl radical generation without transition metal catalysis and tyrosine nitration during oxidation of the anti-tubercular drug, isonicotinic acid hydrazide. Biochem. Pharmacol. 48 (1994) 2033-42.

[28] Ashish Garg, Om Prakash Meena, Pandey Ykar. Study of electrode kinetics and thermodynamic parameters of antituberculosis drug isoniazid at D.M.E. Int. J. Pharm. Pharm. Sci. 4 (2012) 154-7.

[29] Tosk JM. Method of determining the concentration of reducing agents. Google Patents; 1981.

[30] Bannister JV, Bellavite P, Serra MC, Thornalley PJ, Rossi F. An EPR study of the production of superoxide radicals by neutrophil NADPH oxidase. FEBS lett. 145 (1982) 323-6.

[31] Singh R, Wiseman B, Deemagarn T, Jha V, Switala J, Loewen PC. Comparative study of catalase-peroxidases (KatGs). Arch. Biochem. Biophys. 471 (2008) 207-14.

[32] Wei C-J, Lei B, Musser JM, Tu S-C. Isoniazid Activation Defects in Recombinant Mycobacterium tuberculosis Catalase-Peroxidase (KatG) Mutants Evident in InhA Inhibitor Production. Antimicrob. Agents Chemother. 47 (2003) 670-5.

[33] Wengenack NL, Rusnak F. Evidence for Isoniazid-Dependent Free Radical Generation Catalyzed by Mycobacterium tuberculosis KatG and the Isoniazid-Resistant Mutant KatG(S315T). Biochemistry 40 (2001) 8990-6.

[34] Singh R, Wiseman B, Deemagarn T, Donald LJ, Duckworth HW, Carpena X, et al. Catalase-peroxidases (KatG) Exhibit NADH Oxidase Activity. J. Bio. Chem. 279 (2004) 43098-106.

[35] Furst A, Berlo RC, Hooton S. Hydrazine as a Reducing Agent for Organic Compounds (Catalytic Hydrazine Reductions). Chem. Rev. 65 (1965) 51-68.

[36] Lowe DM, Redford PS, Wilkinson RJ, O'Garra A, Martineau AR. Neutrophils in tuberculosis: friend or foe? Trends Immunol. 33 (2012) 14-25.

[37] Fox S, Leitch AE, Duffin R, Haslett C, Rossi AG. Neutrophil Apoptosis: Relevance to the Innate Immune Response and Inflammatory Disease. J. Innate Immun. 2 (2010) 216-27.

[38] Henson PM, Bratton DL. Antiinflammatory effects of apoptotic cells. J. Clin. Invest. 123 (2013) 2773-4.

[39] Gregory CD, Devitt A. The macrophage and the apoptotic cell: an innate immune interaction viewed simplistically? Immunology. 113 (2004) 1-14.

[40] Repasy T, Martinez N, Lee J, West K, Li W, Kornfeld H. Bacillary replication and macrophage necrosis are determinants of neutrophil recruitment in tuberculosis. Microbes Infect. 17 (2015) 564-74.

2.8 FIGURE AND LEGENDS

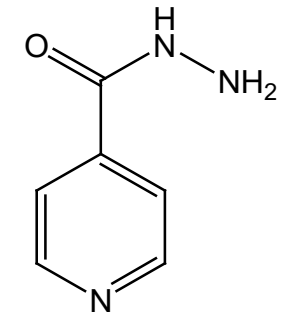

Isoniazid (INH)

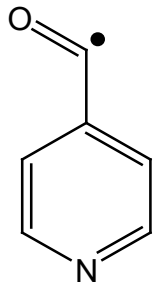

Isonicotinoyl radical (INH$^{\bullet}$)

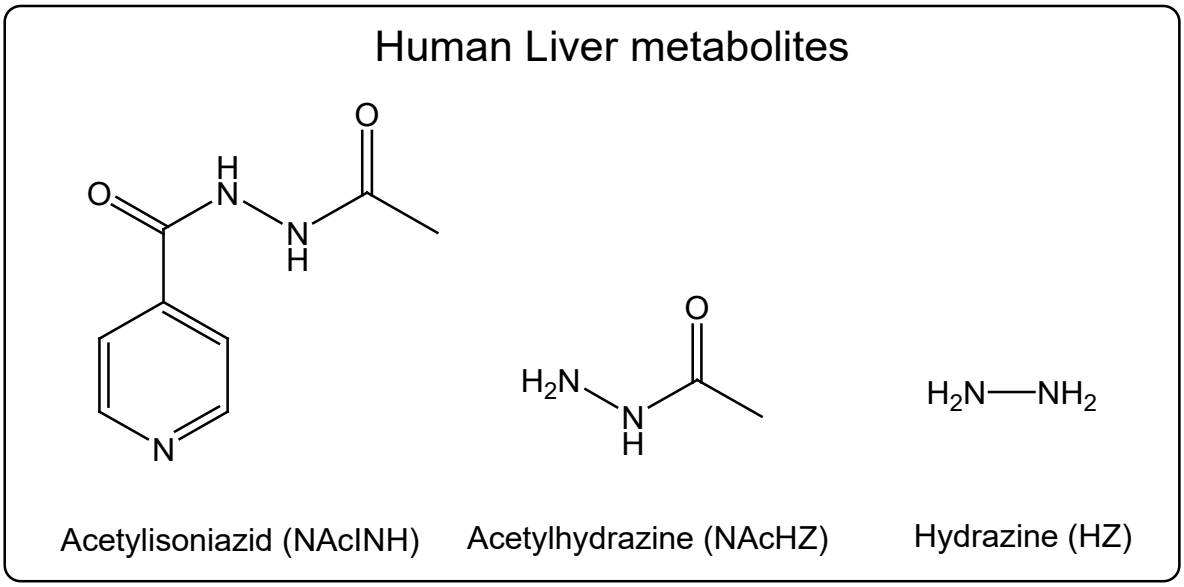

2.8.1 Figure 1. Chemical structure of INH and INH metabolites used and referred to in this study.

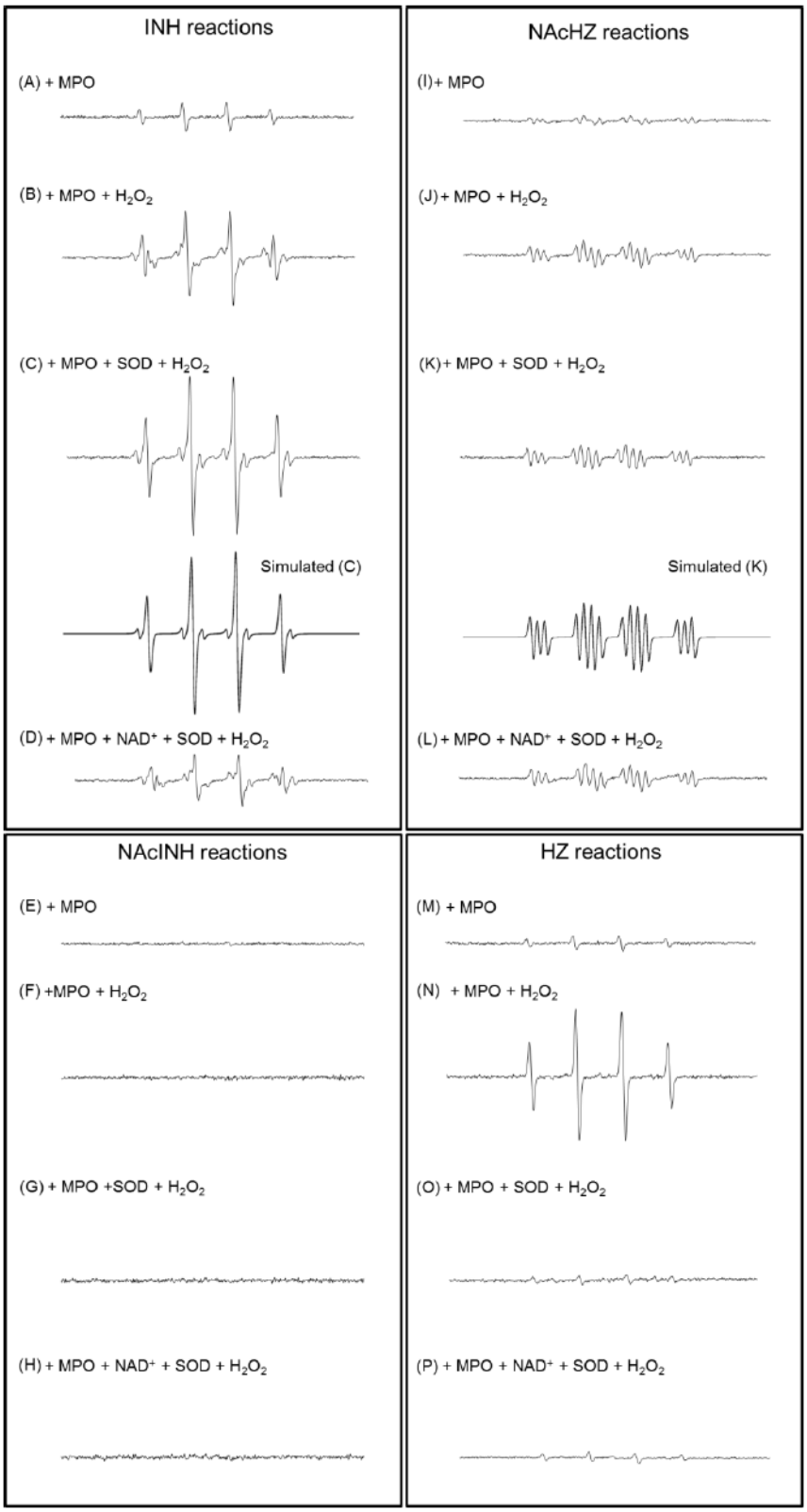
INH reactions
(A) + MPO
(B) + MPO + H_2O_2
(C) + MPO + SOD + H_2O_2
Simulated (C)
(D) + MPO + NAD^+ + SOD + H_2O_2
NAcHZ reactions
(I) + MPO
(J) + MPO + H_2O_2
(K) + MPO + SOD + H_2O_2
Simulated (K)
(L) + MPO + NAD^+ + SOD + H_2O_2
NAcINH reactions
(E) + MPO
(F) +MPO + H_2O_2
(G) + MPO +SOD + H_2O_2
(H) + MPO + NAD^+ + SOD + H_2O_2
HZ reactions
(M) + MPO
(N) + MPO + H_2O_2
(O) + MPO + SOD + H_2O_2
(P) + MPO + NAD^+ + SOD + H_2O_2

2.8.2 Figure 2. EPR spin-trapping studies of INH and its metabolites using MPO. Each reaction was carried out in 200 µl of Chelex®-100-treated 0.1 M sodium phosphate buffer (pH 7.4) containing 100 µM DTPA, and has 0.1 µM of MPO with or without 100 µM of H_2O_2. 2 mM of either INH or any of its metabolites (NAcINH, NAcHZ, and HZ) were used for treatment. 2.5 µM of SOD was added to eliminate spectra arising from the trapping of superoxide ($O_2^{\bullet-}$). In addition, 2 mM of NAD^+ was further used to find the role of NAD^+ in each reaction. The reactions with INH (A –D), NAcINH (E-H), NAcHZ (I-L) and HZ (M-P) are shown. There are two simulated spectra to identify the radical species: Simulated (C) is the simulation of INH reaction C, and simulated (K) is the simulation of NAcHZ reaction K. The parameters for simulated (C) of INH reaction "C": $a^N_{nitroxide}$ = 14.69 G, a^H_{carbon} = 21.75 G, r = 0.99; the parameters for simulated (K) of AcHZ reaction "K": $a^N_{nitroxide}$ = 15.01 G, a^N = 2.32 G, a^H = 17.84 G, r = 0.97. EPR settings are described in Materials & Methods.

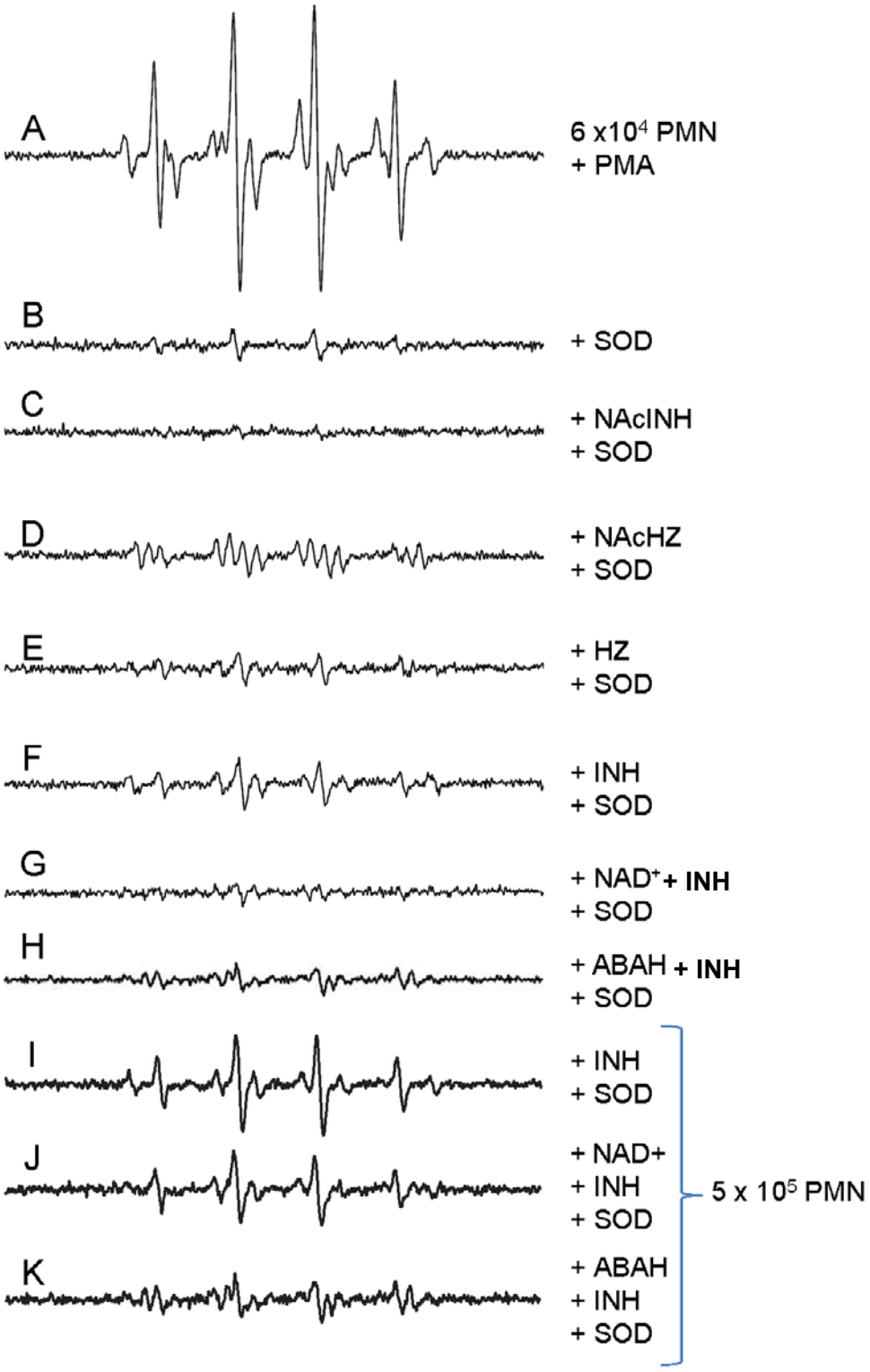
A
6 x10⁴ PMN
+ PMA
B
+ SOD
C
+ NAcINH
+ SOD
D
+ NAcHZ
+ SOD
E
+ HZ
+ SOD
F
+ INH
+ SOD
G
+ NAD⁺ + INH
+ SOD
H
+ ABAH + INH
+ SOD
I
+ INH
+ SOD
J
+ NAD+
+ INH
+ SOD
K
+ ABAH
+ INH
+ SOD
5 x 10⁵ PMN

2.8.3 Figure 3. EPR study of INH and its metabolites in human neutrophil activated by PMA. Each 200 µl of reaction contained $6x10^4$ or 5×10^5 neutrophils activated by 0.8 µM of PMA, and 100 mM DMPO. 2 mM of either INH or any of its metabolites (NAcINH, NAcHZ, and HZ) were used for treatment and the reaction was incubated for 15 min at 37 ºC. 2.5 µM of SOD was added to eliminate spectra arising from the trapping of superoxide ($O_2^{\bullet -}$) due to activation of neutrophils. In addition, 2 mM of NAD^+ was further used to find the role of NAD^+ in each reaction. All reactions were carried out in Chelex®-100-treated 0.1 M sodium phosphate buffer (pH 7.4) containing 100 µM DTPA. A is the typical spectrum of activated neutrophils (neutrophils + PMA + DMPO), and B is the same reaction after adding SOD. In order to discern drug/metabolite radical species, SOD was used for all subsequent reactions. The spectrum of activated neutrophils treated with NAcINH (C), NAcHZ (D), HZ (E), and INH (F) are shown. The addition of NAD^+ (G) or ABAH (H) to reaction F is shown. Spectra I, J and K were run under the same conditions as F, G, and H, respectively, but used a greater density of neutrophils as indicated.

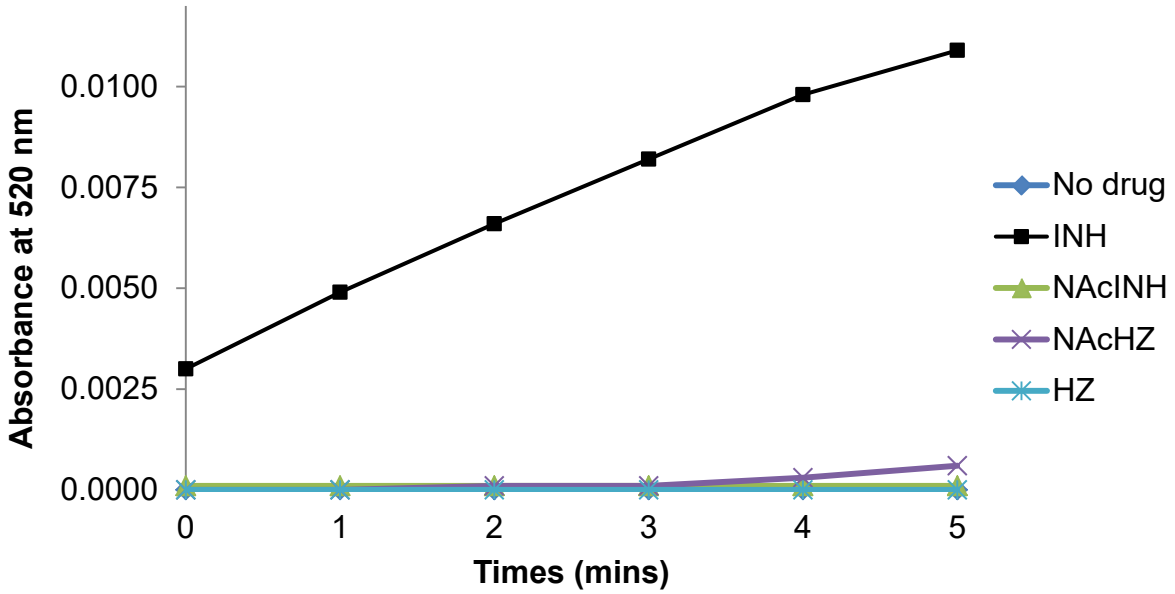

3.8.4 Figure 4. NBT reduction assay of INH and its human metabolites. Reactions contained 1 mM of either INH, NAcHZ, AcINH, or HZ in the mixture of 200 µM NBT, 50 nM MPO, and 50 µM H_2O_2. The absorption of the reduced NBT (formazan) was measured at 520 nm. All reactions were carried out in Chelex®-100-treated 0.1 M sodium phosphate buffer (pH 7.4) containing 100 µM DTPA.

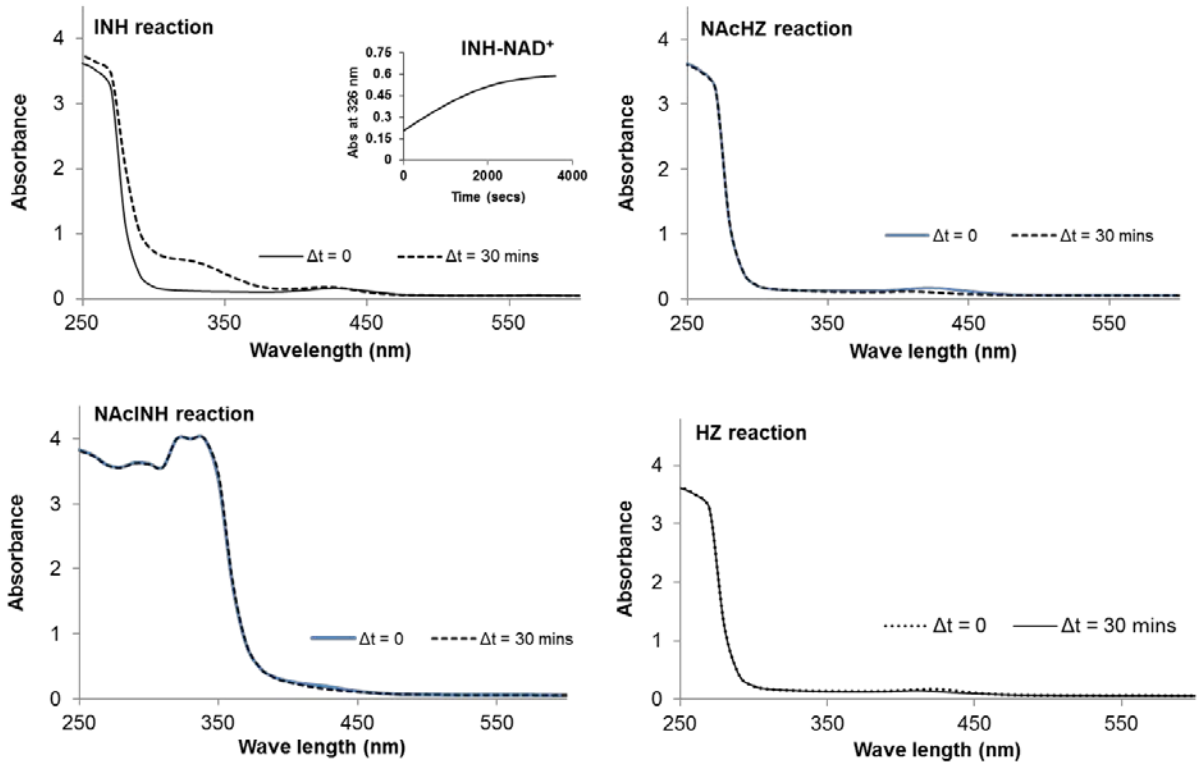

3.8.5 Figure 5. UV-Vis, study for drug-NAD$^+$ adduct formation in MPO system. 500 µM of each chemical (INH, NAcINH, NAcHZ, and HZ) was exposed to 500 µM of NAD$^+$, 1 µM of MPO, 10 mU GOx, and 5 mM glucose. Each reaction was carried for 30 minutes followed by compared the spectrum (Δt = 30 mins) with the initial time point (Δt = 0) spectrum. INH showed significant changes of spectra over time. A UV-Vis kinetic spectroscopy was carried out for INH at 326 nm (inset of INH reaction). It showed the formation of INH-NAD$^+$ adduct over time. All reactions were carried out in Chelex®-100-treated 0.1 M sodium phosphate buffer (pH 7.4) containing 100 µM DTPA.

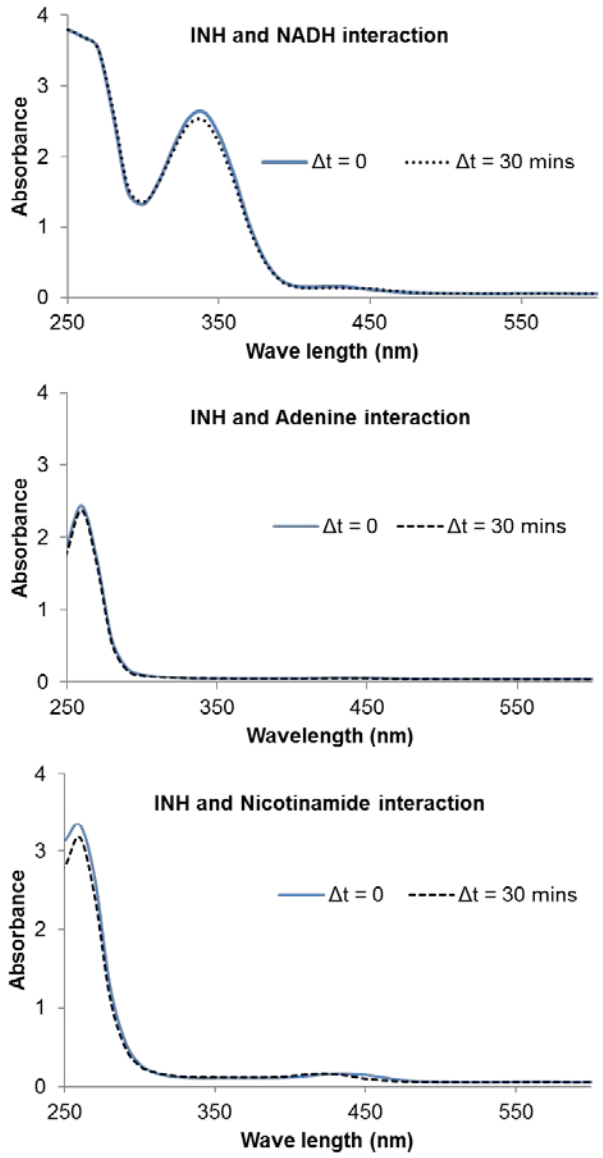

3.8.6 Figure 6. UV-Vis studies for INH interactions with any of these compounds (NADH, adenine, and nicotinamide) in MPO system. 500 µM of each compound (NADH, adenine, and nicotinamide) was exposed to 500 µM of NAD^+, 1 µM of MPO, 10 mU GOx and 5 mM glucose. Each reaction was carried for 30 minutes followed by compared the spectrum (Δt = 30 mins) with the initial time point (Δt = 0) spectrum. The results showed that none of them are reactive with INH. All reactions were carried out in Chelex®-100-treated 0.1 M sodium phosphate buffer (pH 7.4) containing 100 µM DTPA

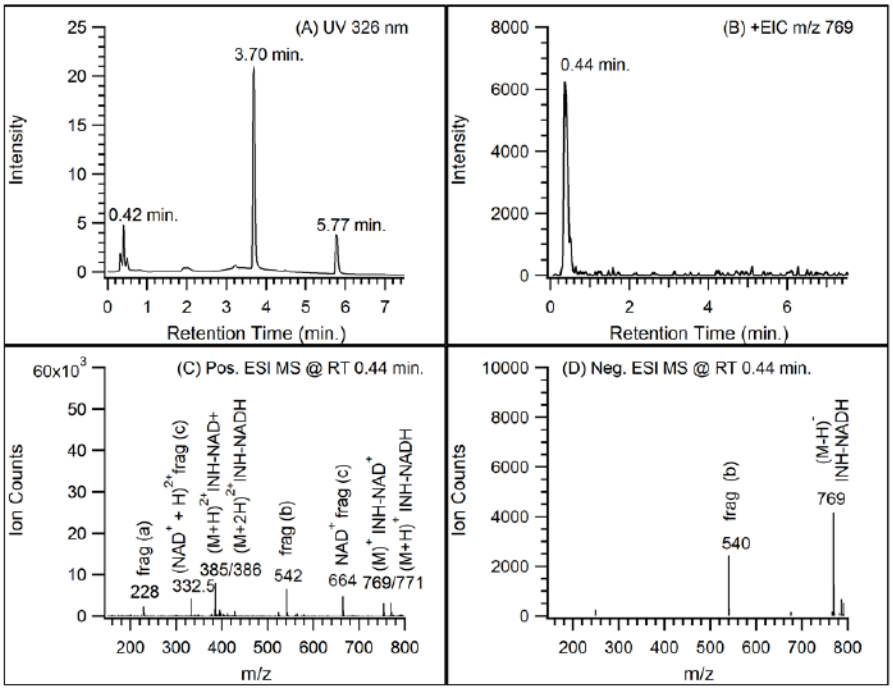
(A) UV 326 nm
3.70 min.
0.42 min.
5.77 min.
Intensity
Retention Time (min.)
(B) +EIC m/z 769
0.44 min.
Intensity
Retention Time (min.)
(C) Pos. ESI MS @ RT 0.44 min.
60x10^3
Ion Counts
frag (a)
228
(NAD+ + H)2+ frag (c)
332.5
(M+H)2+ INH-NAD+
385/386
(M+2H)2+ INH-NADH
frag (b)
542
NAD+ frag (c)
664
(M)+ INH-NAD+
769/771
(M+H)+ INH-NADH
m/z
(D) Neg. ESI MS @ RT 0.44 min.
Ion Counts
frag (b)
540
(M-H)- INH-NADH
769
m/z

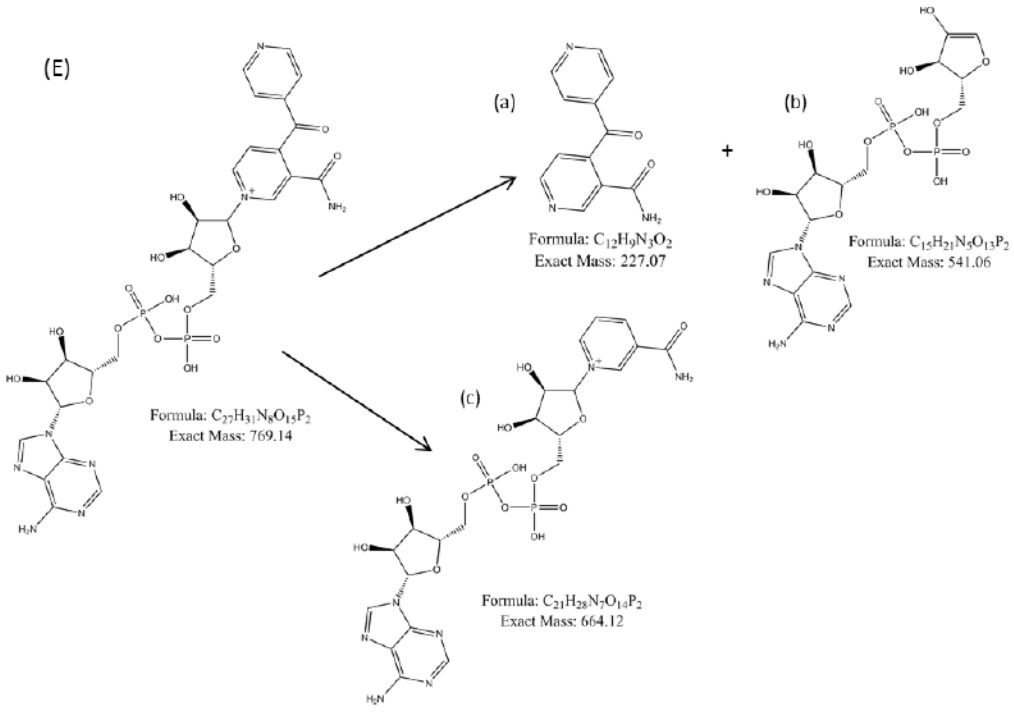
(E)
(a)
Formula: C12H9N3O2
Exact Mass: 227.07
(b)
Formula: C15H21N5O13P2
Exact Mass: 541.06
Formula: C27H31N8O15P2
Exact Mass: 769.14
(c)
Formula: C21H28N7O14P2
Exact Mass: 664.12

3.8.7 Figure 7. LC-MS study of INH-NAD^+ adduct formation in MPO system. (A) Three major peaks at λ = 326 nm in LC chromatogram at retention times 0.42, 3.70, and 5.77 min. (B) The LC-MS positive ion extracted-ion chromatogram for INH-NAD^+ at m/z 769. (C) The positive-ion ESI mass spectrum at RT 0.44 min showing INH-NAD^+ (M^+) at m/z 769 and its doubly charged peak at m/z 385 as well as expected fragments at m/z 228, 542 and 664. INH-NADH $(M+H)^+$ at m/z 771 was also observed (see text for explanation). (D) The negative ion mass spectrum at RT 0.44 min showing INH-NADH $(M-H)^-$ at m/z 769 and the neutral-loss fragment at m/z 540 (see test for explanation). (E) The proposed structures of the INH-NAD^+ fragments observed in the mass spectrum.

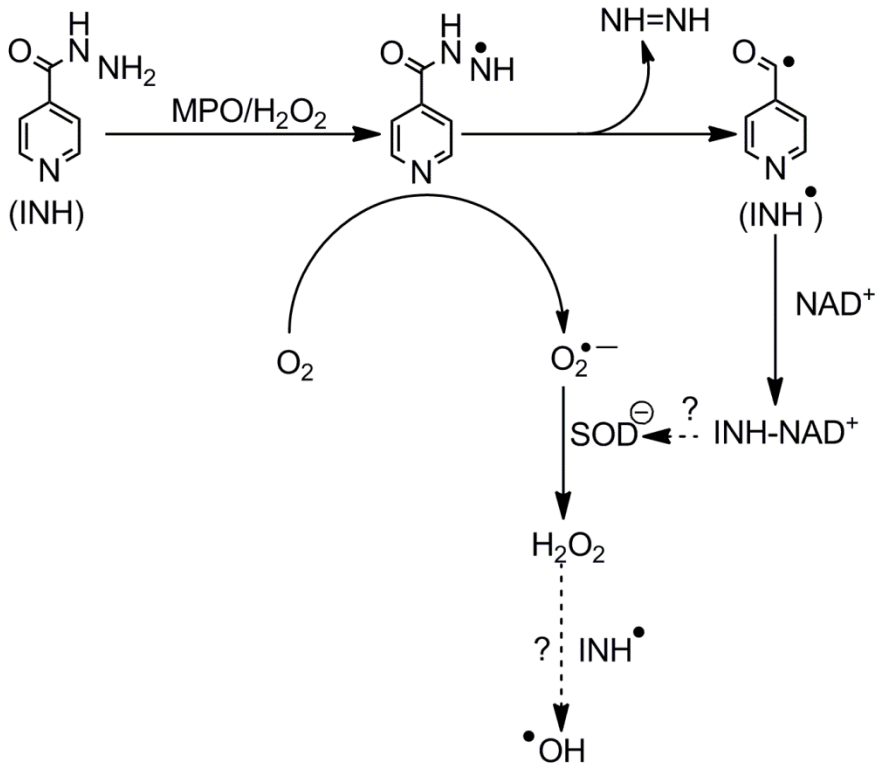

3.8.8 Figure 8: The summary of INH interactions with MPO/H_2O_2 system in the presence of SOD and SOD/NAD^+. INH was oxidized into isonicotinyl radical ($INH^•$) by activated MPO. It enhanced superoxide ($O_2^{•-}$) formation via oxygen reduction. In the presence of SOD, $O_2^{•-}$ is converted into H_2O_2 which we speculate is further reduced to $^•OH$ due to the presence of $INH^•$ (which is a strong reducing intermediate species). In the presence of NAD^+, $INH^•$ forms INH-NAD^+ which may have an inhibitory effect on SOD (based on EPR spectra)**.** The dashed arrows indicate speculated pathways which require further study.

CHAPTER 3:

ISONIAZID INCREASES OXIDATIVE STRESS TOLERANCE OF IMMUNE CELLS

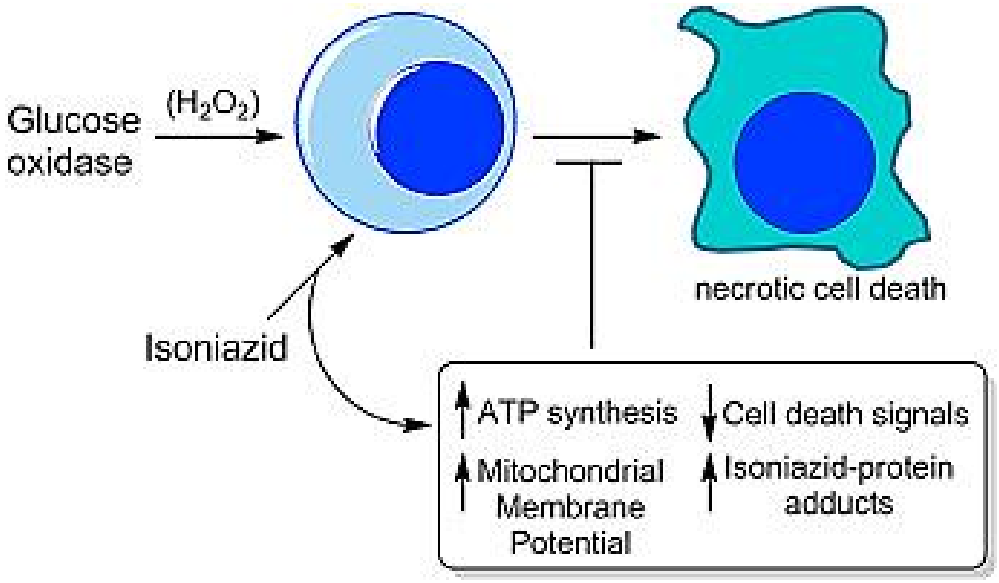

[This work has already been published as Saifur R. Khan *et. al.*, *Cytoprotective effect of isoniazid against H2O2 derived injury in HL-60 cells*, Chemico-Biological Interactions, Volume 244, 25 January 2016, Pages 37-48.]

3.1 ABSTRACT

To combat tuberculosis (TB), host phagocytic cells need to survive against self-generating oxidative stress-induced necrosis. However, the effect of isoniazid (INH) in protecting cells from oxidative stress-induced necrosis has not been previously investigated. In this *in vitro* study, the cytotoxic effect of H_2O_2 generation using glucose oxidase (a model of oxidative stress) was found to be abrogated by INH in a concentration-dependent manner in HL-60 cells (a human promyelocytic leukemia cell). In cells treated with glucose oxidase, both ATP and mitochondrial membrane potential were found to be decreased. However, treatment with INH demonstrated small but significant attenuation in decreasing ATP levels, and complete reversal for the decrease in mitochondrial membrane potential. Quantitative proteomics analysis identified up-regulation of 15 proteins and down-regulation of 14 proteins which all together suggest that these proteomic changes signal for increasing cellular replication, structural integrity, ATP synthesis, and inhibiting cell death. In addition, studies demonstrated that myeloperoxidase (MPO) was involved in catalyzing INH-protein adduct formation. Unexpectedly, these covalent protein adducts were correlated with INH-induced cytoprotection in HL-60 cells. Further studies are needed to determine whether the INH-protein adducts were causative in the mechanism of cytoprotection.

KEY WORDS: Isoniazid, cytoprotection, myeloperoxidase, covalent binding, HL-60 cells, hydrogen peroxide.

3.2 INTRODUCTION

Isoniazid (INH), a synthetic antibiotic, was first used against active *Mycobacterium tuberculosis* (*Mtb*) infection in 1952, and was later recommended as a monotherapy in prevention and treatment of latent tuberculosis (TB) in 1967. Currently, it is a first line choice of drug in both active and latent TB [1]. However, INH is also known for idiosyncratic adverse drug reactions resulting in toxicity such as hepatotoxicity (approximately 5% patients) and autoimmune toxicity, e.g., systemic lupus erythematosus and few case reports of agranulocytosis. Although the mechanisms of these idiosyncratic drug reactions are not fully elucidated, it is suspected that INH reactive metabolites and the adaptive immune responses are involved (http://livertox.nih.gov/Isoniazid.htm). Interestingly, the pharmacological mechanism of action of INH also appears to involve reactive metabolites.

The postulated bactericidal action of INH, based on *in vitro* studies, is through enzymatic oxidation of INH by *Mtb* catalase-peroxidase (KatG) to generate a proposed isonicotinoyl acyl radical metabolite; the latter rapidly reacts with reduced form of nicotinamide adenine dinucleotide (NAD^+) forming an isonicotinoyl acyl-NAD (INH-NAD^+) adduct, which is a potent inhibitor of mycolic acid biosynthesis (inhibits enoyl acyl-carrier-protein reductase) preventing *Mtb* cell wall formation [2, 3]. However, this proposed mechanism of action has yet to be proven in either animal models or humans [3].

Recent studies of *Mtb* pathophysiology reveal that macrophage-dominant phagocytic cells are the host's first-line immune defense against *Mtb*. After entering into lung airways, *Mtb* is engulfed by resident alveolar macrophages, and form granuloma by recruiting other immune cells. However, *Mtb* that escape the granuloma enter into the bloodstream and will encounter

neutrophils as the dominant phagocytic cell [4, 5]. Neutrophils express myeloperoxidase (MPO), and monocytes can be induced to express MPO during infection [6]. MPO is an enzyme that shares some catalytic resemblance to *Mtb* catalase-peroxidase (KatG) to produce reactive metabolites (through the peroxidation cycle) [7], but additionally generates hypochlorous acid (HOCl, through the chlorination cycle) [8].

For pathogen killing during phagocytosis, macrophages mainly rely on their reactive nitrogen species (RNS) production [9], whereas neutrophils rely on reactive oxygen species (ROS) production [10]. Each type of phagocytic cell usually can produce nanomolar (nM) amounts of their respective reactive species (RNS/ROS). If the bacterial load is high, the surrounding activated macrophages and CD4+T cells (within granuloma) release extrinsic death signals (TNF-α, IFN-γ) to initiate apoptosis, leading to successful eradication of *Mtb* [11]. However, *Mtb* has extra-ordinary survival strategies to escape ROS/RNS mediated killing and can induce necrosis of phagocytic cells [12] . *Mtb* possesses very high tolerance for ROS (up to 50 mM H_2O_2) whereas tolerance against RNS is relatively lower (few nM to 5 mM of reactive nitrogen species is bacteriostatic; above 5 mM is bactericidal) [13].

From extensive studies on TB pathophysiology, it is well-known that virulent *Mtb* strains induce necrosis in infected phagocytic cells via mitochondrial damage due to excessive reactive species production by phagocytic cells themselves [14]. To combat *Mtb*, phagocytic cells need to survive first by preventing the oxidative stress-induced self-destruction (oxidative necrosis). However, the effect of INH against oxidative necrosis has never been investigated. Moreover, if INH is cytoprotective against oxidative necrosis, this novel phenomenon can justify its effectiveness against TB by overcoming the limitations of its aforementioned postulated

antibacterial mechanism. Therefore, we hypothesize that INH increases oxidative stress tolerance of immune cells. In this study, we performed *in vitro* experiments by using human promyelocytic leukemia (HL-60) cells which have a high content of MPO and have potential to differentiate into various phagocytic cells such as neutrophils, monocytes and macrophages [15]. As *Mtb* has been described to withstand oxidative or nitrosative injury, we therefore used a surrogate system to produce redox imbalance in HL-60 cells to simulate events that phagocytic cells would be exposed to during *Mtb* infection by using glucose oxidase and glucose system (GOx), which produces a flux of H_2O_2 per unit time.

Studies have shown that both GOx and HOCl trigger the intrinsic pathway for cell death where mitochondrial damage is the common feature [16, 17]. This mitochondrial damage is usually characterized by a loss in mitochondrial membrane potential ($\Delta\psi_m$) and depletion of ATP due to disruption in the electron transport chain. Depending on the severity of mitochondrial damage, the intrinsic cell death pathway follows either apoptosis (caspase-dependent or independent) or necrosis. In general, a high burden of oxidative stress similar to that induced by *Mtb*-infected phagocytic cells can cause excessive mitochondrial damage which usually leads to necrosis. In this study, GOx was used to induce necrosis through mitochondrial damage in HL-60 cells and evaluate the effect of INH.

3.3 MATERIALS & METHODS

3.3.1 Chemicals and Kits

Both heavy and light lysine ($^{13}C_6$-L-Lysine and$^{12}C_6$-L-Lysine) and arginine ($^{13}C_6$-L-arginine and $^{12}C_6$-L-arginine) were purchased from Invitrogen (Carlsbad, CA). FITC annexin-V was purchased from BD Biosciences (San Jose, CA). CellTiter-Glo® Luminescent Cell Viability

Assay kit was purchased from Promega, (Madison, WI). All chemicals unless otherwise noted were from Sigma Chemical Co (Oakville, ON).

3.3.2 Antibodies and enzymes

The glucose oxidase enzyme was purchased from Sigma-Aldrich Canada Co (Oakville, ON). The horseradish peroxidase (HRP) enzyme was purchased from Amresco LLC (Solon, OH). The rabbit polyclonal anti-INH was generously donated by Dr. Uetrecht (University of Toronto). The rabbit anti-GAPDH was purchased from Santa Cruz Biotechnology, Inc. Horseradish peroxidase (HRP) labeled goat anti-rabbit IgG secondary was purchased from Thermo Scientific (USA).

3.3.3 HL-60 cells

HL-60 cells were obtained from ATCC (Cat No. CCL-240, Manassas, VA). The cells were grown in media containing RPMI-1640 medium (Gibco ® Reference No. 11875-093), 10% fetal bovine serum (FBS) (Gibco® Cat No. 12483) and 1% of Antibiotic-Antimycotic (Gibco® Reference No. 15240-062). Cells were maintained in an atmosphere with 5% CO_2 at 37°C, with media change occurring every 2 days. All HL-60 cells used during experiments had a passage number less than 30.

3.3.4 Trypan blue exclusion cytotoxicity assay

HL-60 cells were either pre-treated for 4 h with different concentrations (1 μM to 10 mM) of INH and exposed to 5 mM glucose and 25 mU/mL glucose oxidase (GOx) for 1 h, or co-exposed with both different concentrations (1 μM to 10 mM) of INH and GOx for 1 h in 96-well plates at 1×10^6 cells/ml (>95% viability) at 5% CO_2 and 37°C. 5 mM glucose was always used wherever GOx is indicated. At the end of the experiment, a cell sample from each reaction and 0.4%

trypan blue reagent (Lonza, Anaheim, CA) were mixed at a 1:1 ratio and the cell viability was measured by using a TC-10 automated cell counter (Bio-Rad Laboratories). Data was expressed as means ± SD.

3.3.5 Flow cytometry

We carried out a standard protocol which was adapted for our experimental settings [18]. Briefly, flow cytometry was performed on HL-60 cells (1×10^6/mL, 0.5 mL) pre-treated with varying concentrations (1 μM to 1 mM) of INH for 4 h followed by GOx as described for trypan blue exclusion assays. We did not run the co-exposure experiments here. HL-60 cells were treated with GOx for 1 h (as a positive control for cell death) or HL-60 cells were untreated (used as a negative control) for annexin-V and PI only staining (i.e. cells only treated with one and not the other). Following the reactions, cells were washed with 1 annexin-V binding buffer [0.01 M HEPES (pH 7.4), 0.14 M NaCl, and 2.5 mM $CaCl_2$] twice at RT. Binding buffer (100 μL), 5 μL of FITC annexin-V and 10 μL of 50 μg/mL of PI were added to the cell pellet and resuspended. The samples were incubated at room temperature in the dark with constant shaking of 500 rpm for 15 minutes before being diluted with 400 μL with binding buffer and subsequently analyzed. Fluorescence was induced with an argon laser and detected on FL1 (525 nm BP filter) and FL3 (620 nm LP filter) on a Beckman Coulter Quanta SC flow cytometer. A total of 10,000 events were collected per sample. Compensation was performed using Cell Lab Quanta analysis software to account for fluorophore spectral overlap; data was expressed as means ± SE.

3.3.6 MPO activity assay

A spectrophotometric assay of MPO activity was used in which guaiacol oxidation was measured by changes of absorbance at 470nm (ε = 26.6 mM^{-1}/cm^{-1}[33]). 5 nM of MPO (dissolved in Millipore water) was placed in each well of clear 95-well plate and different concentrations (1µM to 1mM) of either INH or ABAH (4-Aminobenzoic acid hydrazide) were added. Afterwards, 10 mM guaiacol was added into each well. The reactions were started by adding 500 µM of H_2O_2 into each well. Activity of MPO was calculated in nmol tetraguaiacol formed/min/5nM of MPO. The data were acquired using SpectraMax M5.

3.3.7 H_2O_2 flux by GOx

The flux of H_2O_2 per unit time generated by GOx in this study has been measured as described elsewhere [19]. In brief, HRP was used to oxidize phenol red in the presence of various concentrations (1 – 60 µM) of H_2O_2. The reactions with H_2O_2 were carried out for 5 minutes, and the color change of oxidized phenol red was stabilized at pH 12.5 by adding 11.42 mM of sodium hydroxide. This produced a stable purple-mauve coloured product. The absorbance was then measured at 610 nm followed by construction of a linear calibration curve. Afterwards, GOx was tested by replacing H_2O_2 in the same reaction over a 1 hour period with readings at every 15 minutes (4 time points) to calculate the total H_2O_2 production over 1 hour followed by calculating the rate of H_2O_2 generation per minute.

3.3.8 SILAC

3.3.8.1 SILAC Cell culture

HL-60 cells, were purchased from ATCC (Manassas, VA), were cultured in both heavy and light media. Firstly, the RPMI-1640 medium without L-lysine, L-arginine and L-leucine was purchased from Sigma Chemical Co. We added L-leucine to the RPMI-1640 medium as 0.05 mg/mL. 10% dialyzed fetal bovine serum (FBS), obtained from Invitrogen, was also added to RPMI-1640 medium. Afterward, the RPMI-1640 was divided equally into two parts to make either heavy or light media. For heavy medium, heavy L-lysine and L-arginine ($^{13}C_6$-L-Lysine and$^{13}C_6$-L-Arginine) were added to make a final concentration of 0.04 mg/mL and 0.2 mg/mL respectively into one part of RPMI-1640 medium. To make light medium, we added unlabeled L-lysine and L-arginine in as same concentrations as in heavy medium into other part of RPMI-1640. Cells were then maintained in both heavy and light media separately under a humidified atmosphere with 5% CO_2 at 37ºC. Medium renewal was every 2-3 days depending on cell density. The HL-60 cells were cultured in both heavy and light media separately for at least 7 passages to achieve complete isotope incorporation [20].

3.3.8.2 SILAC Cell treatment and lysis

Heavy and light cells were treated with GOx (control) or both GOx and 2.5 mM INH (treatment) for 4 hours in an incubator with 5% CO_2 at 37°C. The reactions were as follows: Sample A – the forward labeled sample was the mixture of control "GOx treated HL-60 cells treated, cultured in the light media" and the treatment "both GOx and INH treated HL-60 cells, cultured in the heavy (containing $^{13}C_6$-L-Lysine and$^{13}C_6$-L-Arginine) media". Sample B – the reverse labeled sample was the same as sample A but the labeling was reversed.

The control and treatment of both sample A (forward labeled sample) and sample B (reverse labeled sample) were lysed separately by using RIPA (0.05 g sodium deoxycholate, 100 µL of Triton X-100, and 0.01 g of SDS in 10 mL of PBS). For preparing either sample A or B, the protein content in control and treatment have to be in a 1:1 ratio. This was achieved by SDS-PAGE of the samples, followed by staining the gel with Coomassie blue, destaining and scanning the gel using LI-COR Odyssey gel scanner. The intensity of protein content in each lane provided a quantitative check the ratio of protein between control and treatment of each sample.

3.3.8.3 SDS-PAGE & Gel-Digestion

2× Loading buffer (0.5 M Tris-HCl pH 6.8, 10% SDS, 1.5% Bromophenol Blue, 20% glycerol and 5% β-mercaptoethanol) was mixed with cell lysates and the heavy and light labeled samples were combined in a 1:1 ratio. The samples were then heated to 95ºC for 5 minutes and then resolved on a 1.0 mm thick 10% polyacrylamide gel. After electrophoresis, the SDS gel was stained with Coomassie Brilliant Blue and destained using 10% acetic acid solution to visualize the bands and lanes. The entire gel lanes were excised into 12 equal pieces for in gel digestion.

3.3.8.4 In-gel digestion and LC-MS/MS analysis

In-gel digestion and LC-MS/MS analysis were carried out according to an in-house standard protocol which was described in one of our recently published paper [18]. A total of 1459 and 1712 proteins were identified in sample A and B, respectively. Proteins those were reproducibly identified in both samples (390 proteins) were taken for further analysis. The expression-changes were determined from the ratios of protein abundance followed by log2 calculation. The proteins

which were also reproducibly either down- or up-regulated by 0.5 on a log2 scale (~ over 40% changes in abundance) in both samples were reported here.

3.3.9 Relative Cellular ATP analysis

Cellular ATP levels were determined by using CellTiter-Glo® Luminescent Cell Viability Assay kit (Promega, WI, USA) as per their protocol. In brief, CellTiter-Glo® reagent was prepared by mixing substrate and buffer (which was thawed by storing at room temperature 24 hours). Run all the reactions in PBS as same as before. 100 µl (approximately 5×10^4 cells) of each reaction with three replica were placed into each well of opaque-walled 96-well plate. 100 µl of freshly prepared CellTiter-Glo® reagent was added to each well and shake the plate for 2 minutes on a shaker. After 10 minutes of incubation at RT, luminescent signals were recorded using a platereader (SpectraMax M5).

3.3.10 Mitochondrial Membrane Potential Change (ΔΨm) analysis

The mitochondrial membrane potential was measured by using JC-1 dye according to a previous protocol [21]. In brief, HL-60 cells were suspended in 1.5 ml micro test tubes at a density of 0.5×10^6 cells/ml of serum free RPMI 1640 media and the reactions were prepared as described before. After completion of reactions, cells were centrifuged at 500g to discard the supernatant. The same volume of PBS containing 0.3 µM of JC-1 was added to the cells, which were resuspended, and incubated for 30 min at 37ºC. The sample was then washed twice at 200 g for 5 minutes to discard the unincorporated free dye. The cells were resuspended in PBS and incubated at 37ºC again for 20 minutes, and 300 µl of cell suspension were added to a black 96-well polystyrene microplate. The fluorescence intensity was measured as ratio of red aggregates/green monomers. For red aggregates, the parameter setting of the plate reader

(SpectraMax M5) was fixed at the excitation 490 nm and emission 595 nm whereas green monomers were measured by changing only the emission to 535 nm. The ratio of red aggregates/green monomers was then calculated. Known mitochondrial toxins (5 μM of antimycin A and 50 μM of carbonyl cyanide 3-chlorophenylhydrazone (CCCP) were used as positive controls for the assay [22].

3.3.11 SDS-PAGE and anti-INH immunoblots

The amount of protein in the lysed samples was determined by the BCA assay and equal amounts of lysate from each reaction were loaded onto an SDS-PAGE (1.0 mm 10% polyacrylamide gel). Before loading, lysates were reduced by 2× loading buffer (0.5 M Tris-HCl pH 6.8, 10% SDS, 1.5% bromophenol blue, 20% glycerol and 5% β-mercaptoethanol), and proteins were denatured for 5 min at 95°C with shaking at 600 rpm followed by cooling to room temperature. After completion of gel running, the proteins were transferred from the gel onto a nitrocellulose membrane which was blocked overnight at 4°C with 5% bovine serum albumin (BSA) in washing buffer (TBS-T). The membrane was then treated with a rabbit anti-INH (1:1000) or rabbit anti-GAPDH (1:1000) for 1 h at room temperature (RT) with constant shaking. Afterwards, the membrane was washed and treated with goat anti-rabbit HRP-conjugated secondary antibody (1:5000 in TBS-T) for 1 h at RT. The membrane was again washed and treated with chemiluminescence HRP substrate (Millipore Corp., Cat No. WBKLS0500) reagent for 2 min and the signals were measured by using luminescent image analyzer (GE ImageQuant LAS 4000 mini).

3.3.12 Statistics

Data were expressed as mean ± standard deviation of mean (SD) of separate experiments (n≥5) performed on separate days using freshly prepared reagents. Statistical significance was performed by a one-way pairwise multiple comparison ANOVA followed by Holm-Sidak post-hoc analysis using SigmaPlot 11.0 software.

3.4 RESULTS

3.4.1 Cytoprotective effects of INH

In this study, HL-60 cells which were treated with GOx (glucose/glucose oxidase as described in Materials & Methods) for three hours were either pre-incubated for 4 h or co-exposed with different concentrations of INH (1 μM to 1 mM). GOx was added to the reactions to provide continuous production of H_2O_2. The rate of H_2O_2 production by GOx was calculated as 2.928 ± 0.072 μmol • U^{-1} • ml^{-1} • h^{-1} (see Materials & Methods). One hour and 3 h after adding GOx, cell viability was determined by trypan blue exclusion. The trypan blue exclusion assay results (Fig. 1) showed that GOx significantly decreased the cell viability (ϕ p <0.001), and both INH pre-incubation and co-exposure showed concentration dependent cytoprotection. INH co-exposure with GOx (Fig. 1a) showed significant INH cytoprotection from 20 μM after 1 h (*P<0.001) and 50 μM INH after 3 h (*P<0.001). However, INH pre-incubation for 4 h prior to adding GOx (Fig. 1b) showed significant cytoprotection from 1 μM (*P<0.001) at both time points. Therefore, INH pre-incubation was found to be more cytoprotective than INH co-exposure at micro molar concentrations of INH (up to 100 μM). However, there was no significant difference between pretreatment or cotreatment of INH when concentrations more than 100 μM were used.

3.4.2 Isoniazid attenuates necrosis/late apoptosis induced by GOx

A representative dot plot of the cell population shown in Fig. 2a illustrates a large proportion of cells in Q2 (PI+ and annexin-V+) when treated with GOx; this was attenuated with a 4 h preincubation of 20 μM INH (Fig. 2b). INH showed a concentration-dependent cytoprotective effect against H_2O_2 (GOx) from 1 μM based on cell population in Q3 (PI- and annexin-V-; ¤ $P <$ 0.005) (Fig. 2c). The cytoprotection of INH was statistically significant from 10 μM to 1 mM (*$P < 0.001$) (Fig. 2c). The flow cytometry analysis also confirmed the type of cytoprotection. GOx induced mainly late apoptosis/necrotic-like cell death (PI+, annexinV+) (Fig. 2e) since cells in the early apoptosis phase (PI-, annexin V+) were not detected with this treatment (Fig. 2d). However, INH cytoprotection against GOx was prominent against necrosis/late apoptosis (Fig. 2e) in a concentration dependent manner. The cytoprotective capacity of INH was detected from 1 μM (¤ $P < 0.005$) and was enhanced with 10 μM to 1 mM of INH (* $P < 0.001$). The statistical analysis also showed 100 μM and 1 mM of INH were significantly more protective against oxidative stress in comparison to 1 μM of INH.

3.4.3 INH is a relatively poor MPO inhibitor

To assay the effect of INH on MPO activity, we used four different concentrations (1 μM, 10 μM, 100 μM and 1 mM) of INH or the well-known peroxidase inhibitor, 4-aminobenzoic acid hydrazide (ABAH), as a positive control for MPO inhibition. The IC_{50} of INH was found 253.7 ± 7.83 μM. Our results for INH inhibition were similar to those published by Huang et al., which reported INH IC_{50} = 277.10 ± 6.65 μM [23]. Forbes et al. compared the loss in specific activity of MPO induced by INH and ABAH and reported a 30% loss in MPO specific activity for the

former; however, ABAH completely inactivated MPO [7]. Collectively, these findings indicate that INH is a relatively poor inhibitor of MPO.

3.4.4 INH protein adducts and role of MPO

HL-60 cells pretreated with INH (1 μM to 1 mM) for 4 h were exposed to GOx for an additional 1 h after which they were lysed and probed for protein bound covalent adducts using an anti-isonicotinyl antibody (anti-INH). In Fig. 3, anti-INH Western blots showed that the INH-protein covalent adducts were increased with INH concentration from 10 μM to 1 mM in GOx treated cells. However, we did not find any adducts in absence of either GOx and/or INH during this time period (Fig. 4, lane 1, 2, 7 & 8). Moreover, anti-INH Western blots showed that MPO inhibition by ABAH (lanes 5 & 6) attenuated INH-protein adduct (Fig. 4). Taken together, these findings suggest that MPO activity is a catalyst for the formation of INH-derived reactive metabolites which apparently bind with proteins to form covalent adducts.

3.4.5 INH induced protein expressions

The replicate SILAC analysis of the INH and GOx treated HL60 cells in comparison to the GOx treated control cells resulted in a total of 390 proteins were reproducibly identified and quantified using highly stringent data analysis. The quantified data of the ratios of protein abundance shown in **Figure 5A** reveals that the majority of proteins do not significantly change in abundance upon treatment. Only 29 proteins were identified for their reproducibly significant change in abundance either down- or up-regulated by 0.5 on a log2 scale (~ over 40% changes in abundance) upon treatment. These 29 proteins were listed in **Table 1**. String (version 9.1) analysis revealed that both upregulated and downregulated proteins demonstrated associations

through co-expression analysis (Fig. 5B and 5C). This suggests that these associated proteins are likely to be involved in specific signaling pathways.

In case of down-regulated proteins, the majority were ribosomal proteins (10 in total) along with some nucleosomal proteins such as RNA-binding protein FUS and three histone proteins (Histone H2A type 1-H, Histone H2B type 1-K and Histone H4). The ribosomal proteins were associated with one another (Fig 5C) and the overall trends appeared to be downregulation of protein expression. However, the downregulation of those nucleosomal proteins could be interpreted as either DNA damage followed by cell death or the preparatory stage for replication. In this study, it has already shown that INH is cytoprotective. Therefore, the down regulation of those nucleosomal proteins might involve in replication process. The up-regulated proteins were found to involve one of the following functions: replication process (DNA replication licensing factor MCM2, Ran-specific GTPase-activating protein and proliferating cell nuclear antigen), structural integrity maintenance activity (tubulin beta chain, tubulin alpha-1B chain, α-actinin-1, stathmin, actin-cytoplasmic 1, T-complex protein 1 subunit eta and Prostaglandin E synthase 3), ATP synthesis (ATP synthase subunit alpha, isoform 2 of 3-hydroxyacyl-CoA dehydrogenase type-2) and blocking of cell death signals (isoform 2 of transcription intermediary factor 1-beta and programmed cell death 6-interacting protein).

3.4.6 Effect of INH on ATP levels

The ATP assay was performed based on proteomic findings that ATP synthesis was upregulated in response to INH treatment. In Fig. 6a, the relative ATP levels of GOx challenged cells were significantly decreased (ϕ $P < 0.001$) within 1 h of exposure. In the INH co-exposure group, 50 μM and 1 mM of INH treated cells showed a significant increase in relative ATP levels versus

GOx challenged cells (¤¤ $P < 0.005$, ¤ $P < 0.05$ respectively). In the INH 4 h preincubated group, both 50 μM and 1 mM INH increased ATP level with similar significance (* $P < 0.001$). At the 3 h timepoint (Fig. 6b), only the higher concentration (1 mM) of INH preincubated for 4 h significantly increased ATP levels (ɵ $P < 0.05$).

3.4.7 Effect of INH on mitochondria membrane potential

The mitochondria membrane potential assay (Fig. 7) showed that GOx treatment significantly reduced the mitochondrial membrane potential compared to untreated cells (* $P < 0.001$). Positive controls for decreasing the mitochondria membrane potential reveal that HL-60 cells produced expected responses toward mitochondrial poisons such as the complex-III inhibitor, antimycin A, or the uncoupler, CCCP. Interestingly, INH significantly attenuated the drop in mitochondrial membrane potential of GOx challenged HL-60 cells (* $P < 0.001$) from 1 μM. This capacity of INH was also found to be significantly greater (• $P < 0.001$) for 100 μM and 1 mM INH compared with 1 and 10 μM INH.

3.5 DISCUSSION

In this study, we have reported the cytoprotective effect of INH in HL-60 cells challenged with H_2O_2 (produced from GOx); this effect was observed with a concentration as low as 1 μM in 4 h preincubation group while relatively higher concentrations (20 to 50 μM) of INH were needed for the co-exposed group. The cytoprotective effect in both groups was in concentration dependent manner. The predominant mechanism of cell death induced by GOx treatment was late apoptosis/necrosis. This study was not able to examine the INH-induced cytoprotection capacity against early apoptosis induced by GOx, since this form of cell death was not observed for the conditions used in this study.

The involvement of mitochondria was investigated through both the relative ATP analysis and mitochondrial membrane potential assays. Both ATP and mitochondrial membrane potential play important roles in the intrinsic pathway of both apoptosis and necrosis. In this study, the increase in ATP induced by INH was minor. As HL-60 cells are cancer cells, their ATP is derived mostly from glycolysis process; as such, the role of mitochondrial ATP is expected to be minor in relation to the mechanism of cell death; however mitochondrial membrane potential appeared to be a major factor in cell death. In this study, the effect of INH on mitochondrial membrane potential was quite marked. Therefore, INH effects on mitochondria played an important role to counteract H_2O_2/HOCl injury in HL-60 cells.

Several studies have demonstrated a different effect of INH on mitochondria [24]. It was shown that mitochondrial dysfunction induced through mitochondrial complex I and II poisoning was enhanced in the presence of INH and proposed that mitochondrial dysfunction was an underlying cause of INH-induced toxicity [24]. However, the effect of INH against mitochondrial poison-induced dysfunction does not appear related with the effect of INH against ROS-induced mitochondrial damage in our study. It is possible that the cell type can dictate the response caused by INH since we used HL-60 cells, but the aforementioned studies were carried out in mouse hepatocytes.

The role of MPO in cytoprotection/cytotoxicity was also explored in this study. MPO is a peroxidase enzyme found abundantly in HL-60 cells. In the presence of H_2O_2, resting or native MPO (Fe^{+3}) is oxidized into its active form, compound I (Fe^{+4}), which can be either reduced back to its resting form (chlorination cycle) or form compound II (Fe^{+4}) through one electron redox reaction where it produces free radical metabolite of favourable 1-electron donor

substrates (peroxidase cycle). Compound II can go through another step of 1 electron reduction back to its native form by generating more free radical metabolites [23, 25, 26].

These free radical species/metabolites may have deleterious effects [27], but this depends on the specific donor substrate. Many xenobiotics and electrophilic (non-radical) metabolites can form covalent protein adducts with electron dense regions of proteins through substitution or addition reactions [28]. Covalent adducts which interfere with biological pathways by disrupting the function of the involved proteins, may be linked with diseases or toxicity [28]. However, it is possible that adduct formation may protect a biomolecule from possible oxidation or degradation which can induce beneficial effects.

For example, it has been shown that the beneficial effect of olive oil is derived from oleuropein (an electrophilic catechol quinone metabolite of olive oil) which hydrolyzes to the catechol hydroxytyrosol quinone and functions as a hydrophilic phenolic antioxidant. It can readily form Michael adducts with thiol nucleophiles in glutathione and proteins. During redox cycling, they can be easily oxidized and back to their native forms (catechol quione and proteins) [29]. A comparison between large dose of acetaminophen (4'-hydroxyacetanilide) and its *m*-hydroxy isomer (3'-hydroxyacetanilide) showed that the latter produced more covalent protein adducts, yet only acetaminophen produced hepatotoxicity [30]. Studies showed that the difference between the toxicity profiles of these two isomers of acetaminophen were related with the difference of reactive metabolite localization and protein targets [31, 32]. In brief, reactive species (RS) also can play a crucial role for cell survival and regeneration through protein oxidation or covalent binding. A review on post-transcriptional oxidative modification by reactive species and the beneficial effects on health and disease has been recently published [33].

From INH-induced liver injury and autoimmunity perspectives, the INH-protein covalent adduct is of great interest [34]. A study on patients under prophylaxis treatment with INH showed the presence of INH-protein adducts in their blood serum if they had liver failure. However, in the case of mild to moderate liver injury, this adduct was not detected [35]. Another study showed that INH treatment on rats and mice up to 5 weeks did not produce liver injury. However, their liver microsomes showed INH-protein adducts [36]. A recent study showed a paradoxical effect of INH. Mice were first induced with mild autoimmune hepatitis, were subsequently treated with INH for 5 weeks. It was expected that this would enhance liver injury, however, INH treatment markedly attenuated hepatitis [37]. Therefore, the role of INH-protein adduct are still elusive.

In this study, anti-INH immunoblots were used to detect covalently bound protein adducts (INH-protein adduct). We found that INH increased the formation of protein adducts concentration dependently. Interestingly, INH induced cytoprotection against GOx concentration dependently also. Therefore, there was a correlation observed between cytoprotection and INH covalent protein binding in this study. Additionally, ABAH (a potent MPO inhibitor) showed a significant decrease in covalent adduct formation. Therefore, MPO activity played a major role in the adduct formation through oxidation of INH.

A recent study demonstrated that INH auto-oxidation for 16 h leads to covalent adducts with lysine, human serum albumin, and human plasma in cell free system [38]. Thus, MPO appeared to act as a true catalyst in HL-60 cells as it greatly accelerated the process that leads to covalent protein binding. The exact relationship between the latter and cytoprotection (i.e., whether covalent protein binding is causative or correlated with cytoprotection) is beyond the

scope of this study; future studies should be conducted to identify the proteins involved in the adduct formation.

One possible mechanism of INH-induced cytoprotection could be related to its inhibition of MPO. A study compared the MPO inhibition capacity of different inhibitors including INH. INH ranked at the bottom of the list with an IC_{50} of 277.10±6.65 μM, whereas ABAH ranked most potent, with an IC_{50} of 0.5±0.03 μM [23]. This finding was similar with our experimental results (data not shown). The reason behind the INH's poor inhibitory capacity was explained by its slow production of superoxide in aerobic conditions through auto-oxidation [39]. Superoxide converts MPO into compound III through a one-step oxidation [39]. Compound III is very unstable and converts into native MPO within a few minutes at room temperature [26, 27]. In presence of reducing agent such as ascorbic acid, it also can be converted into the native enzyme [40]. Therefore, given the potency and mechanism of INH inhibition of MPO, it is highly unlikely that the low micro molar concentrations of INH exerted cytoprotection by MPO inhibition. It is possible that the higher concentrations of INH have the added effect of MPO inhibition, particularly when using concentrations beyond its IC_{50} for MPO. Other mechanisms, however, must be at play for cytoprotection at low micro molar concentrations. This may involve covalent binding to proteins which may provide protection against oxidative damage and/or upregulation of some protective proteins.

Several studies have previously shown that GOx-induced cell death in various systems is not via classical caspase-dependent apoptosis; rather caspase-independent apoptosis or necrosis depending on the GOx concentration [41-43]. In brief, the cell death signal is initiated through oxidative stress-induced mitochondrial damage. It causes mitochondrial membrane depolarization and loss of potential which disrupts electron transport system and ultimately

reduces ATP synthesis markedly [44]. However, cancer cells can overcome the reduction of ATP synthesis, since they mainly rely on glycolysis for ATP production but not for mitochondria. The mitochondrial damage releases AIF to execute apoptosis through caspase-independent pathway [41]. Again, if the mitochondrial damage is extensive due to oxidative stress, it can lead to necrosis [44]. In our study, it is possible to follow either caspase-independent apoptosis or necrosis due to nature of GOx and its concentration. We made many attempts to detect AIF in our studies, but were unsuccessful likely due to technical difficulty in isolating mitochondria from these cells (personal communication, Dr. Paige Lacy, University of Alberta).

In quantitative global protein expression experiments (using SILAC) we found 29 proteins that had significantly changed expression. Using a bioinformatic tool, String 9.1, we found protein-protein associations between these proteins through co-expression/association analysis. These associations suggested that the interacting proteins were involved in certain biological pathways, and most likely are involved with replication process, structural integrity maintenance activity, ATP synthesis and blocking of cell death signals.

In conclusion, our study showed that the detrimental effect of a flux of H_2O_2 was abrogated through both ATP generation and mitochondrial membrane potential recovery, which could involve the upregulation of multiple protective proteins. Besides, replication process, structural integrity maintenance activity and blocking of cell death signals may also play important role. MPO was found essential in INH-protein adduct formation. The role of INH-protein adducts may be either causative or correlated with INH-induced cytoprotection, which is currently unknown. To determine the role of protein covalent adducts, the identification of involved proteins is necessary. The summary of the findings have been illustrated in Figure 8. In case of TB, we have already discussed that the prevention of necrosis of *Mtb*-infected phagocytic

cells has an important role in the prevention of the disease. The *Mtb*-induced necrosis process is executed mainly through oxidative stress and subsequent mitochondrial damage. In this study, we showed INH has a protective role in this perspective. Therefore, INH-induced cytoprotection is plausible mechanism of action of INH though further research is required in appropriate cell models of TB.

3.6 ACKNOWLEDGEMENTS

The authors are grateful to Dr. Jack Uetrecht (University of Toronto) and Dr. Imir Metushi (La Jolla Institute) for generously providing the anti-isonicotinyl antibody. Saifur R. Khan (supervised by Arno G. Siraki) is supported by an Alberta Innovates Graduate Scholarship of Alberta Innovates Technology Futures (AITF). Mr. N. Aljuhani was supported by Taibah University through Saudi Arabian Cultural Bureau in Canada. This work was supported by the Canadian Institutes of Health Research (202034) and the Natural Sciences and Engineering Research Council (#RGPIN-2014-04878).

3.7 REFERENCES

[1] I.G. Sia, M.L. Wieland, Current concepts in the management of tuberculosis, Mayo Clin. Proc. 86 (2011) 348-361.

[2] V. Bernardes-Genisson, C. Deraeve, A. Chollet, J. Bernadou, G. Pratviel, Isoniazid: an update on the multiple mechanisms for a singular action, Curr. Med. Chem. 20 (2013) 4370-4385.

[3] B. Lei, C.J. Wei, S.C. Tu, Action mechanism of antitubercular isoniazid. Activation by Mycobacterium tuberculosis KatG, isolation, and characterization of inha inhibitor, J. Biol. Chem. 275 (2000) 2520-2526.

[4] V.B. Antony, S.A. Sahn, R.N. Harada, J.E. Repine, Lung repair and granuloma formation. Tubercle bacilli stimulated neutrophils release chemotactic factors for monocytes, Chest 83 (1983) 95S-96S.

[5] N. Perskvist, L. Zheng, O. Stendahl, Activation of Human Neutrophils by Mycobacterium tuberculosis H37Ra Involves Phospholipase Cγ2, Shc Adapter Protein, and p38 Mitogen-Activated Protein Kinase, J. Immunol. 164 (2000) 959-965.

[6] M.T. Silva, When two is better than one: macrophages and neutrophils work in concert in innate immunity as complementary and cooperative partners of a myeloid phagocyte system, J. Leukoc. Biol. 87 (2010) 93-106.

[7] L.V. Forbes, P.G. Furtmüller, I. Khalilova, R. Turner, C. Obinger, A.J. Kettle, Isoniazid as a substrate and inhibitor of myeloperoxidase: Identification of amine adducts and the influence of superoxide dismutase on their formation, Biochem. Pharmacol. 84 (2012) 949-960.

[8] S.J. Klebanoff, Myeloperoxidase: friend and foe, J. Leukoc. Biol. 77 (2005) 598-625.

[9] N.M. Iovine, S. Pursnani, A. Voldman, G. Wasserman, M.J. Blaser, Y. Weinrauch, Reactive Nitrogen Species Contribute to Innate Host Defense against Campylobacter jejuni, Infect. Immun. 76 (2008) 986-993.

[10] H.L. Wright, R.J. Moots, R.C. Bucknall, S.W. Edwards, Neutrophil function in inflammation and inflammatory diseases, Rheumatology, 49 (2010) 1618-1631.

[11] S. Behar, C. Martin, M. Booty, T. Nishimura, X. Zhao, H. Gan, M. Divangahi, H. Remold, Apoptosis is an innate defense function of macrophages against Mycobacterium tuberculosis, Mucosal Immunol. 4 (2011) 279-287.

[12] S. Ehrt, D. Schnappinger, Mycobacterial survival strategies in the phagosome: Defense against host stresses, Cell. Microbiol. 11 (2009) 1170-1178.

[13] M.I. Voskuil, I. Bartek, K. Visconti, G.K. Schoolnik, The response of Mycobacterium tuberculosis to reactive oxygen and nitrogen species, Front. Microbiol. 2 (2011).

[14] M. Chen, H. Gan, H.G. Remold, A Mechanism of Virulence: Virulent Mycobacterium tuberculosis Strain H37Rv, but Not Attenuated H37Ra, Causes Significant Mitochondrial Inner Membrane Disruption in Macrophages Leading to Necrosis, J. Immunol. 176 (2006) 3707-3716.

[15] G.D. Birnie, The HL60 cell line: a model system for studying human myeloid cell differentiation, Br. J. Cancer. Suppl. 9 (1988) 41-45.

[16] S.W. Ballinger, C. Patterson, C.-N. Yan, R. Doan, D.L. Burow, C.G. Young, F.M. Yakes, B. Van Houten, C.A. Ballinger, B.A. Freeman, M.S. Runge, Hydrogen Peroxide– and Peroxynitrite-Induced Mitochondrial DNA Damage and Dysfunction in Vascular Endothelial and Smooth Muscle Cells, Circ. Res. 86 (2000) 960-966.

[17] M. Whiteman, J.P.E. Spencer, H.H. Szeto, J.S. Armstrong, Do Mitochondriotropic Antioxidants Prevent Chlorinative Stress-Induced Mitochondrial and Cellular Injury?, Antioxid. Redox Signal. 10 (2007) 641-650.

[18] S.R. Khan, A. Baghdasarian, P.H. Nagar, R. Fahlman, P. Jurasz, K. Michail, N. Aljuhani, A.G. Siraki, Proteomic profile of aminoglutethimide-induced apoptosis in HL-60 cells: Role of myeloperoxidase and arylamine free radicals, Chem. Biol. Interact. 239 (2015) 129-138.

[19] E. Pick, Y. Keisari, A simple colorimetric method for the measurement of hydrogen peroxide produced by cells in culture, J. Immunol. Methods 38 (1980) 161-170.

[20] S.R. Khan, A. Baghdasarian, R.P. Fahlman, K. Michail, A.G. Siraki, Current status and future prospects of toxicogenomics in drug discovery, Drug Discov. Today 19 (2014) 562-578.

[21] M. Reers, T.W. Smith, L.B. Chen, J-aggregate formation of a carbocyanine as a quantitative fluorescent indicator of membrane potential, Biochemistry 30 (1991) 4480-4486.

[22] K.K. Lee, U.A. Boelsterli, Bypassing the compromised mitochondrial electron transport with methylene blue alleviates efavirenz/isoniazid-induced oxidant stress and mitochondria-mediated cell death in mouse hepatocytes, Redox Biol. 2 (2014) 599-609.

[23] J. Huang, F. Smith, P. Panizzi, Ordered Cleavage of Myeloperoxidase Ester Bonds Releases Active site Heme Leading to Inactivation of Myeloperoxidase by Benzoic Acid Hydrazide Analogs, Arch. Biochem. Biophys. 548 (2014) 74-85.

[24] U.A. Boelsterli, K.K. Lee, Mechanisms of isoniazid-induced idiosyncratic liver injury: Emerging role of mitochondrial stress, J. Gastroenterol. Hepatol. 29 (2014) 678-687.

[25] B.E. Svensson, Myeloperoxidase oxidation states involved in myeloperoxidase-oxidase oxidation of thiols, Biochem. J. 256 (1988) 751-755.

[26] I. Yamazaki, K.-n. Yokota, Oxidation states of peroxidase, Mol. Cell. Biochem. 2 (1973) 39-52.

[27] S.M. Attia, Deleterious effects of reactive metabolites, Oxid. Med. Cell. Longev. 3 (2010) 238-253.

[28] R.M. LoPachin, A.P. DeCaprio, Protein Adduct Formation as a Molecular Mechanism in Neurotoxicity, Toxicol. Sci. 86 (2005) 214-225.

[29] D.G. Cornwell, J. Ma, Nutritional Benefit of Olive Oil: The Biological Effects of Hydroxytyrosol and Its Arylating Quinone Adducts, J. Agric. Food Chem. 56 (2008) 8774-8786.

[30] Myers TG1, Dietz EC, Anderson NL, Khairallah EA, Cohen SD, N. SD., A comparative study of mouse liver proteins arylated by reactive metabolites of acetaminophen and its nonhepatotoxic regioisomer, 3'-hydroxyacetanilide., Chem. Res. Toxicol. 8 (1995) 403-413.

[31] A.M. Matthews, J.A. Hinson, D.W. Roberts, N.R. Pumford, Comparison of covalent binding of acetaminophen and the regioisomer 3′-hydroxyacetanilide to mouse liver protein, Toxicol. Lett. 90 (1997) 77-82.

[32] A.M. Matthews, D.W. Roberts, J.A. Hinson, N.R. Pumford, Acetaminophen-induced hepatotoxicity. Analysis of total covalent binding vs. specific binding to cysteine, Drug Metab. Dispos. 24 (1996) 1192-1196.

[33] Z. Cai, L.J. Yan, Protein Oxidative Modifications: Beneficial Roles in Disease and Health, J. Biochem. Pharmacol. Res. 1 (2013) 15-26.

[34] I.G. Metushi, P. Cai, X. Zhu, T. Nakagawa, J.P. Uetrecht, A Fresh Look at the Mechanism of Isoniazid-Induced Hepatotoxicity, Clin. Pharmacol. Ther. 89 (2011) 911-914.

[35] I.G. Metushi, C. Sanders, G. The Acute Liver Study, W.M. Lee, J. Uetrecht, Detection of anti-isoniazid and anti–cytochrome P450 antibodies in patients with isoniazid-induced liver failure, Hepatology 59 (2014) 1084-1093.

[36] I.G. Metushi, T. Nakagawa, J. Uetrecht, Direct Oxidation and Covalent Binding of Isoniazid to Rodent Liver and Human Hepatic Microsomes: Humans Are More Like Mice than Rats, Chem. Res. Toxicol. 25 (2012) 2567-2576.

[37] I.G. Metushi, P. Cai, L. Vega, D.M. Grant, J. Uetrecht, Paradoxical Attenuation of Autoimmune Hepatitis by Oral Isoniazid in Wild-Type and N-Acetyltransferase–Deficient Mice, Drug Metab. Dispos. 42 (2014) 963-973.

[38] X. Meng, J.L. Maggs, T. Usui, P. Whitaker, N.S. French, D.J. Naisbitt, B.K. Park, Auto-oxidation of Isoniazid Leads to Isonicotinic-Lysine Adducts on Human Serum Albumin, Chem. Res. Toxicol. 28 (2015) 51-58.

[39] H. A., l. Shoeb, B. U., J. Bowman, A. C., l. Ottolenghi, A.J. Merola, Enzymatic and Nonenzymatic Superoxide-Generating Reactions of Isoniazid, Antimicrob. Agents Chemother. 27 (1985) 408-412.

[40] L.A. Marquez, H.B. Dunford, Reaction of compound III of myeloperoxidase with ascorbic acid, J. Biol. Chem. 265 (1990) 6074-6078.

[41] C. Candé, I. Cohen, E. Daugas, L. Ravagnan, N. Larochette, N. Zamzami, G. Kroemer, Apoptosis-inducing factor (AIF): a novel caspase-independent death effector released from mitochondria, Biochimie, 84 (2002) 215-222.

[42] J.Q. Ho, M. Asagiri, A. Hoffmann, G. Ghosh, NF-κB Potentiates Caspase Independent Hydrogen Peroxide Induced Cell Death, PLoS ONE, 6 (2011) e16815.

[43] Y.-O. Son, Y.-S. Jang, J.-S. Heo, W.-T. Chung, K.-C. Choi, J.-C. Lee, Apoptosis-inducing factor plays a critical role in caspase-independent, pyknotic cell death in hydrogen peroxide-exposed cells, Apoptosis, 14 (2009) 796-808.

[44] W.-X. Zong, C.B. Thompson, Necrotic death as a cell fate, Genes & Dev. 20 (2006) 1-15.

3.8 FIGURES AND LEGENDS

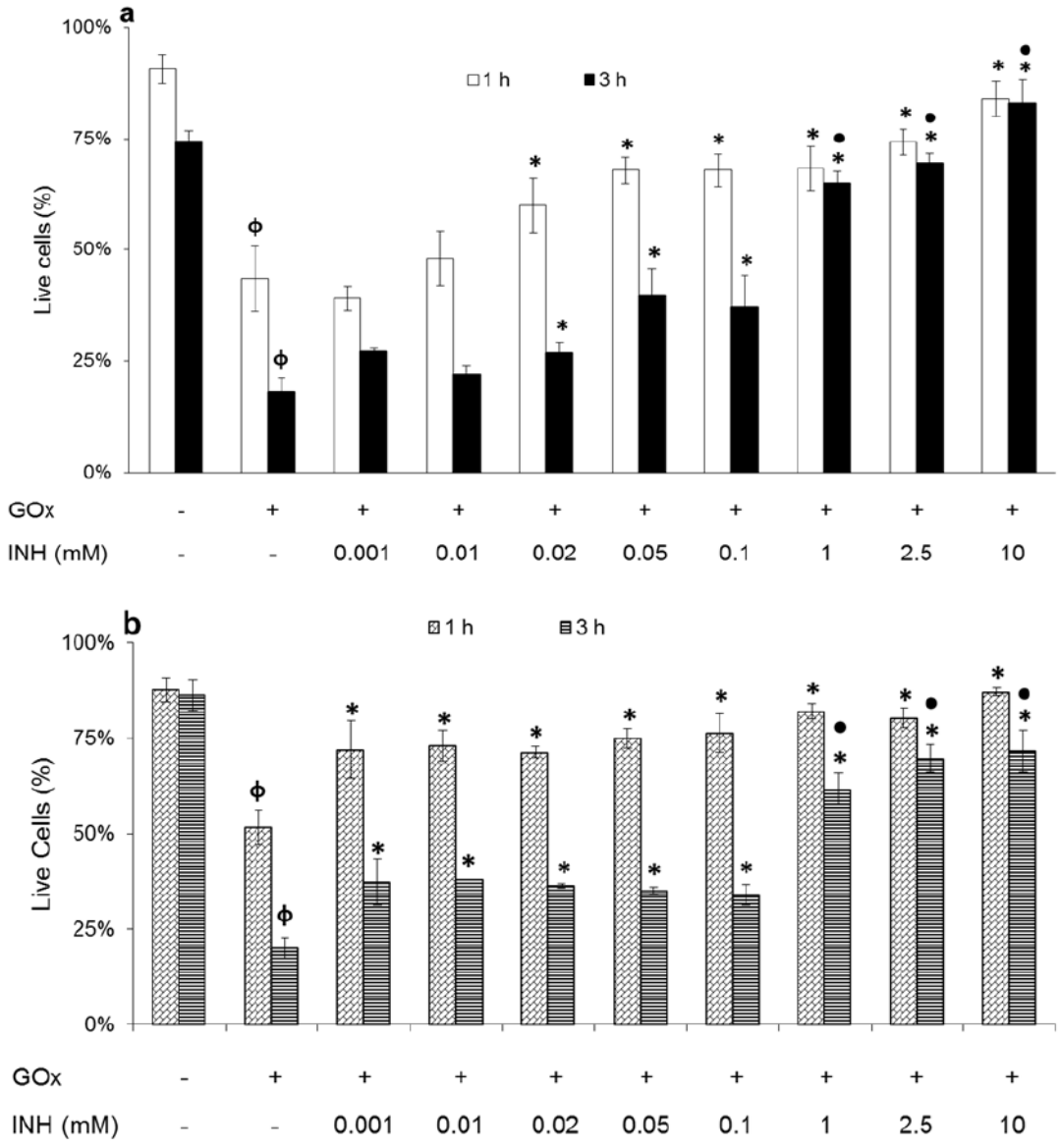

3.8.1 Figure 1. Trypan blue exclusion cell viability assay. Effect of INH without preincubation on HL-60 cells treated with GOx for 1 h and 3 h (a). ϕ $P < 0.001$ compared to untreated HL-60

cells (bar 1), * $p < 0.001$ compared to GOx (25 mU/mL) treated cells (bar 2); • $p < 0.001$ compared to INH (1 – 100 μM). Effect of INH preincubation (4 h) on HL-60 cells treated with GOx for 1 and 3 h (b); ϕ $P<0.001$ compared to untreated HL-60 cells (bar 1), * $p < 0.001$ compared to GO treated cells (bar 2). ● $p < 0.001$ compared to INH (1 – 100 μM). Data represent 3 independent experiments.

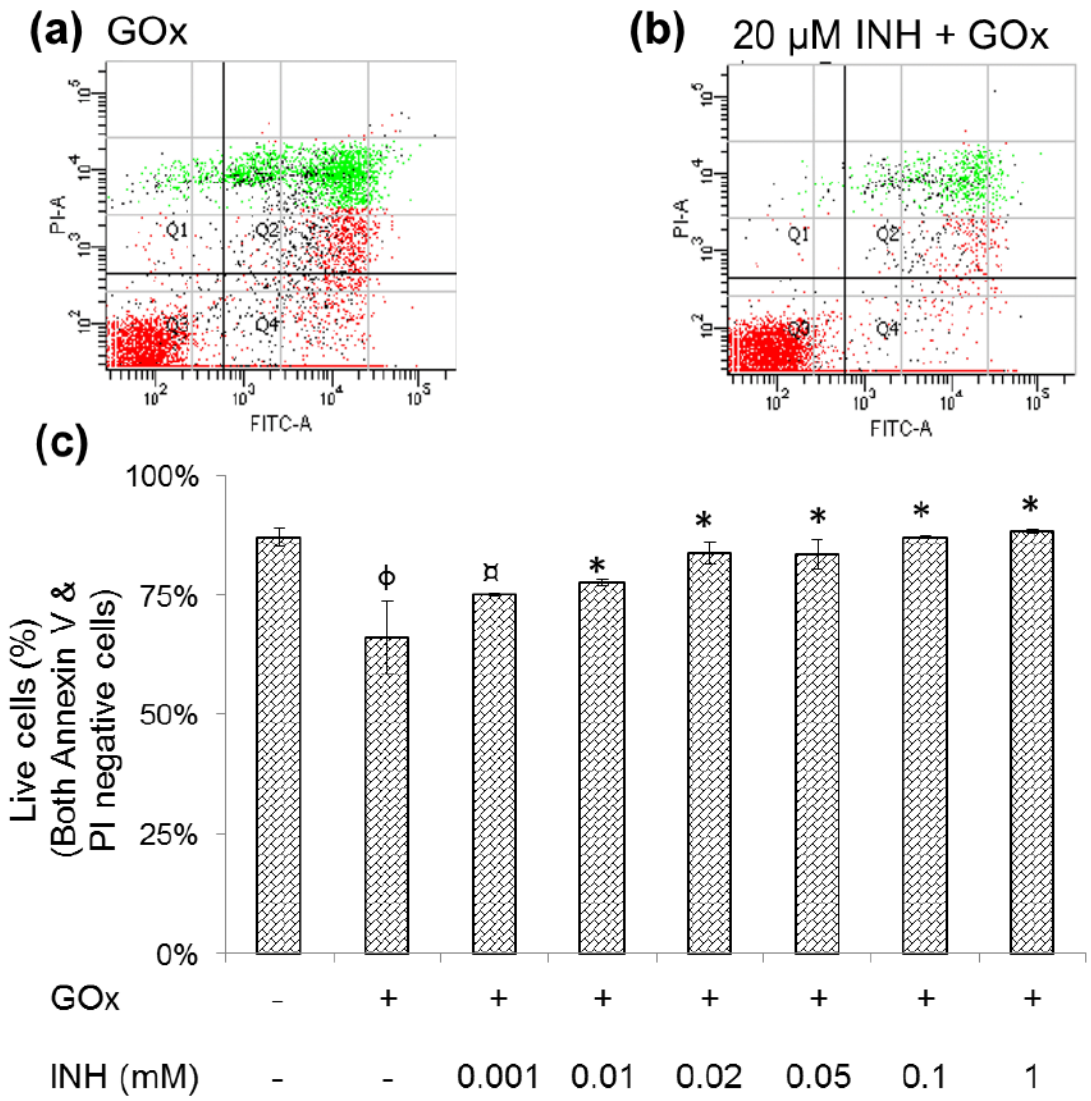
(a) GOx
(b) 20 μM INH + GOx
PI-A
FITC-A
Q1
Q2
Q3
Q4
(c)
Live cells (%)
(Both Annexin V &
PI negative cells)
100%
75%
50%
25%
0%
GOx
INH (mM)
-
-
0.001
0.01
0.02
0.05
0.1
1

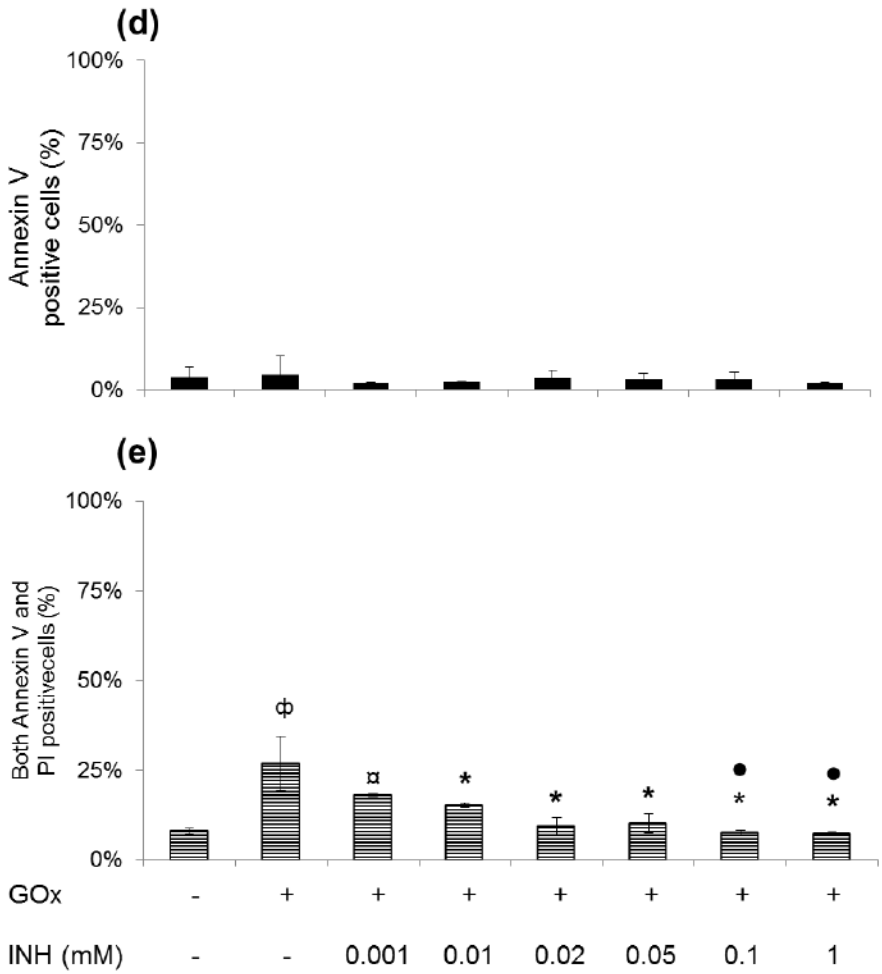

3.8.2 Figure 2. Flow cytometry analysis for INH 4 h preincubated HL-60 cells. Representative dot plots (a and b) demonstrating the population of cells at different stages (live cells – Q3; early apoptosis – Q4; late apoptosis/necrosis – Q2; dead/necrotic cells – Q1). The cytoprotective effect of 20 μM INH preincubated for 4 h against GOx (25 mU/mL) injury is shown for visual comparison; (c) live cell count (negative for both Annexin V and PI staining) after 1 h of GOx exposure on HL-60 cells preincubated (4 h) with INH; (d) Early apoptotic death (Annexin-V positive only) after 1 h of GOx exposure on HL-60 cells preincubated (4 h) with INH, and (e) INH preincubation (4 h) significantly reduces GOx-induced late apoptosis/necrosis

(both Annexin-V and PI positive). ϕ $p < 0.001$ in comparison with untreated HL-60 cells, ¤ $p < 0.005$ GOx vs GOx + (0.001 mM) INH preincubated cells, * $p < 0.001$ GOx vs. GOx + (0.01 to 1 mM) INH preincubated cells.

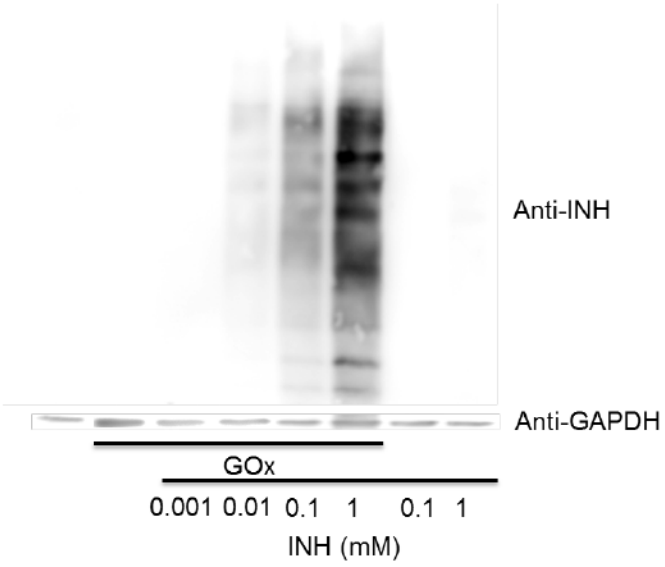

3.8.3 Figure 3. Concentration-dependent formation of INH-protein adducts in HL-60 cells. Cells were treated with INH for 4 h after which GOx (25 mU/mL) was added (where indicated) and incubated further for 1 h before cell lysis. INH-protein adducts appeared to require the presence of INH and GOx during these incubation periods.

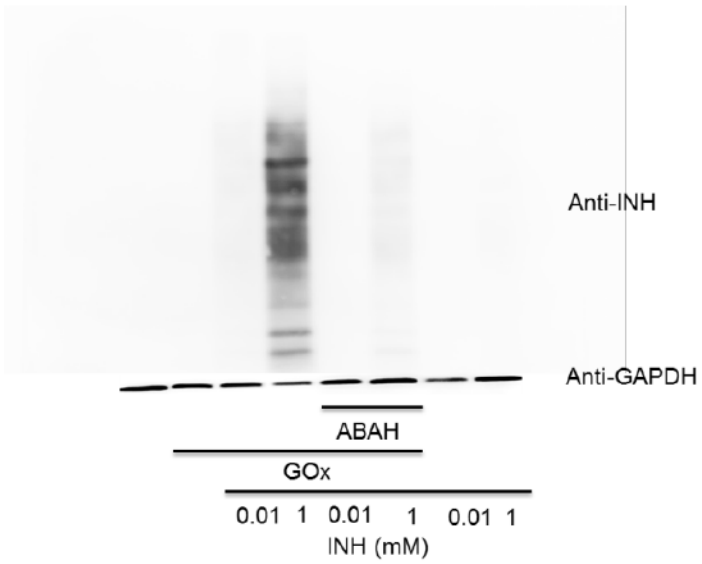

3.8.4 Figure 4. Role of MPO in INH-protein adduct formation. Cells were treated with INH (lanes 7 & 8), INH and GOx (lanes 3 & 4), or with INH, GOx, and 100 μM ABAH (MPO inhibitor; (lane 5 & 6). INH-protein adduct formation was dependent on the presence of GOx, suggesting H_2O_2 was necessary for INH oxidation to reactive metabolites. Comparison between lane 4 and lane 6 as well as lane 3 and lane 5 showed that MPO inhibition significantly decreased INH-protein adduct formation. (This blot is representative of at least 3 independent experiments).

5A

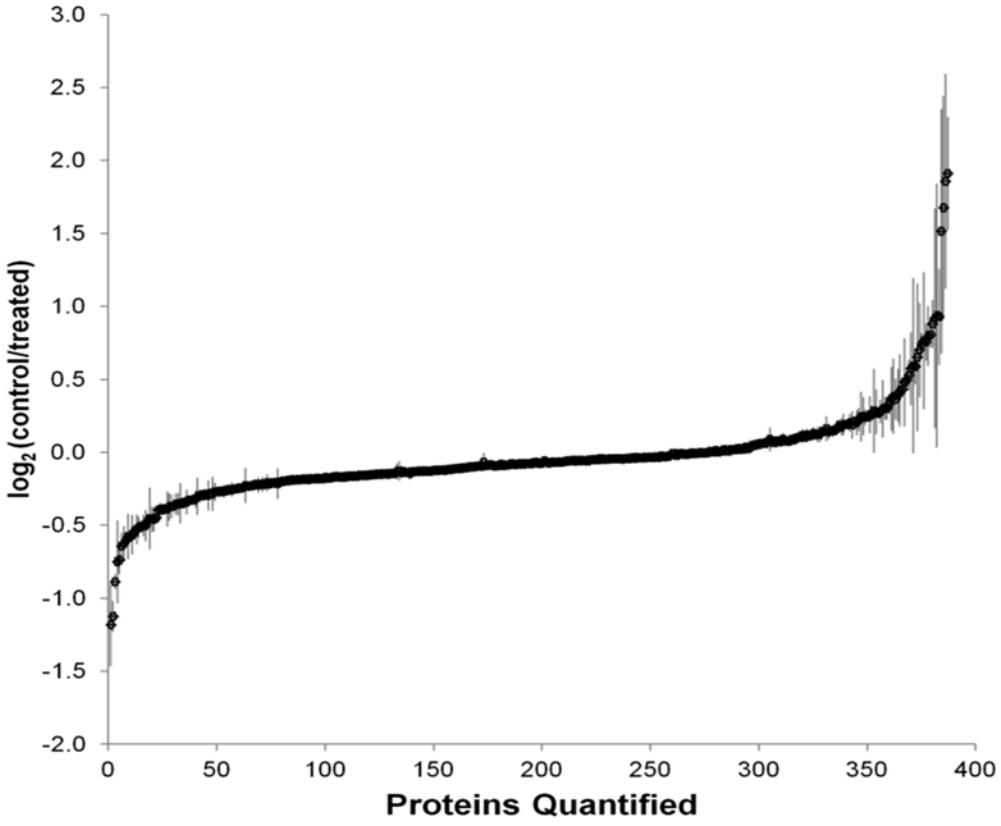
3.0
2.5
2.0
1.5
1.0
0.5
0.0
-0.5
-1.0
-1.5
-2.0
log2 (control/treated)
0
50
100
150
200
250
300
350
400
Proteins Quantified

5B

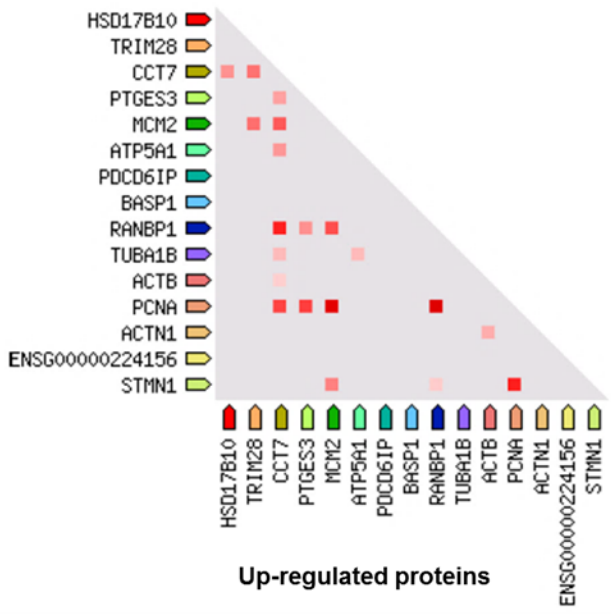
HSD17B10
TRIM28
CCT7
PTGES3
MCM2
ATP5A1
PDCD6IP
BASP1
RANBP1
TUBA1B
ACTB
PCNA
ACTN1
ENSG00000224156
STMN1
Up-regulated proteins

5C

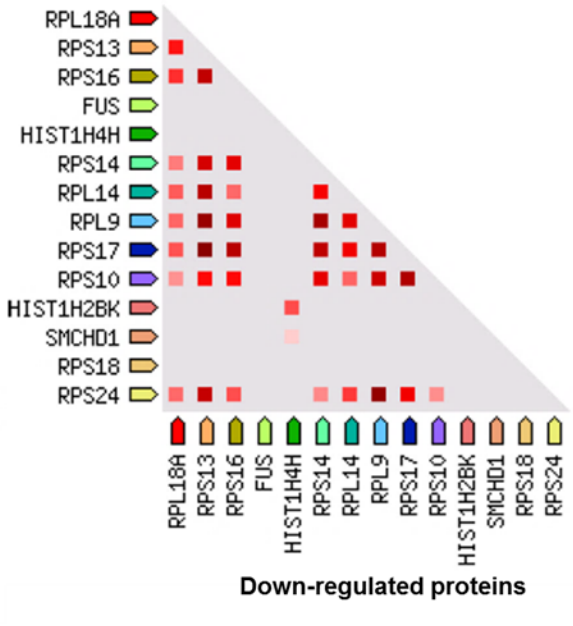
RPL18A
RPS13
RPS16
FUS
HIST1H4H
RPS14
RPL14
RPL9
RPS17
RPS10
HIST1H2BK
SMCHD1
RPS18
RPS24
Down-regulated proteins


- Coexpression -
association score
0.0
1.0

3.8.5 Figure 5. Protein changes in abundance and coexpression analysis. All reproducible proteins in both sample A and B were analyzed here for their changes in expression based on Log2 value in figure 5A. It showed that most of the proteins were not changed in abundance upon treatment of INH on GOx treated HL-60 cells. Later, the proteins which were significantly changed in abundance (reported on Table 1) were further analyzed for coexpression by using String v.9.1. The association score for up-regulated proteins (15 proteins) were showed in figure 5B, whereas the association score for down-regulated proteins (14 proteins) were showed in figure 5C. Darker points indicate a stronger association, as shown by the association score gradient.

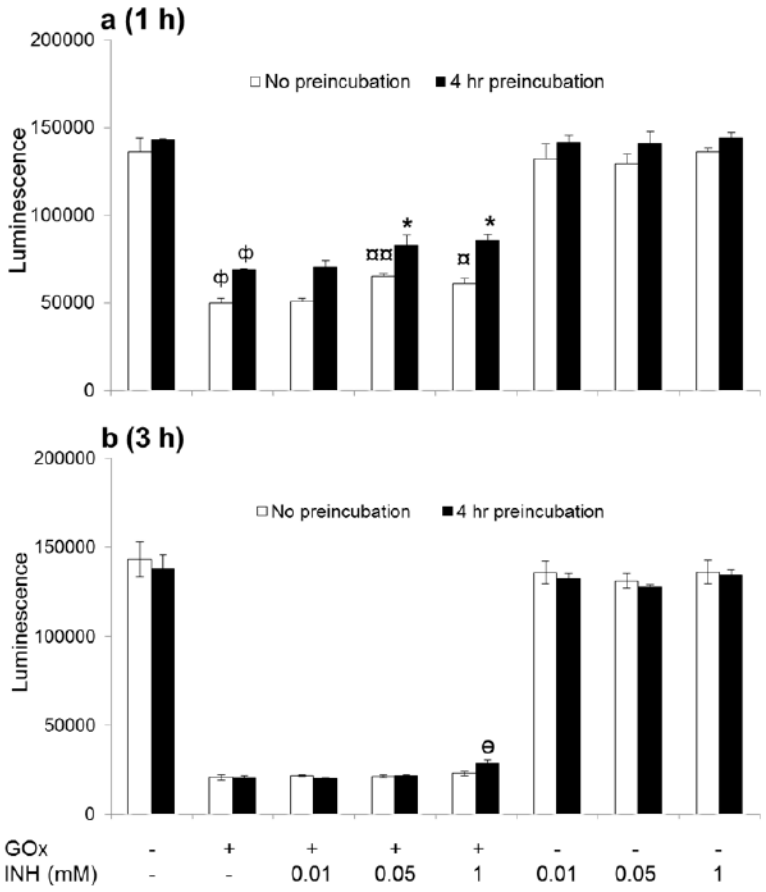

3.8.6 Figure 6. INH attenuated ATP decrease induced by GOx at 1 h, but not at 3 h. (a) Relative ATP levels after 1 h of GOx exposure on 0 h and 4 h INH pre-incubated HL-60 cells; ϕ $p < 0.001$ compared to untreated HL-60 cells. * $p < 0.001$ compared to GOx treated cells. ¤ $p < 0.05$ and ¤¤ $p < 0.005$ compared to GOx treated cells. (b) Relative ATP levels after 3 h between 0 h and 4 h INH pre-incubated HL-60 cells; ɵ $p < 0.05$ compared to GOx treated cells.

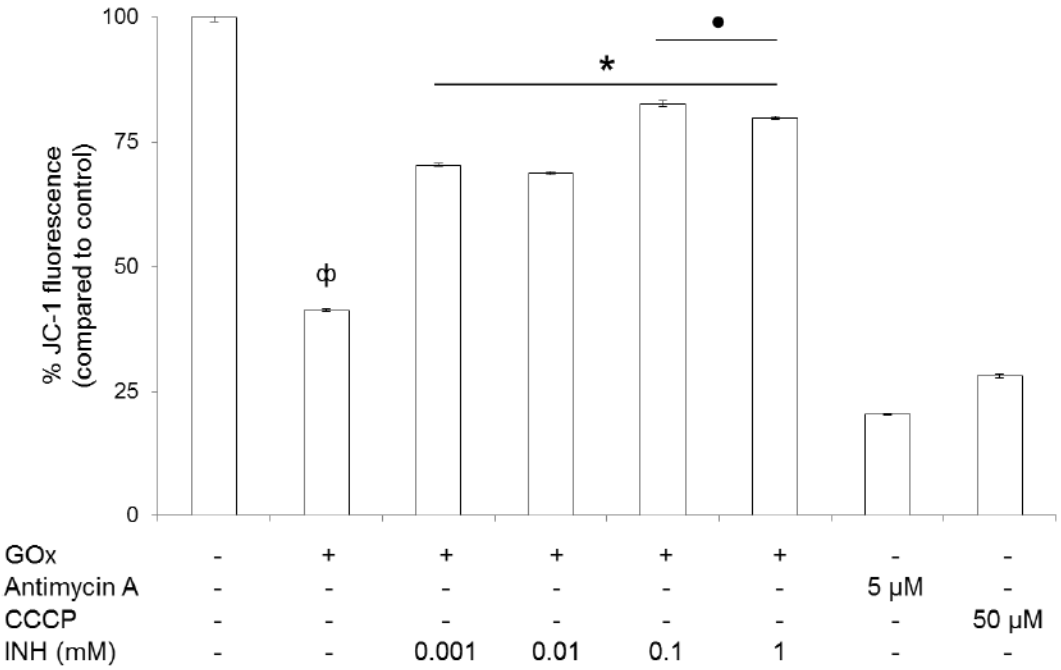

3.8.7 Figure 7. Effect of INH on mitochondrial membrane potential of GOx challenged HL-60 cells. Cells were pretreated with INH for 4 h and then treated with GOx for 1 h. Mitochondrial membrane potential was then assessed using JC-1 fluorescence as described in Materials and methods followed by converted into percentage by taking the fluorescence measurement of untreated cells as 100%. Each measurement represents n=6. ϕ $P < 0.001$ compared to untreated cells. * $P < 0.001$ compared to GOx treated cells. • $P < 0.001$ compared to lower INH concentrations (0.001 - 0.01 mM).

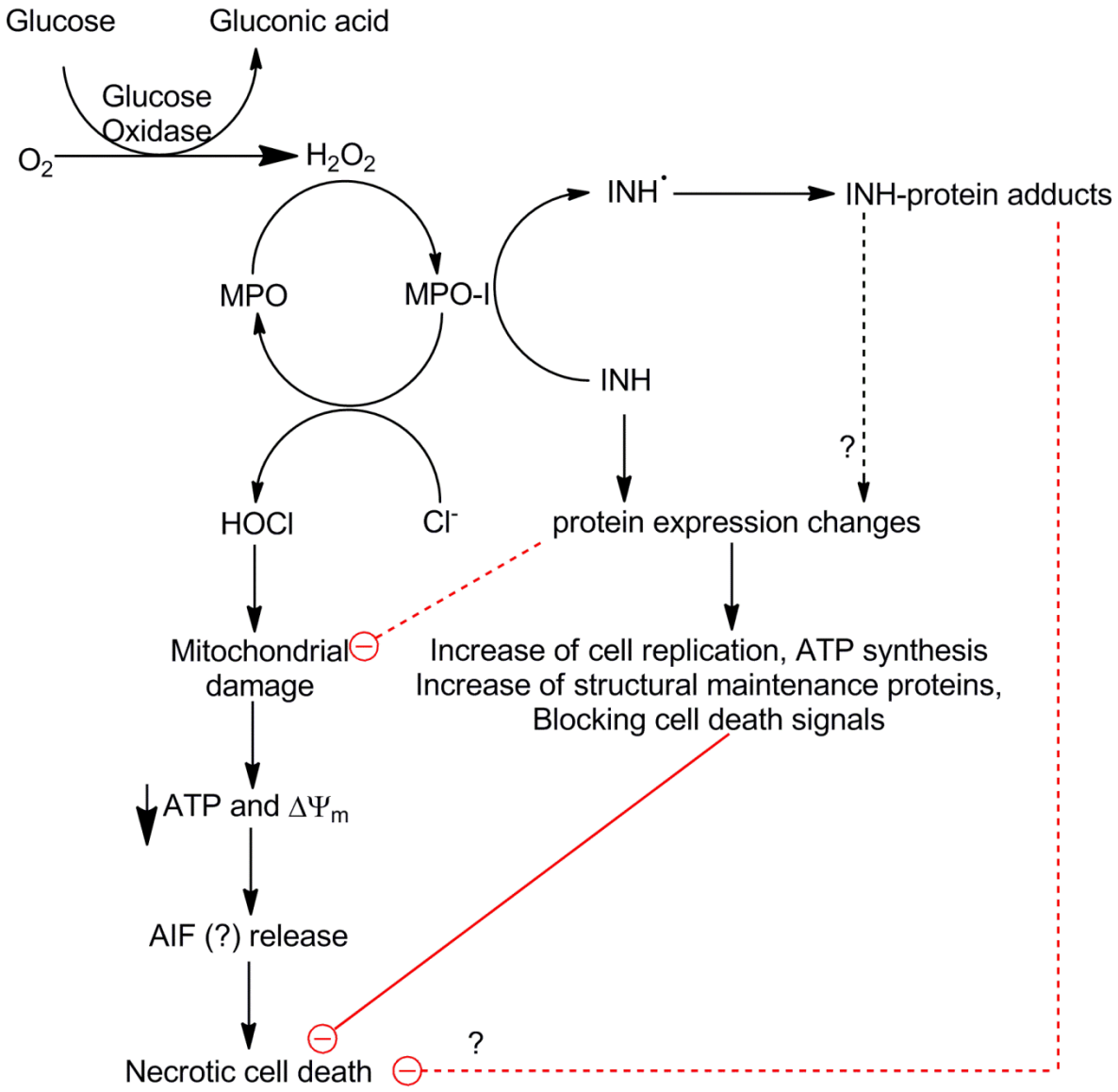

3.8.8 Figure 8: Summary of INH-induced cytoprotection against ROS. ROS (H_2O_2) generated through GOx activated MPO which can oxidize INH to INH•. INH has dual effects on activated MPO. At high concentrations (~ 1 mM), INH can inhibit MPO as well as change the expression of numerous proteins. These proteins' functions are involved in increasing the cell replication process, ATP synthesis and structural maintenance, and inhibition of apoptosis. At

low concentration (~ 100 μM), INH can be oxidized into INH• and form covalent adducts with various proteins. There was an apparent correlation between INH-protein adducts and cytoprotective activity; however, it is not known if INH-protein adducts were causative in this effect.

3.9 TABLE

Table 1. Up and Down- regulated proteins observed upon INH treatment.

Accession	Description	Unique Peptides Sample A	Unique Peptides Sample B	Average Change (control/treated) +/- SD
	Up Regulated Proteins			
Q99714	Isoform 2 of 3-hydroxyacyl-CoA dehydrogenase type-2	7	7	0.44±0.11
P12004	Proliferating cell nuclear antigen	2	3	0.46±0.04
P80723	Brain acid soluble protein 1	5	7	0.54±0.03
C9JXG8	Ran-specific GTPase-activating protein (Fragment)	2	2	0.60±0.23
Q13263	Isoform 2 of Transcription intermediary factor 1-beta	3	3	0.60±0.08
P49736	DNA replication licensing factor MCM2	2	4	0.64±0.09
P07437	Tubulin beta chain	5	5	0.65±0.12
P68363	Tubulin alpha-1B chain	8	13	0.66±0.06
P12814	Alpha-actinin-1	4	5	0.67±0.18
P16949	Stathmin	3	3	0.67±0.03
Q8WUM4	Programmed cell death 6-interacting protein	2	3	0.68±0.16
P60709	Actin, cytoplasmic 1	22	23	0.69±0.02

Q99832	T-complex protein 1 subunit eta	9	10	0.70±0.14
A8K092	ATP synthase subunit alpha	3	4	0.70±0.10
B4DP21	Prostaglandin E synthase 3	5	4	0.70±0.06

Down Regulated Proteins

P62269	40S ribosomal protein S18	8	8	1.44±0.29
P32969	60S ribosomal protein L9	4	4	1.49±0.64
P46783	40S ribosomal protein S10	2	2	1.504±0.30
P62277	40S ribosomal protein S13	4	6	1.67±0.17
B4DR70	RNA-binding protein FUS	2	2	1.69±0.28
P62249	40S ribosomal protein S16	6	5	1.74±0.45
P62847	Isoform 2 of 40S ribosomal protein S24	3	4	1.75±0.20
P50914	60S ribosomal protein L14	3	4	1.84±0.34
B4DM74	60S ribosomal protein L18a	2	4	1.89±1.55
P62263	40S ribosomal protein S14	3	4	1.91±0.67
Q96KK5	Histone H2A type 1-H	5	7	2.86±1.6
P08708	40S ribosomal protein S17	4	3	3.20±1.46
P62805	Histone H4	9	10	3.63±1.43
O60814	Histone H2B type 1-K	3	3	3.76±0.76

CHAPTER 4:

ISONIAZID INDUCES MONOCYTIC DIFFERENTIATION IN HL-60 CELLS

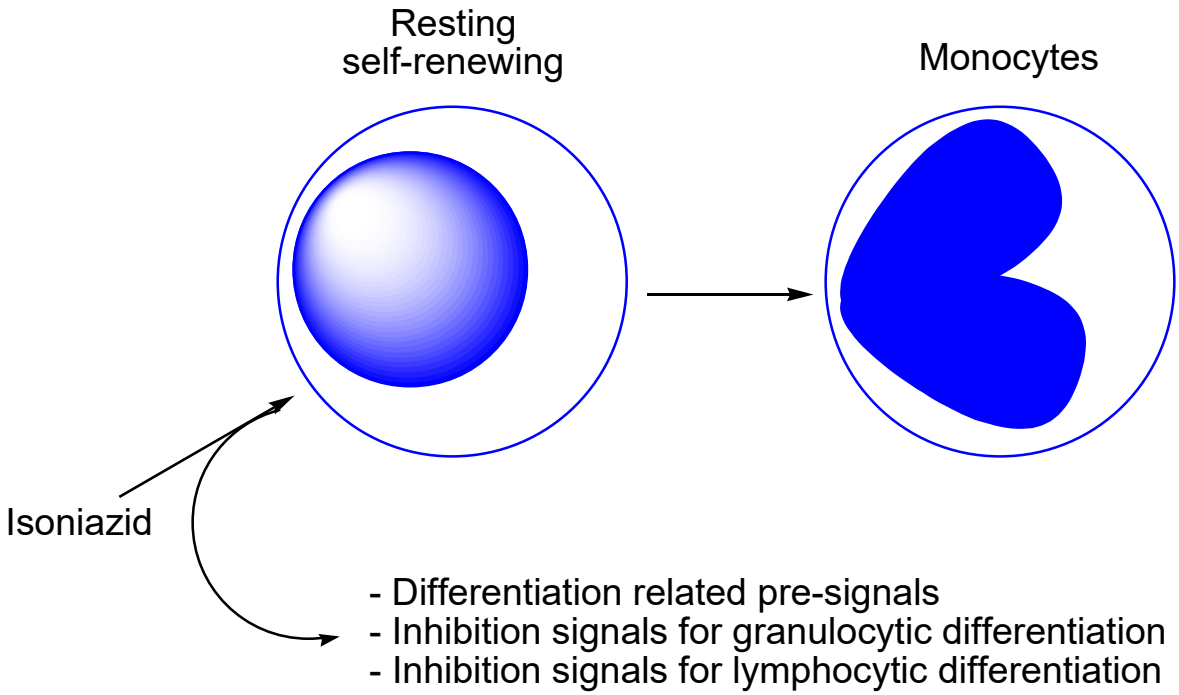

4.1 ABSTRACT

Monocytes and monocyte-derive macrophages play an important role in host immune defense against tuberculosis (TB). Although isoniazid (INH) is an important drug used for both latent and active TB, it is unknown whether INH has any role in monocytic differentiation from myeloid progenitor stem cells. In this *in vitro* study, HL-60 cells, a model myeloid progenitor cell line which is capable of differentiating into granulocytes, monocytes, and dendritic cells, was treated with different concentrations of INH. Quantitative proteomics revealed 21 proteins that were down-regulated significantly. The protein-protein interactions analysis of these proteins showed a high degree of association and was indicative for the pre-signals of monocytic differentiation. INH-induced monocytic differentiation has been confirmed to occur in a concentration-dependent manner through several markers such as nonspecific esterase activity, NADPH oxidase activity and expression of surface markers CD14 and CD16 (characteristic of monocytes). This study revealed INH as a chemical stimulus for monocytic differentiation in HL-60 cells and confirmed at least 25% cells were differentiated within the range of the pharmacological concentrations of INH.

Keywords: Differentiation, Monocytes, GM progenitor stem cells, Isoniazid.

4.2 INTRODUCTION

Isoniazid (INH) is still the mainstay of the treatment of both active and latent tuberculosis (TB) [1, 2]. It has been proposed as a synthetic antibiotic which inhibits the mycolic acid biosynthesis, an essential cell wall component of *Mycobacterium tuberculosis* (*Mtb*) [3]. INH is a prodrug and is activated by a bacterial enzyme, known as KatG. [3]. Our group has shown that INH can be bioactivated in human neutrophils through myeloperoxidase activity [4]. Beside its antibacterial properties, there is little known about its effects on host systems except its toxicities [5].

Macrophages are considered as the host's first-line immune defense against *Mtb*. After engulfing *Mtb* from lung airways, the alveolar macrophages either kill the bacilli or form granuloma by recruiting other immune cells to halt the dissemination of infection [6, 7]. In granulomas, bacilli remain non-replicating but energy-generating [8], which are capable of killing the immune cells through necrosis [9]. A possible mechanism of *Mtb*-induced necrosis has been described by the macrophage itself producing excessive reactive species (RS) which damage its own mitochondria and leads to necrotic cell death [10]. It is noteworthy that our recent study showed the cytoprotective effect of INH against oxidative stress in HL-60 cells; the latter is a human promyelocytic leukemia cell line which can be differentiated like granulocyte-monocyte (GM) progeny stem cells [11, 12].

To prevent active TB, the corner-stone of the host defense mechanism is to halt the *Mtb* within granuloma. The death of macrophages within the granuloma during TB infection will weaken the host defense. To compensate for macrophage death, both or one of following necessary steps should be adopted by our host system: (1) inhibition of the death of macrophage, and (2)

recruitment of more monocytes at the granuloma. We have already shown that INH may have a role to inhibit the necrotic cell death of macrophage [11]; however, it is not known if INH has any role in the recruitment of more monocytes at the granuloma.

For more monocytes recruitment at the granuloma, more monocytes are needed in circulation. For more monocytes in circulation, more monocytic differentiation is required from GM progeny stem cells. One study revealed that niacin (structurally similar to INH) can induce granulocytic differentiation in HL-60 cells [13]; and another study in HL-60 cells showed that isonicotinic acid (a metabolite of INH) can induce expression of CD38, a surface marker of resting monocytes [14]. Although these studies point towards the role of INH in immune cell differentiation, there is no such "INH-induced differentiation" study. Therefore, it has been hypothesized here that INH may play an important role in monocytic differentiation from GM progeny stem cells. In this study, a global proteomics study was conducted initially to understand the effects of INH at protein levels; which indicates INH-induced certain type of differentiation in HL-60 cells, particularly it may be monocytic differentiation. Further studies were carried out to identify such differentiation with its subpopulations.

4.3 METHODS AND MATERIALS

4.3.1 Chemicals and Kits

Isoniazid (INH), 1α, 25-Dihydroxyvitamin D_3 (VitD3), retinoic acid (RA), sodium fluoride (NaF), nitrotetrazolium blue chloride (NBT), phorbol 12-myristate 13-acetate (PMA), and α-naphthyl acetate (non-specific esterase) (Product No.: 91A) were purchased from Sigma-Aldrich Canada Co. (Oakville, ON). Diphenyleneiodonium chloride (DPI) was purchased from Santa Cruz biotechnology (Dallas, TX). Pierce™ BCA Protein Assay Kit was purchased from

ThermoFisher Scientific (Burlington, ON). All other chemicals, unless otherwise noted, were from Sigma Chemical Co (Oakville, ON).

4.3.2 Antibodies and enzymes

PE-mouse anti-human CD16 (PE-CD16) and APC mouse anti-human CD14 (APC-CD14) were purchased from BD Biosciences (San Jose, CA).

4.3.3 HL-60 cells

HL-60 cells were purchased from ATCC (Cat No. CCL-240, Manassas, VA). The cell growth medium contained RPMI-1640 medium (Gibco ® Reference No. 11875-093), 10% fetal bovine serum (FBS) (Gibco® Cat No. 12483) and 1% of Antibiotic-Antimycotic (Gibco® Reference No. 15240-062). An incubator was used to maintain cells at 5% CO_2 and 37°C, and media was changed every 2 days. No HL-60 cells were used in experiments that had a passage number more than 30.

4.3.4 Monocyte isolation from human blood

Human monocytes were collected from the blood of healthy donors by consent granted from the Human Ethics Research Office of the University of Alberta by a methodology described elsewhere [15]. In brief, the peripheral whole blood was drawn and diluted with PBS in 1:1 ratio. The diluted whole blood was layered on 15 ml of ficoll in a 50 ml tube. It was then centrifuged at 400 g for 30 mins with the brakes-off setting. It produced four distinct layers where the second layer from the top layer was peripheral blood mononuclear cells (PBMCs). It was collected and again diluted with 1X PBS, followed by centrifugation at 300 g for 10 mins. The cell pellets were collected and wash with 1X sterile PBS. The RPMI-1640 complete medium was added and

incubated for 30 mins at 37°C. Monocytes adhered on the tube surface. By discarding the supernatant, monocytes were isolated from all other PBMCs.

4.3.5 Trypan blue exclusion cytotoxicity assay

HL-60 cells were treated with different concentrations (1 μM to 10 mM) of INH for 12 h in 6-well plates at 1×10^6 cells/ml (>95% viability) at 5% CO_2 and 37°C. At the end of the experiment, a cell sample from each reaction and 0.4% trypan blue reagent (Lonza, Anaheim, CA) were mixed at a 1:1 ratio and the cell viability was measured by using a TC-10 automated cell counter (Bio-Rad Laboratories).

4.3.6 SILAC Experiment

4.3.6.1 SILAC Cell culture

For this method, HL-60 cells were cultured in two different types of media: heavy and light. Firstly, the RPMI-1640 medium without L-lysine, L-arginine and L-leucine was purchased from Sigma Chemical Co. We added L-leucine to the RPMI-1640 medium (0.05 mg/mL). 10% dialyzed fetal bovine serum (FBS), obtained from Invitrogen, was also added to RPMI-1640 medium. Afterward, the RPMI-1640 was divided equally into two parts to make either heavy or light media. For heavy medium, heavy L-lysine and L-arginine ($^{13}C_6$-L-Lysine and $^{13}C_6$-L-Arginine) were added to make a final concentration of 0.04 mg/mL and 0.2 mg/mL respectively into one part of RPMI-1640 medium. To make a light medium, we added unlabeled L-lysine and L-arginine in as same concentrations as in heavy medium into another part of RPMI-1640. Cells were then maintained in both heavy and light media separately under a humidified atmosphere with 5% CO_2 at 37ºC. The medium renewal was every 2-3 days depending on cell density. The

HL-60 cells were cultured in both heavy and light media separately for at least 7 passages to achieve complete isotope incorporation [16].

4.3.6.2 SILAC Cell treatment and lysis

Heavy and light cells were treated with 2.5 mM INH for 4 hours in an incubator with 5% CO_2 at 37°C. The reactions were as follows: Sample A – the forward labeled sample was the mixture of control "untreated HL-60 cells, cultured in the light media" and the treatment "INH-treated HL-60 cells, cultured in the heavy (containing $^{13}C_6$-L-Lysine and$^{13}C_6$-L-Arginine) media". Sample B – the reverse labeled sample was the same as sample A but the labeling was reversed.

The control and treatment of both sample A (forward labeled sample) and sample B (reverse labeled sample) were lysed separately by using RIPA (0.05 g sodium deoxycholate, 100 µL of Triton X-100, and 0.01 g of SDS in 10 mL of PBS). For preparing either sample A or B, the protein content in control and treatment have to be in a 1:1 ratio. This was achieved by SDS-PAGE of the samples, followed by staining the gel with Coomassie blue, destaining and scanning the gel using LI-COR Odyssey gel scanner. The intensity of protein content in each lane provided a quantitative check the ratio of protein between control and treatment of each sample.

4.3.6.3 SDS-PAGE & Gel-Digestion

2× loading buffer (0.5 M Tris-HCl pH 6.8, 10% SDS, 1.5% Bromophenol Blue, 20% Glycerol and 5% β-mercaptoethanol) was mixed with cell lysates and the heavy and light labeled samples were combined in a 1:1 ratio. The samples were then heated to 95ºC for 5 minutes and then resolved on a 1.0 mm thick 10% polyacrylamide gel. After electrophoresis, the SDS gel was

stained with Coomassie Brilliant Blue and destained using 10% acetic acid solution to visualize the bands and lanes. The entire gel lanes were excised into 12 equal pieces for in-gel digestion.

4.3.6.4 In-gel digestion and LC-MS/MS analysis

In-gel digestion and LC-MS/MS analysis were carried out according to an in-house standard protocol which was described in one of our recent publications [17]. A total of 479 and 388 proteins were identified in sample A and B, respectively. Proteins those were reproducibly identified in both samples (260 proteins) were taken for further analysis. The expression changes were determined from the ratios of protein abundance followed by log2 calculation. The proteins which were also reproducible either down- or up-regulated by 0.5 on a log2 scale (~ over 40% changes in abundance) in both samples were reported here.

4.3.7 Non-specific esterase (NSE) activity

4.3.7.1 Reactions

The membrane-bound NSE is an important cytochemical marker for monocytes. These NSEs are mainly neutral serine-carboxyl esterase (80 -95%) which can be inhibited by NaF [18]. Here HL-60 (2.5 x 10^5 per ml) cells were either untreated or treated for 7 days with any of followings: 1 µM of vitD3, 0.1 µM of RA, and different concentration of INH (1µM, 10µM, 100µM, 1mM, and 10 mM). 2mM of NaF treatment was carried out for each of these reactions to inhibit NSE.

4.3.7.2 Colorimetric NSE activity assay

The colorimetric NSE activity assay was adopted from elsewhere [19]. In brief, cell pellets were collected after 7 days treatment and were lysed by using RIPA (0.05 g sodium deoxycholate, 100 µL of Triton X-100, and 0.01 g of SDS in 10 mL of PBS). The concentrations of proteins were

quantified by using Pierce™ BCA Protein Assay Kit and its protocol. 100 µg protein of each reaction was exposed to 100 µM of α-naphthalyl acetate (taken from Sigma-Aldrich, Catalogue number 91A-1KT) for 30 mins at 35°C. NSE is responsible for hydrolyzing α-naphthalyl acetate to free naphthol compounds which can be measured by using UV spectrophotometer (SpectraMax M5, Molecular devices) at 235nm.

4.3.7.3 Cytohistochemical microscopic NSE activity assay

The differentiated monocytes were identified cytohistochemically by α-napthyl acetate as per manufacturer's instructions (Sigma-Aldrich, Product No.: 91A-1KT). In brief, the seeded cells were fixed by using fixation solution (25 ml of 27 mM citrate solution, 65 ml of acetone, and 8 ml of 37% formaldehyde) for 30 secs. The staining solution (1 ml of sodium nitrite, 1 ml of fast blue BB, 40 ml of pre-warmed deionized water, 5 ml of TRIZMAL™ 7.6 concentrate, and 1 ml of α-napthyl acetate solution) was added to the fixed cells and kept in darkness for 30 min. The stained cells were washed three times with 1X PBS. The hematoxylin solution was added and kept for 2 mins followed by washing three times with 1X PBS. Coverslips containing gold antifade mounting medium were placed on top and stored at 4°C for overnight. These were analyzed under a microscope (Axio observer.A1, Zeiss) and its software pack (Axio 4.8). The slides were placed in an upright position on a microscope without water or immersion oil and were focused against white light.

4.3.8 NADPH Oxidase activity assay

NADPH activity is a hallmark enzyme for all professional phagocytic cells including monocytes and macrophages. However, it expresses to a lesser extent in monocytes and macrophages in comparison with neutrophils. It forms superoxide ($O_2^{\bullet-}$) from NADPH and oxygen. The

generated $O_2^{\bullet-}$ can reduce NBT to formazan which can be detected by UV spectrophotometer [20, 21]. Here, HL-60 (2.5 x 10^5 per ml) cells were either treated with any of followings: 1 µM of vitD3, 0.1 µM of RA, and different concentration of INH (1mM, 2.5mM, and 5 mM) or left untreated for 7 days in RPMI-1640 media containing 10% FBS and 1% antibiotic-antimycotic. Then cell pellets of each reaction were collected and activated by using 10 µM of PMA for 1 hour. Thereafter, NBT (1 mg/mL) was added to the cell pellets and incubated for 30 mins at room temperature. All reactants from pellets were removed by fixation through methanol, followed by centrifugation at 400 g for 5 min. A mixture of 1 M of sodium hydroxide, DMSO and isopropanol were used to dissolve the fixed pellets, followed by measuring the absorbance (λ_{max} 620 nm) by using HBSS media as a diluent in a spectrophotometer (SpectraMax M5, Molecular devices). 10 µM of DPI for 1 h pre-treatment was used to inhibit NADPH oxidase.

4.3.9 Image Stream Flow Cytometry

All reactions except 1 mM and 10 mM of INH were used here as described above (*3.2.7* NSE activity). After 7 days of incubation with INH, all reactions were assessed for live cells by using trypan blue exclusion method. 2x10^6 cells per reaction were taken for image stream flow cytometry study. Twice washed cell pellets were stained by staining solution (APC-CD14: PE-CD16: stain buffer 1:1:2), and incubated in darkness for 30 minutes at 4°C. The stained cells were twice washed with staining buffer at 4°C. Cytofix BD was used here to fix the stained cells (20 min incubation), followed by washing twice with staining buffer. Except the unstained control, all samples were further incubated with Hoescht stain solution for 20 mins at 4°C in the dark, followed by washing twice with stain buffer. Finally, cells were resuspended in 100 µl of

stain buffer and analyzed by Amnis ImageStream mkII and its software package, INSPIRE, as per its standard protocol.

4.3.10 Statistics

Data were expressed as mean ± standard deviation of mean (SD) of separate experiments (n≥3) performed on separate days using freshly prepared reagents. Statistical significance was performed by a one-way pairwise multiple comparison ANOVA followed by Holm-Sidak posthoc analysis by using SigmaPlot 11.0 software.

4.4 RESULTS

4.4.1 INH does not cause cell death

12 h treatment with different concentrations (1 μM to 10 mM) of INH was used to evaluate the cytotoxic effect of INH on HL-60 cells. The trypan blue exclusion assay results showed that there was no difference in live cell counts between untreated cells and any concentration of INH-treated cells (results not shown).

4.4.2 INH-induced changes in protein expressions

The replicate SILAC analysis of the INH-treated HL60 cells in comparison to the untreated control cells resulted in a total of 260 proteins were reproducibly identified and quantified in both analyses using highly stringent data analysis. The quantified data of the ratios of protein abundance shown in **Figure 1A** reveals that the majority of proteins do not significantly change in abundance upon treatment. Only 21 proteins were identified for their reproducibly significant change in abundance by 0.5 on a log2 scale (~ over 40% changes in abundance) upon treatment.

All of these were downregulated (upregulated proteins did not find reproducible and discarded). These 21 proteins were listed in Table 1. String (version 10) analysis revealed that these downregulated proteins demonstrated strong evidence-based association (**fig 1B**). This suggests that these associated proteins are likely to be involved in specific signaling pathways. Among all changed (down-regulated) proteins, 16 were ribosomal proteins, and other five included cathepsin G (CTSG), minichromosome maintenance complex component 3 (MCM3), inosine 5'-monophosphate dehydrogenase 2 (IMPDH2), DEAD (Asp-Glu-Ala-Asp) box helicase 17 (DDX17), and histone H2A type 1-H (HIST1H2AH).

4.4.3 A hallmark sign of monocytic cells: NSE activity

Monocyte-macrophage lineage of immune cells possesses membrane-bound NSE which lacks proteolytic activity, however, hydrolyzes α-naphthyl acetate to naphthanol compounds. This property of NSE provides a unique opportunity for identification of monocytes through both a simple staining procedure and UV spectroscopy [18, 22]. In the colorimetric assay of NSE activity, vitD3 (specific for monocytic differentiation) and different concentrations of INH (1μM to 10 mM) were compared against both untreated HL-60 cells and RA-treated cells (specific for granulocytic differentiation). The results showed that INH increased NSE activity in a concentration-dependent manner. The higher concentration of INH (100 μM to 10 mM) and vitD3 treatment groups showed a significant increase (*$P < 0.005$) in NSE activity in comparison with both untreated and RA treated HL-60 cells (**fig 2**). NaF, an inhibitor of NSE, showed the elimination of NSE activity in all treatment groups (**fig 2**).

In cytohistochemical microscope assay for NSE activity, the results echoed similar patterns with its colorimetric assay. The NSE activity appeared here as dark (black) color cells under a

microscope. The amount of NSE activity has been presented here as the intensity of darkness. The higher the intensity of darkness, the higher the NSE activity, and the higher the number of differentiated monocytic cells. The results showed that both untreated and RA-treated cells were least in darkness while human monocytes and vitD3 showed the highest intensity of darkness (**fig 3**). In the case of INH treatment groups, the intensity of darkness was increased with the concentration of INH (**fig 3**).

4.4.4 A hallmark sign for phagocytic cells: NADPH oxidase activity

A popular assay, NBT reduction, for NADPH oxidase activity was carried out here. All professional phagocytes including monocytes and macrophages express NADPH oxidase which can form $O_2^{\bullet-}$. The $O_2^{\bullet-}$ reduces NBT to its formazan which causes a color change. As HL-60 cell is a promyeloid progenitor cell, it possesses a low level of NADPH oxidase activity [23]. However, this activity increases during differentiation into phagocytic cells [24]. Again, the certainty of the source of $O_2^{\bullet-}$ is NADPH oxidase can be reconfirmed by using an NADPH oxidase inhibitor such as DPI [20]. In this study, the results showed a significant increase (*$P <$ 0.005) of NADPH oxidase activity in all the treatment groups in comparison with untreated HL-60 cells (**fig 4**). At the same time, the DPI-treated cells ceased the NBT reduction for all treatment groups. It confirmed that NADPH oxidase was the main enzyme to produce $O_2^{\bullet-}$ and subsequently reduce NBT (**fig 4**).

4.4.5 Image stream flow cytometry for identification of CD14 and CD16

The expression of CD14 and CD16 surface biomarkers from different treatment groups were analyzed using flow cytometry. A representative dot plot for differential CD14 and CD16 expressions in different treatment groups has been shown in **figure 5A**. The untreated HL-60

cells were mostly congregated at CD14-/CD16- zone in dot plot whereas vitD3-treated cells were at CD14+ zone. The different concentrations of INH-treated HL-60 cells were slowly moved from CD14-/CD16- zone towards other zones, mainly CD14+ zone and partly CD14+/CD16+ as a concentration-dependent manner. A representation image of the dominant cell type of each treatment groups has been shown in **figure 5B**. The resulted images showed that untreated HL-60 cells were free of CD14 and CD16 (nucleus, blue in color), vitD3 treated cells were expressed CD14 (red color surface marker) whereas RA treated cells were expressed CD16 (green color surface marker). Increasing concentrations of INH-treated cells produced a gradual increase in CD14 staining (red color surface marker).

4.4.6 Monocytic subpopulations: CD14+ and CD14+/CD16+

Monocytes are mainly two types: classical monocytes and non-classical monocytes. The classical monocytes express mainly CD14 (shown here as CD14+) whereas non-classical monocytes express both CD14 and CD16 (shown here as CD14+/CD16+). Non-classical monocytes can be further classified based on CD14 expression level which was not carried out in this study. The expression of CD14 of all treatment groups has been compared in **figure 6A**. The result showed that vitD3 and the different concentration of INH (10 μM to 100 μM, and 1μM) increased CD14 expression significantly in comparison with both untreated and RA-treated cells (***P<0.005, **P<0.01, and *P<0.05 respectively). The vitD3 treated HL-60 cells expressed the highest level of CD14 (80 percent of total cells) whereas both the untreated and RA treated HL-60 cells expressed the lowest CD14 (5.7 and 2.4 percent of total cells respectively). In the case of INH treatments, the expression of CD14 was increased in a concentration-dependent manner (20 to 30 percent of total cells). In comparison with CD14+ expression, the CD14+/CD16+ expression for all treatment was low in percentage, however, CD14+/C16+ expressions in different treatment

groups found statistically significant in comparison with untreated HL-60 cells (**fig-6B**). Both the vitD3 and 100 μM of INH-treated groups showed here the most significant expression in comparison with the untreated HL-60 cells (7.57% and 5.12% of total cells respectively, ***P<0.005), followed by 10 μM of the INH-treated group (**P<0.01). Both RA and 1μM of INH treatment also increased CD14+/CD16+ significantly (*P<0.05) in comparison with untreated HL-60 cells.

4.5 DISCUSSION

INH was not found cytotoxic over 12 h treatments, however, 21 proteins were significantly downregulated within 4 h treatment. The string analysis on those downregulated proteins showed strong evidence-based associations in between all ribosomal proteins, particularly DDX17 and IMPDH2. These proteins have been further assessed through rigorous literature review. The DEAD box RNA helicase, DDX17, is highly conserved protein, and functions as a co-regulator of master transcriptional regulators of differentiation with other ribosomal proteins. A recent study observed the downregulation of DDX17 during myogenesis and epithelial-to-mesenchymal transdifferentiation in MCF7 cells [25]. Hence, any change in DDX17 expression can be anticipated as the phenotypic switch of cells, in another word “differentiation”. IMPDH2, a key regulator of lymphocyte proliferation, involves in the oxidation of inosine monophosphate to xanthosine monophosphate which is the rate limiting step in the *de novo* guanine synthetic pathway [26, 27]. A downregulation of IMPDH2 can assume as the inhibition of lymphocytic differentiation. Therefore, these strongly associated proteins indicate INH-induced differentiation which is not definitely lymphocytic.

It is well-known that HL-60 cells behave like GM progenitor cells which can be differentiated into both monocytes and granulocytes depending on the stimulators. Monocytes, macrophages and granulocytes (or neutrophils) possess myeloperoxidase, NADPH oxidase, and cathepsins in different extents. Those are abundant in neutrophils, and to a lesser extent in monocytes and macrophages. A study showed that CTSG, a neutrophilic cathepsin enzyme, was decreased during monocytic differentiation in U937 cells [28]. Hence, the downregulation of CTSG in this study can further indicate that INH-induced differentiation, and this might be towards monocytic phenotypes. In quantitative proteomics, we also found downregulated minichromosome maintenance complex component 3 (MCM3) and histone H2A type 1-H (HIST1H2AH). Both of them participate in DNA replication and cell growth; they are also markers of malignancy where abnormal cell growth is a dominant phenomenon [29, 30]. Since the HL-60 cell is a malignant cell type, it is conceivable why any one of them would not be downregulated. Therefore, the downregulation of these two growth-related proteins without any evidence of cell death in INH treatment can be interpreted as the initiation of malignancy stoppage which means HL-60 cells were undergoing differentiation. Therefore, all significant proteins in SILAC experiment suggest that INH-induced differentiation pathways, particularly towards the monocytes lineage.

HL-60 differentiation was determined in this study by using a number of methods. It revealed the monocytic differentiation capacity of INH. Although this effect of INH was found in a concentration-dependent manner, the millimolar concentration of INH cannot be usable therapeutically since the pharmacological concentration of INH (C_{max}) is 20 μM to 60 μM (5.53 ± 2.92 μg/ml) [31]. Due to a narrow therapeutic window, a number of questions regarding this novel property of INH can be raised. These are: how much differentiation can we expect from

INH's pharmacological concentration, and how this novel property of INH may improve the TB-treatment. As per this study, 10 μM of INH triggered the monocytic differentiation (both types together) approximately 25% of total HL-60 cells whereas 100 μM of INH triggered 35% monocytic cell differentiation. Therefore, the pharmacological concentration of INH triggered monocytic cell differentiation.

Although both macrophages and neutrophils are professional phagocytic cells, the macrophage possesses some unique features which make it a better defender against TB. For pathogen-killing during phagocytosis, macrophages mainly rely on their reactive nitrogen species (RNS) production whereas neutrophils rely on their reactive oxygen species (ROS) production [32, 33]. The bacterial catalase-peroxidase, KatG, can neutralize ROS very effectively [32, 33]. A study showed that *Mtb* possesses a very high tolerance for ROS (up to 50 mM H_2O_2 [34]) whereas tolerance against RNS is relatively lower (few nM to 5 mM of reactive nitrogen species is bacteriostatic; above 5 mM of that is bactericidal [34]). Therefore, more macrophages (which can be converted from recruited circulatory monocytes) would provide better host defense. For more macrophages, more circulatory monocytes are required to be recruited from circulation. For more circulatory monocytes, more monocytic differentiation is required from GM progeny stem cells. In this study, it has been shown that INH has significant capacity to induce monocytic differentiation (fig 6). As such, this novel property of INH can be proposed as its additional mode of action.

4.6 REFERENCES

[1] Sia IG, Wieland ML. Current concepts in the management of tuberculosis. Mayo Clinic proceedings. 2011;86:348-61.

[2] Gafter AKaU. Tuberculosis prophylaxis for the chronically dialysed patient--yes or no? . Nephrology Dialysis Transplantation. 1999;14: 2857-9.

[3] Timmins GS, Deretic V. Mechanisms of action of isoniazid. Molecular microbiology. 2006;62:1220-7.

[4] Khan SR, Morgan AGM, Michail K, Srivastava N, Whital RM, Aljuhani N, et al. Metabolism of Isoniazid by Neutrophil Myeloperoxidase Leads to INH-NAD+ Adduct Formation: A Comparison of the Reactivity of Isoniazid with its Known Human Metabolites. Biochemical Pharmacology.

[5] Metushi IG, Uetrecht J, Phillips E. Mechanism of isoniazid-induced hepatotoxicity: then and now. British Journal of Clinical Pharmacology. 2016:n/a-n/a.

[6] Antony VB, Sahn SA, Harada RN, Repine JE. Lung repair and granuloma formation. Tubercle bacilli stimulated neutrophils release chemotactic factors for monocytes. Chest. 1983;83:95S-6S.

[7] Perskvist N, Zheng L, Stendahl O. Activation of Human Neutrophils by Mycobacterium tuberculosis H37Ra Involves Phospholipase Cγ2, Shc Adapter Protein, and p38 Mitogen-Activated Protein Kinase. The Journal of Immunology. 2000;164:959-65.

[8] Ehlers S, Schaible UE. The Granuloma in Tuberculosis: Dynamics of a Host–Pathogen Collusion. Frontiers in Immunology. 2012;3:411.

[9] Assis PA, Espíndola MS, Paula-Silva FW, Rios WM, Pereira PA, Leão SC, et al. Mycobacterium tuberculosis expressing phospholipase C subverts PGE2 synthesis and induces necrosis in alveolar macrophages. BMC Microbiology. 2014;14:1-10.

[10] Chen M, Gan H, Remold HG. A Mechanism of Virulence: Virulent Mycobacterium tuberculosis Strain H37Rv, but Not Attenuated H37Ra, Causes Significant Mitochondrial Inner Membrane Disruption in Macrophages Leading to Necrosis. The Journal of Immunology. 2006;176:3707-16.

[11] Khan SR, Aljuhani N, Morgan AGM, Baghdasarian A, Fahlman RP, Siraki AG. Cytoprotective effect of isoniazid against H_2O_2 derived injury in HL-60 cells. Chemico-Biological Interactions. 2016;244:37-48.

[12] Khan SR, Baghdasarian A, Fahlman RP, Siraki AG. Global protein expression dataset acquired during isoniazid-induced cytoprotection against H_2O_2 challenge in HL-60 cells. Data in Brief.

[13] Iwata K, Ogata S, Okumura K, Taguchi H. Induction of differentiation in human promyelocytic leukemia HL-60 cell line by niacin-related compounds. Bioscience, biotechnology, and biochemistry. 2003;67:1132-5.

[14] Ida C, Ogata S, Okumura K, Taguchi H. Changes in the Gene Expression of C-myc and CD38 in HL-60 Cells during Differentiation Induced by Nicotinic Acid-Related Compounds. Bioscience, Biotechnology, and Biochemistry. 2008;72:868-71.

[15] Wahl LM, Wahl SM, Smythies LE, Smith PD. Isolation of human monocyte populations. Current protocols in immunology / edited by John E Coligan [et al]. 2006;Chapter 7:Unit 7 6A.

[16] Khan SR, Baghdasarian A, Fahlman RP, Michail K, Siraki AG. Current status and future prospects of toxicogenomics in drug discovery. Drug Discovery Today. 2014;19:562-78.

[17] Khan SR, Baghdasarian A, Nagar PH, Fahlman R, Jurasz P, Michail K, et al. Proteomic profile of aminoglutethimide-induced apoptosis in HL-60 cells: Role of myeloperoxidase and arylamine free radicals. Chemico-Biological Interactions. 2015;239:129-38.

[18] Oseph Yourno, Peter Burkart, Walter Mastropaolo, Frank Lizzi, Tartaglia A. Monocyte Nonspecific Esterase: Enzymologic Characterization of a Neutral Serine Esterase Associated with Myeloid Cell. The Journal of Histochemistry and Cytochemistry. 1986;34:727-33.

[19] Howell DR, Hackett T, Moore WC, Warner JA. Macrophage Derived Non-Specific Esterase and Allergen Stimulation. Journal of Allergy and Clinical Immunology.117:S63.

[20] Babior BM. NADPH oxidase. Current Opinion in Immunology. 2004;16:42-7.

[21] Nathan DG. NBT Reduction by Human Phagocytes. New England Journal of Medicine. 1974;290:280-1.

[22] Salmassi A, Kreipe H, Radzun HJ, Lilischkis R, Charchinajadamoey M, Zschunke F, et al. Isolation of Monocytic Serine Esterase and Evaluation of Its Proteolytic Activity. Journal of Leukocyte Biology. 1992;51:409-14.

[23] Teufelhofer O, Weiss RM, Parzefall W, Schulte-Hermann R, Micksche M, Berger W, et al. Promyelocytic HL60 cells express NADPH oxidase and are excellent targets in a rapid spectrophotometric microplate assay for extracellular superoxide. Toxicological Sciences. 2003;76:376-83.

[24] Hua J, Hasebe T, Someya A, Nakamura S, Sugimoto K, Nagaoka I. Evaluation of the expression of NADPH oxidase components during maturation of HL-60 cells to neutrophil lineage. J Leukoc Biol. 2000;68:216-24.

[25] Dardenne E, Polay Espinoza M, Fattet L, Germann S, Lambert MP, Neil H, et al. RNA helicases DDX5 and DDX17 dynamically orchestrate transcription, miRNA, and splicing programs in cell differentiation. Cell reports. 2014;7:1900-13.

[26] Carcamo WC, Satoh M, Kasahara H, Terada N, Hamazaki T, Chan JYF, et al. Induction of Cytoplasmic Rods and Rings Structures by Inhibition of the CTP and GTP Synthetic Pathway in Mammalian Cells. PLoS ONE. 2011;6:e29690.

[27] Pazik J, Oldak M, Podgorska M, Lewandowski Z, Sitarek E, Ploski R, et al. Lymphocyte counts in kidney allograft recipients are associated with IMPDH2 3757T>C gene polymorphism. Transplantation proceedings. 2011;43:2943-5.

[28] Senior RM, Campbell EJ. Cathepsin G in human mononuclear phagocytes: comparisons between monocytes and U937 monocyte-like cells. Journal of immunology. 1984;132:2547-51.

[29] Freeman A, Morris LS, Mills AD, Stoeber K, Laskey RA, Williams GH, et al. Minichromosome Maintenance Proteins as Biological Markers of Dysplasia and Malignancy. Clinical Cancer Research. 1999;5:2121-32.

[30] Khare SP, Sharma A, Deodhar KK, Gupta S. Overexpression of histone variant H2A.1 and cellular transformation are related in N-nitrosodiethylamine-induced sequential hepatocarcinogenesis. Experimental Biology and Medicine. 2011;236:30-5.

[31] Peloquin CA, Namdar R, Dodge AA, Nix DE. Pharmacokinetics of isoniazid under fasting conditions, with food, and with antacids. Int J Tuberc Lung D. 1999;3:703-10.

[32] DeVito JA, Morris S. Exploring the Structure and Function of the Mycobacterial KatG Protein Using trans-Dominant Mutants. Antimicrobial agents and chemotherapy. 2003;47:188-95.

[33] Chouchane S, Lippai I, Magliozzo RS. Catalase-Peroxidase (Mycobacterium tuberculosis KatG) Catalysis and Isoniazid Activation†. Biochemistry. 2000;39:9975-83.

[34] Voskuil MI, Bartek I, Visconti K, Schoolnik GK. The response of Mycobacterium tuberculosis to reactive oxygen and nitrogen species. Frontiers in Microbiology. 2011;2.

4.7 FIGURES AND LEGENDS

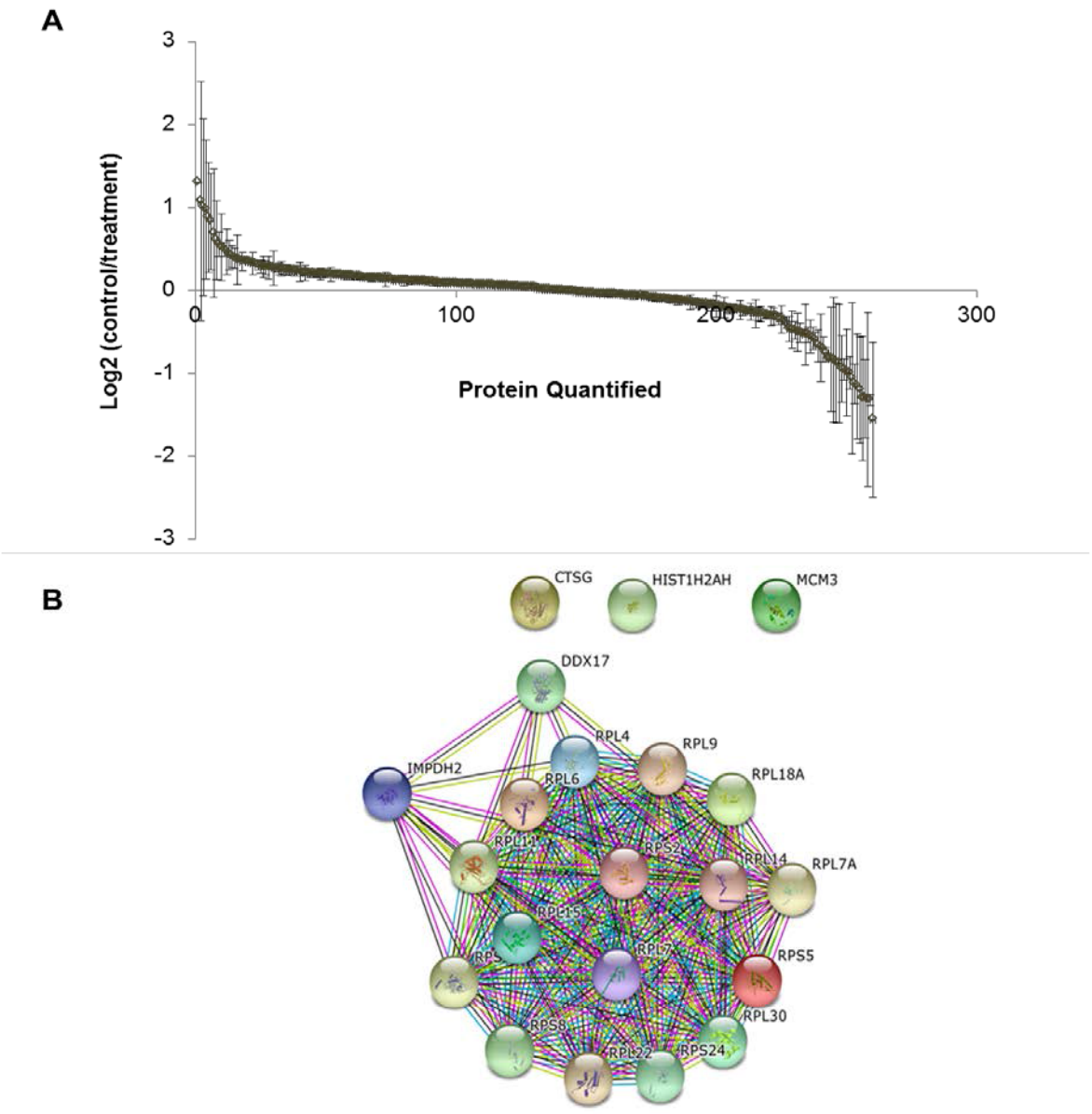

4.7.1 Figure 1: Protein changes in abundance and evidence-based association analysis. (A) All reproducible proteins in both sample A and B were analyzed here for their changes in expression based on Log2 value. It showed that most of the proteins were not changed in abundance upon treatment with INH in HL-60 cells. (B) the proteins which were significantly

changed in abundance (reported in Table 1) were further analyzed for evidence-based analysis by using String v.10 .

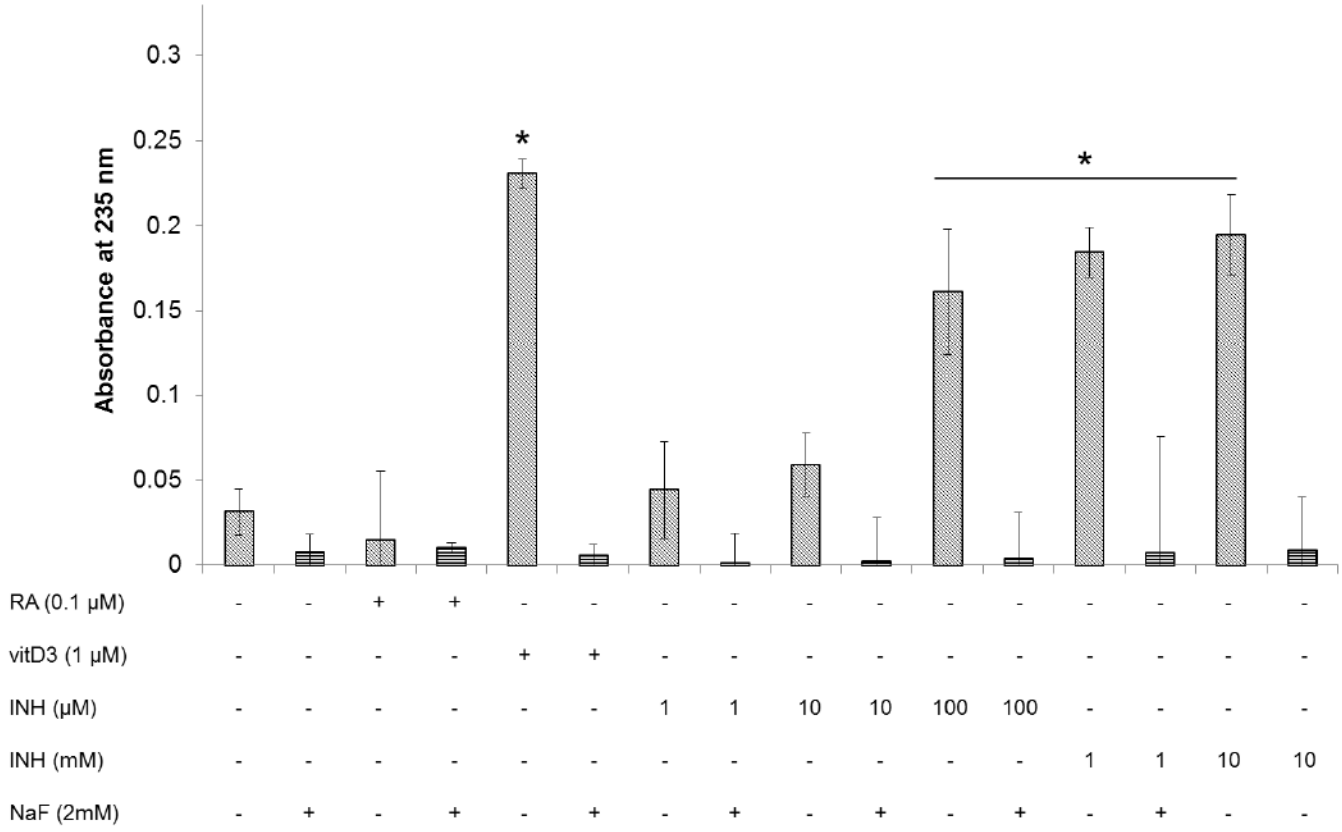

4.7.2 Figure 2: The colorimetric assay for non-specific esterase activity assay (specific for monocytes). * P>0.005 in comparison with both HL-60 cells and RA-treated cells.

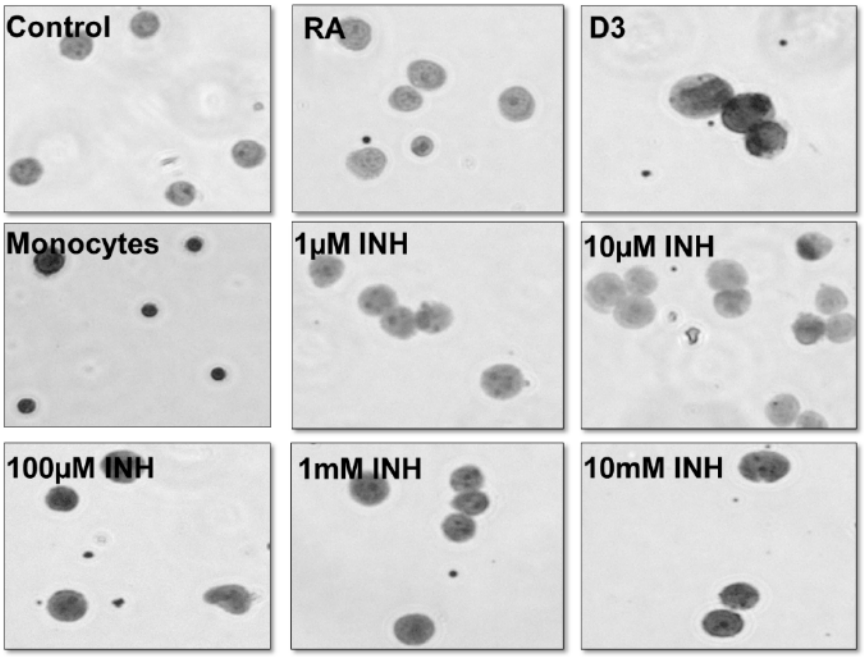

4.7.3 Figure 3: The cytohistochemical microscope for non-specific esterase activity (specific for monocytes).

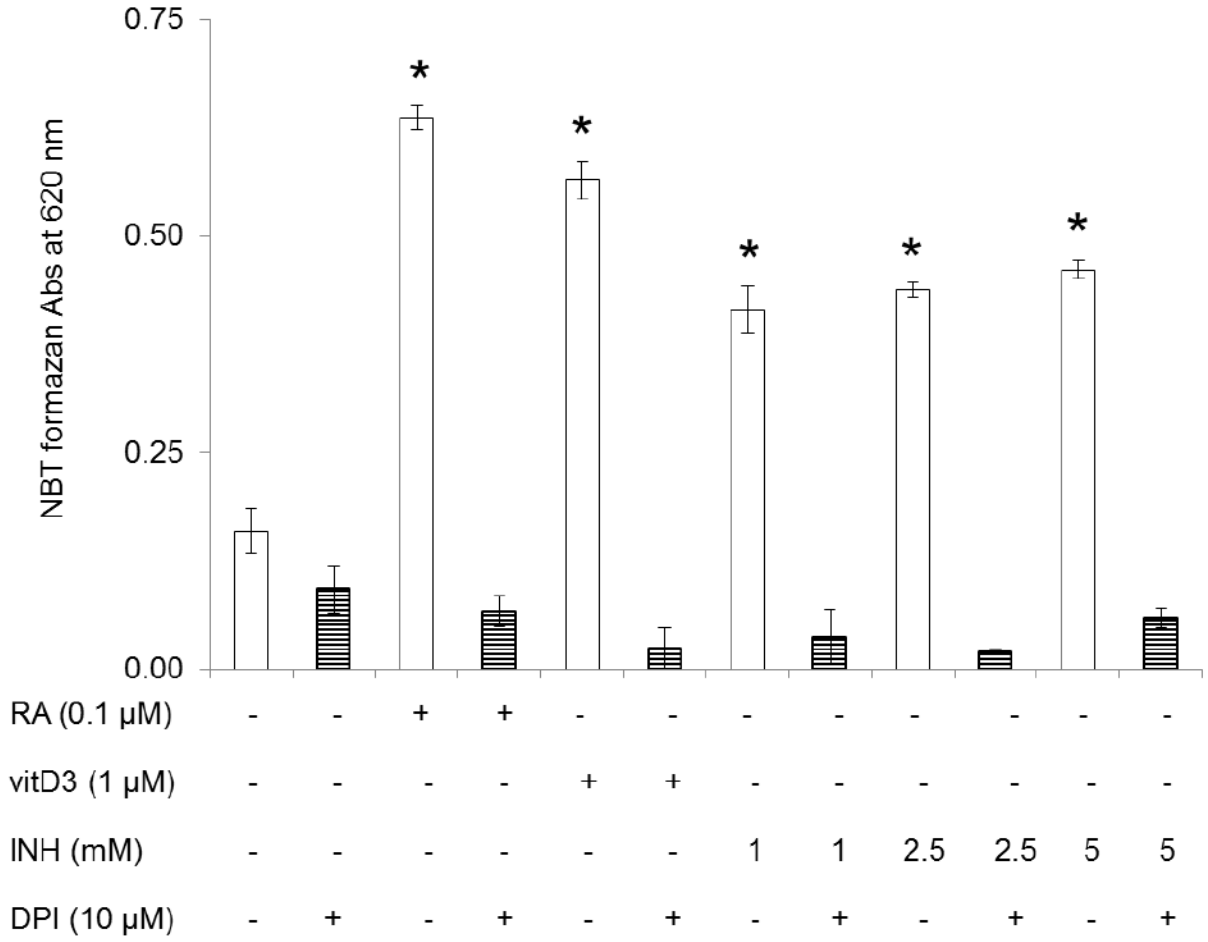

4.7.4 Figure 4: NBT reduction assay. It is a hallmark assay for NADPH activity of phagocytic cells. They reduce NBT upon being stimulated by Phorbol myristate acetate (PMA). PMA induces PKC pathway for superoxide generation through NADPH oxidase activation. DPI (diphenyleneiodonium), an inhibitor of NADPH oxidase, was used in 10 µM for 1-hour pretreatment. * $p > 0.005$ in comparison with HL-60 cells.

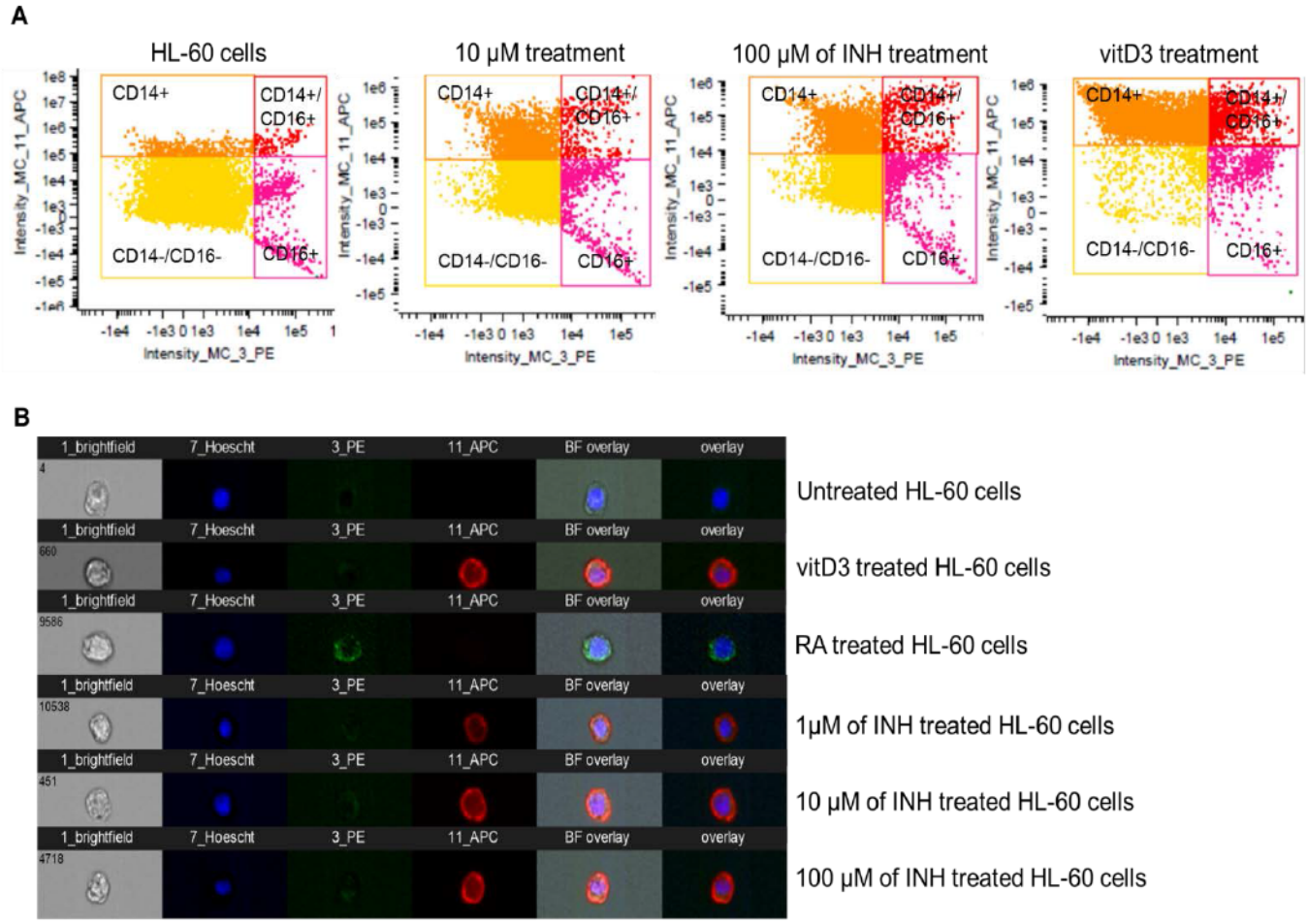

4.7.5 Figure 5: Image stream flow cytometry for CD14 and CD16 surface protein expression. (A) a set of dots plot for untreated HL-60 cells, 10 µM and 100 µM INH-treated HL-60 cells, and vitD3 treated HL-60 cells have been shown here to represent the pattern of monocytic differentiation in INH-treated HL-60 cells. (B) a set of the representative image of the dominant cell type of different reactions.

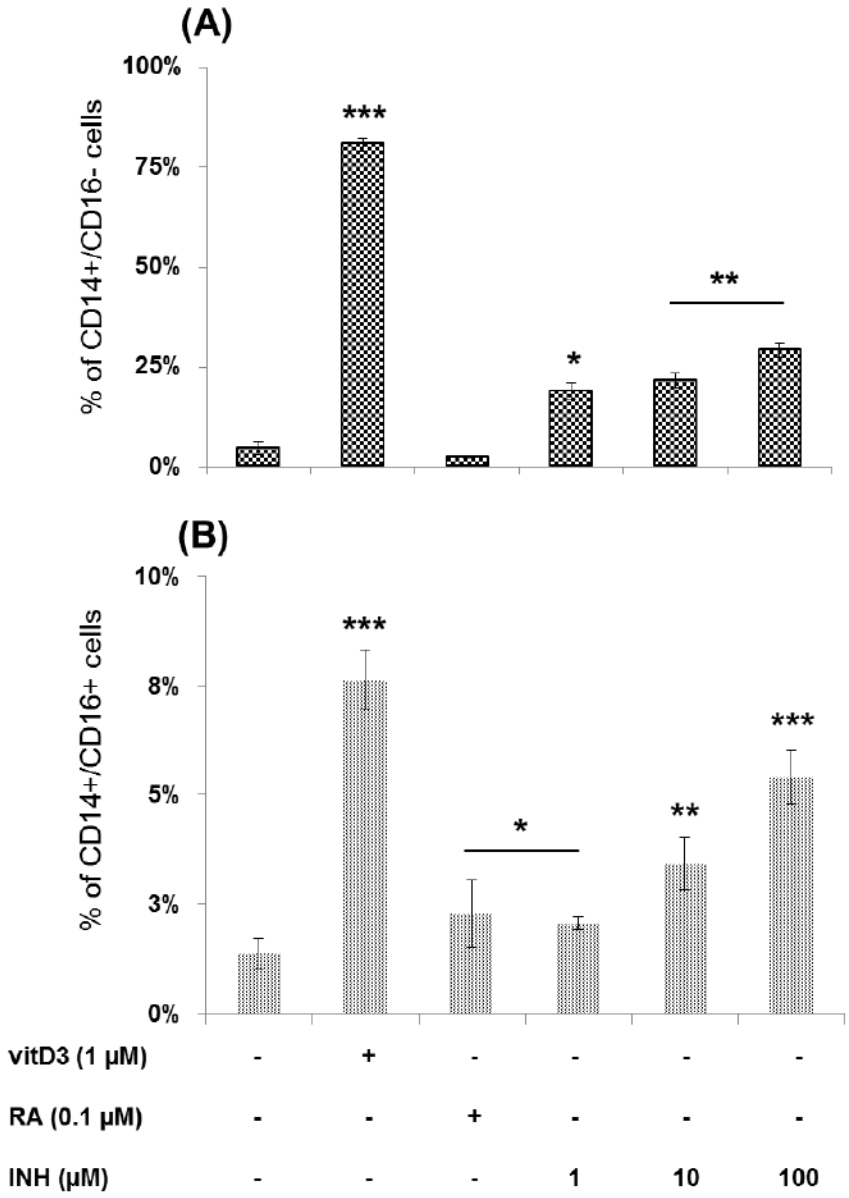

4.7.6 Figure 6: The percentage of monocytic subpopulations in each reaction. (A) Classical monocytic (CD14+) population in each reaction: The vitD3 treated HL-60 cells showed the most significant CD14 expression (80% of total population) in comparison with untreated HL-60 cells (***P<0.005). The different concentrations of INH (1 µM, 10 µM and 100 µM) treated HL-60 cells showed also significant CD14 expression (20% to 30% of total population) in comparison

with untreated HL-60 cells (*P<0.05, and **P<0.01). (B) Non-classical monocytic (CD14+/CD16+) population in each reaction: The vitD3 treated HL-60 cells showed the most significant CD14+/CD16+ expression in comparison with untreated HL-60 cells (***P<0.005). The different concentrations of INH (1 μM, 10 μM, and 100 μM) treated HL-60 cells and RA-treated cells showed also significant CD14 expression in comparison with untreated HL-60 cells (*P<0.05, and **P<0.01).

3.8 TABLES

3.8.1 Table 1. All significant proteins (downregulated) observed in SILAC experiment upon INH treatment.

Accession	Description	Unique Peptides Sample A	Unique Peptides Sample B	Average Change (control/treated) +/- SD
E5RI99	Ribosomal protein L30 (RPL30)	5	5	0.66 ± 0.10
P62701	Ribosomal protein S4, X-linked (RPS4)	5	8	0.40 ± 0.02
Q5JR95	Ribosomal protein S8 (RPS8)	5	5	0.43 ± 0.27
H0YEN5	Ribosomal protein S2 (RPS2)	4	5	0.51 ± 0.07
P08311	Cathepsin G (CTSG)	3	6	0.63 ± 0.39
A8MUD9	Ribosomal protein L7 (RPL7)	9	5	0.46 ± 0.26
F8W181	Ribosomal protein L6 (RPL6)	7	5	0.39 ± 0.04
D6RAN4	Ribosomal protein L9 (RPL9)	4	3	0.40 ± 0.32
P62847	Ribosomal protein S24 (RPS24)	2	2	0.51 ± 0.28
B4DM74	Ribosomal protein L18a (RPL18a)	2	3	0.40 ± 0.14
E7EQV9	Ribosomal protein L15 (RPL15)	3	3	0.47 ± 0.10
P35268	Ribosomal protein L22 (RPL22)	3	2	0.70 ± 0.01
E7EPB3	Ribosomal protein L14 (RPL14)	4	2	0.44 ± 0.24
H0Y4R1	Inosine 5'-monophosphate dehydrogenase 2 (IMPDH2)	8	5	0.59 ± 0.00
Q5T8U3	Ribosomal protein L7a (RPL7a)	2	3	0.5 ± 0.10
Q96KK5	Histone H2A type 1-H (HIST1H2AH)	5	2	0.67 ± 0.16
P25205	Minichromosome maintenance complex component 3 (MCM3)	6	9	0.61 ± 0.05
P46782	Ribosomal protein S5 (RPS5)	4	2	0.54 ± 0.24
P62913	Ribosomal protein L11 (RPL11)	3	2	0.61 ± 0.13
Q92841	DEAD (Asp-Glu-Ala-Asp) box helicase 17 (DDX17)	3	6	0.71 ± 0.15
B4DMJ2	Ribosomal protein L4 (RPL4)	2	2	0.40 ± 0.28

CHAPTER 5:

DISCUSSION

Our studies revealed three novel pharmacological findings regarding INH and its conceivable roles on the host immune system. In the first study (chapter 2), neutrophil myeloperoxidase (MPO) was shown to metabolize INH (similar to KatG), which forms a key antibacterial compound: INH-NAD^+ adduct (an inhibitor of enoyl-acyl carrier protein reductase which is the key enzyme for mycolic acid synthesis). This finding may explain how INH could kill *Mtb* without penetrating into granuloma. In addition, this additional role for neutrophils in INH activation puts forward several questions, such as the rationale for stopping INH treatment in KatG mutation related INH-resistant TB cases, and whether the neutrophils should be considered as a "Trojan horse" during INH treatment (see below). The second study (chapter 3) revealed the cytoprotective role of INH against oxidative stress-induced necrosis in HL-60 cells, a model cell line which can generate oxidative stress itself in the presence of H_2O_2 and undergoes necrosis. This type of self-generating oxidative stress-induced necrosis is the underlying cause of phagocytic cell death followed by granuloma degradation in TB. The cytoprotective role of INH could describe how it can strengthen the granuloma mediated host immune defense, and induce the latency of *Mtb*. The third study (chapter 4) revealed the capacity of INH to induce monocytic differentiation in HL-60 cells, which served as a model cell line such as GM progenitor stem cells. This finding is important since monocyte-derived macrophages are known to play the major role in killing both latent and active *Mtb* due to its capacity to generate NO for which *Mtb* does not possess any defense mechanism. To understand the connection of these novel pharmacological actions with the possible mode of actions of INH, a comprehensive knowledge of both TB pathophysiology and limitations of the existing mode of action of INH is essential. The limitations of the existing mode of action of INH have already been discussed in

"Introduction". The TB pathophysiology has been discussed below briefly by highlighting the role of neutrophils, monocytes, and necrosis.

At the early stage of TB infection, neutrophils are promptly recruited around the alveolar macrophage (which has already engulfed *Mtb*) due to reactive species induced inflammatory signals [1-3]. In the case of healthy people, macrophages usually kill *Mtb* with NO through its inducible NO synthase (iNOS) activity; however, neutrophils cannot kill *Mtb* since bacterial KatG can neutralize both the acidic compounds and the reactive oxygen species (ROS) through its catalase-peroxidase activity [4, 5]. If macrophages kill *Mtb* successfully, they will undergo apoptotic cell death [6]. Neutrophils will engulf these apoptotic cells and carry their contents to lymph nodes to activate T cells [7]. T cells defend the host against further active TB infection and *Mtb* latency [8]. The opposite scenario is the failure of macrophages to kill *Mtb.* In this case, macrophages form granuloma by recruiting more macrophages, macrophage-like immune cells, and a few lymphocytes. It can effectively stop the *Mtb* dissemination through the body [9]. This stage is known as latent TB. The success of macrophages depends on the several factors such as the number of *Mtb* and their virulence, the number of macrophages and individual host [2, 9]. If the host's immune system is compromised (due to HIV-infection or malnutrition), the granuloma cannot provide sufficient protection due to lack of monocyte-derived macrophages, and can cause active TB. Based on the individual host variations, the possible outcomes of the battle in between *Mtb* and host immune defense have been illustrated in figure 1.

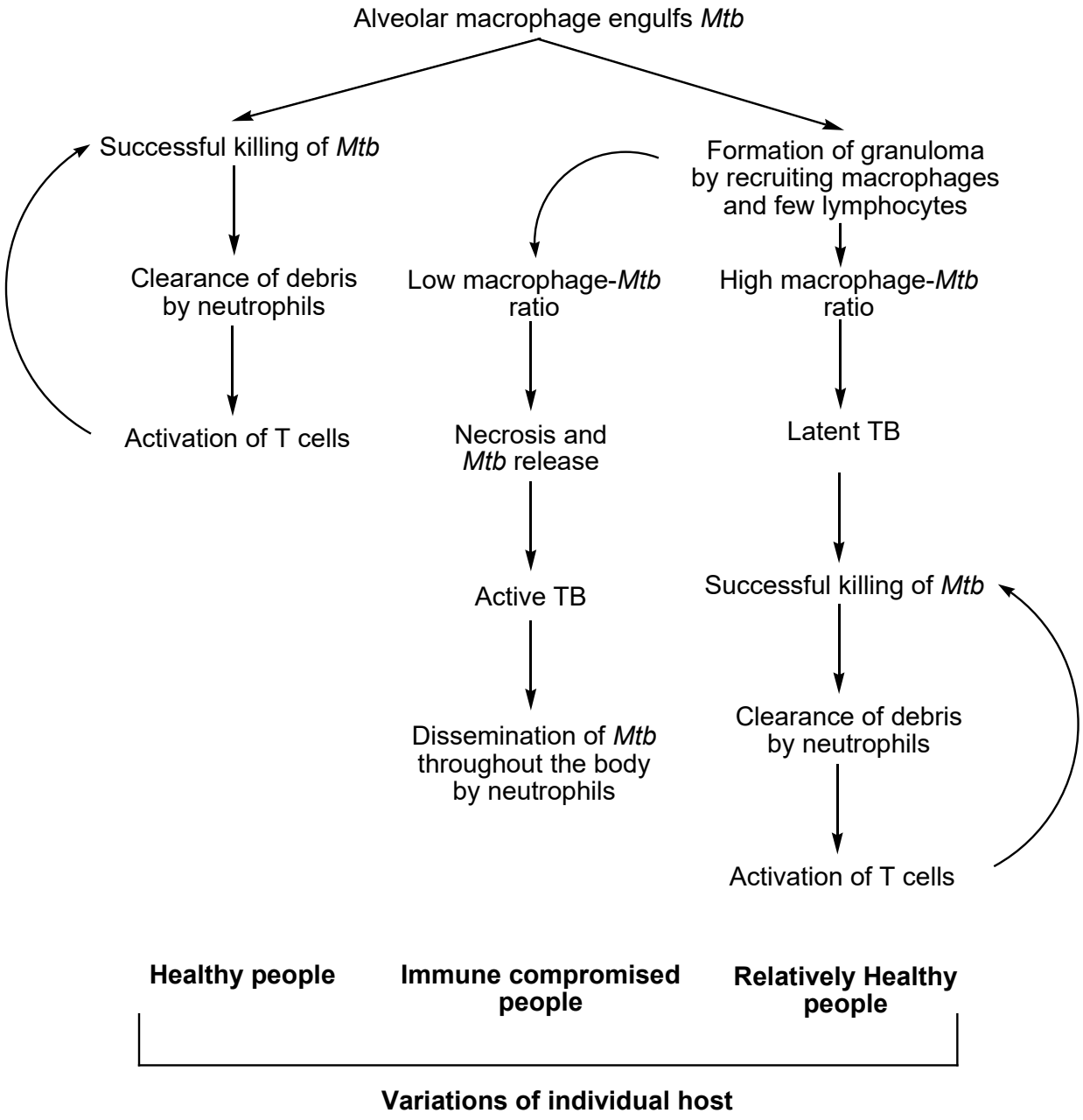

Figure-1: The possible scenario of TB infections based on individual host immunity.

In the latent stage (within the granuloma), *Mtb* loses its typical cell wall, and remains non-replicating but high energy generating [10]. This condition influences host immune cells to generate continuous reactive species (RS) which create high oxidative stress within the

granuloma. *Mtb* exhibits unusual high tolerance to such ROS and remains safe [4]. However, such a high concentration of ROS leads to mitochondrial damage followed by necrotic cell death of infected macrophages [6]. After necrosis, *Mtb* escapes the granuloma. Neutrophils engulf those *Mtb*. As neutrophils do not possess iNOS activity, they cannot kill bacteria; however, they help to disseminate bacteria throughout the body [2]. Hence, neutrophils are known as the "Trojan Horse" for TB infection [2, 3], and this pathological condition is known as active TB [6]. From above discussion, the following aspects of TB pathophysiology are plausible: (1) neutrophils are involved in *Mtb* spreading throughout of the body; (2) oxidative stress-induced necrosis is the rate-limiting step for active TB, and (3) macrophage recruitment into granulomas can strengthen the host immune defense against *Mtb*.

Although neutrophils do not have iNOS, they have myeloperoxidase (MPO) which has approximately 10^4 times more peroxidase activity than the bacterial (*Mtb*) catalase-peroxidase, KatG. In the first study (chapter 2), it was shown that neutrophil MPO can oxidize INH which forms an antibacterial INH-NAD^+ adduct in the presence of NAD^+. Since neutrophils engulf granuloma-escaped *Mtb*, its antibacterial INH-NAD^+ adduct formation capacity during INH treatment could play a vital role in *Mtb* killing directly. This possibility has been proposed here as the part of the mode of action of INH (fig 2). In addition, this finding argues against the concept where KatG was claimed as the only site of INH activation. Therefore, mutations in KatG gene may not such important consideration for INH resistance (discussed later).

The necrotic cell death of macrophages in granuloma has been described here as the rate-limiting step for active TB. However, the prevention of this necrosis not only averts active TB but also strengthens the host defense against latency. In the second study (chapter 3), it was shown that INH provides significant cytoprotection against oxidative stress-induced

mitochondrial damage and subsequent necrotic cell death. The possible mechanisms of such cytoprotection were: (1) the increase of the cell replication process; (2) an increase of ATP synthesis, and (3) an increase of structure maintenance proteins expression and blocking of some cell-death signals. In addition, a correlation between MPO-dependent protein-adduct formation and the cytoprotective effect of INH was observed. Since it is yet to identify the involved proteins in those adducts, it is difficult to draw a conclusive relationship of those protein adducts with INH-induced cytoprotection. However, it is possible that INH could increase oxidative stress tolerance of phagocytic cells (both macrophages and neutrophils). This property of INH definitely adds advantages during INH-treatment in both latent and active TB and has been proposed here another part of INH's mode of action (fig 2).

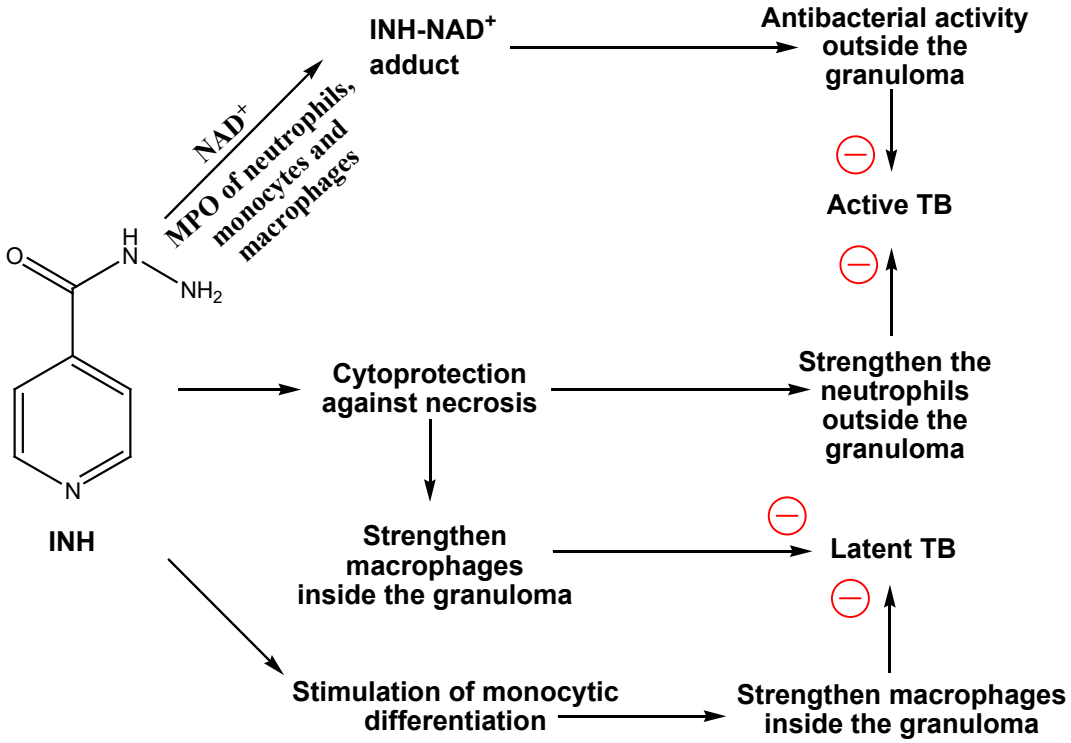

Figure-2: The proposed mode of actions of INH.

The strength of the granuloma will not only ensure the blockade of active TB occurrences but also help to destroy slowly the latent *Mtb*. Certainly, the greater the macrophage: *Mtb* ratio is in the granuloma, the greater the ability of the host to defend TB. There is no data available on whether INH can signal monocyte recruitment; however, the third study (chapter 4) showed that INH can stimulate monocytic differentiation. It could be helpful in the case of immune compromised TB patients whose macrophage: *Mtb* ratio is unusually low. This dangerous condition can favor switching to active TB (Fig-1). However, the stimuli for more monocyte differentiation from GM progenitor stem cells will increase the monocyte populations in circulation. It will ensure the availability of circulating monocytes to be recruited inside the granuloma if needed. Therefore, the monocytic differentiation stimulus of INH could have a great impact on TB recovery and has been proposed as the part of its mode of action (fig 2); however, this requires confirmation using GM progenitor stem cells or CD34+ stem cells.

Since the existing mode of action of INH has a number of limitations which suggest INH may have another mode of action(s), these novel pharmacological findings of INH could be combined to propose its possible mode of action as per figure 2. This proposed mode of action can explain how INH could exert antibacterial action without penetrating into the granuloma, why INH is very effective against latent TB treatment, and why does INH need relatively long-term treatment period. In addition, it also disputes the justification of the stoppage of INH in INH-resistant TB which is considered as the first step of all other types of drug resistances. The drug resistance is usually diagnosed *in vitro* through either phenotypic drug susceptibility test or PCR-based molecular drug susceptibility test (http://www.cdc.gov/tb/) both of which completely overlook the drug's systemic effects (e.g., the host immune modulation). Moreover, the mutation of KatG has been identified for approximately 45% of total clinical INH-resistant TB cases [11].

It interferes with INH binding site at KatG and makes the enzyme relatively less efficient [12]. In this study, neutrophil MPO was found as an alternative of KatG for INH metabolism. It further suggests using INH in the cases of INH-resistant TB, particularly in KatG mutations.

FUTURE DIRECTIONS

As a whole, our studies showed that INH is not only an anti-bacterial drug, but also a host immune modulator. Although our first study revealed neutrophil MPO as an alternative of KatG for INH metabolism, it is necessary to compare their enzymatic capacity in term of the rate of INH-NAD^+ adduct formation. Our second study found the cytoprotective effect of INH in HL-60 cells; however, it is necessary to evaluate this effect of INH in primary phagocytic cells, such as monocyte-derived macrophages. Our third study found INH as a chemical stimulus for monocytic differentiation of HL-60 cells. However, it is also essential to estimate this potentiality of INH in human GM progenitor stem cells. It is difficult to get such cells directly from blood, however, commercially available human hematopoietic CD34+ stem cells can be switched into human GM progenitor stem cells by using StemSpan™ myeloid expansion supplement (Stem Cell Biotechnology, catalog# 02693).

Our studies suggest rethinking the use of INH in the case of KatG-mutation related INH-resistant TB. Since number of host immune cells such as neutrophils, monocytes and macrophages possess MPO which can be the alternative sites for INH oxidation and formation of INH-NAD^+ adduct in the presence of NAD^+. In such instance, KatG is not mandatory. Moreover, INH usage will further beneficial due to its immune modulatory effects (cytoprotection and monocytic differentiation). Initially, a suitable animal model can be infected by KatG mutated *Mtb*, followed by treated with INH to understand the possibility of using INH in patients infected by similar types of *Mtb* strains. Thereafter, a double-blind clinical trial where INH will be given additionally with the current therapy specific for KatG mutation related INH-resistant TB can be carried out to compare the outcomes. It would provide valuable information regarding INH therapy in INH-resistant TB treatment.

REFERENCES

[1] Fialkow L, Wang Y, Downey GP. Reactive oxygen and nitrogen species as signaling molecules regulating neutrophil function. Free radical biology & medicine. 2007;42:153-64.

[2] Lowe DM, Redford PS, Wilkinson RJ, O'Garra A, Martineau AR. Neutrophils in tuberculosis: friend or foe? Trends in immunology. 2012;33:14-25.

[3] Eruslanov EB, Lyadova IV, Kondratieva TK, Majorov KB, Scheglov IV, Orlova MO, et al. Neutrophil Responses to Mycobacterium tuberculosis Infection in Genetically Susceptible and Resistant Mice. Infection and Immunity. 2005;73:1744-53.

[4] Voskuil MI, Bartek I, Visconti K, Schoolnik GK. The response of Mycobacterium tuberculosis to reactive oxygen and nitrogen species. Frontiers in Microbiology. 2011;2.

[5] Forman HJ, Torres M. Redox signaling in macrophages. Molecular aspects of medicine. 2001;22:189-216.

[6] Behar SM, Martin CJ, Booty MG, Nishimura T, Zhao X, Gan HX, et al. Apoptosis is an innate defense function of macrophages against Mycobacterium tuberculosis. Mucosal immunology. 2011;4:279-87.

[7] Abadie V, Badell E, Douillard P, Ensergueix D, Leenen PJ, Tanguy M, et al. Neutrophils rapidly migrate via lymphatics after Mycobacterium bovis BCG intradermal vaccination and shuttle live bacilli to the draining lymph nodes. Blood. 2005;106:1843-50.

[8] Sud D, Bigbee C, Flynn JL, Kirschner DE. Contribution of CD8+ T Cells to Control of Mycobacterium tuberculosis Infection. The Journal of Immunology. 2006;176:4296-314.

[9] Guirado E, Schlesinger LS. Modeling the Mycobacterium tuberculosis Granuloma - the Critical Battlefield in Host Immunity and Disease. Front Immunol. 2013;4:98.

[10] Wolfe LM, Mahaffey SB, Kruh NA, Dobos KM. Proteomic Definition of the Cell Wall of Mycobacterium tuberculosis. Journal of Proteome Research. 2010;9:5816-26.

[11] Guo H, Seet Q, Denkin S, Parsons L, Zhang Y. Molecular characterization of isoniazid-resistant clinical isolates of Mycobacterium tuberculosis from the USA. Journal of medical microbiology. 2006;55:1527-31.

[12] Yu S, Girotto S, Lee C, Magliozzo RS. Reduced Affinity for Isoniazid in the S315T Mutant ofMycobacterium tuberculosis KatG Is a Key Factor in Antibiotic Resistance. Journal of Biological Chemistry. 2003;278:14769-75.